ANDRÉ THOMAZINI

SPATIAL AND TEMPORAL VARIABILITY OF CO_2 DYNAMIC AND SOIL ATTRIBUTES IN MARITIME ANTARCTICA.

Tese apresentada à Universidade Federal de Viçosa, como parte das exigências do Programa de Pós-graduação em Solos e Nutrição de Plantas, para obtenção do título de *Doctor Scientiae*.

VIÇOSA
MINAS GERAIS - BRASIL
2016

Ficha catalográfica preparada pela Biblioteca Central da Universidade Federal de Viçosa - Câmpus Viçosa

T

T465s
2016

Thomazini, André, 1988-
Spatial and temporal variability of CO2 dynamic and soil attributes in Maritime Antarctica / André Thomazini. – Viçosa, MG, 2016.
xii, 127f. : il. (algumas color.) ; 29 cm.

Orientador: Márcio Rocha Francelino.
Tese (doutorado) - Universidade Federal de Viçosa.
Inclui bibliografia.

1. Solos - Antárctica, Península. 2. Dióxido de carbono atmosférico - Antárctica, Península. 3. Aquecimento global. I. Universidade Federal de Viçosa. Solos. Programa de Pós-graduação em Solos e Nutrição de Plantas. II. Título.

CDD 22. ed. 631.4

ANDRÉ THOMAZINI

SPATIAL AND TEMPORAL VARIABILITY OF CO_2 DYNAMIC AND SOIL ATTRIBUTES IN MARITIME ANTARCTICA

Tese apresentada à Universidade Federal de Viçosa, como parte das exigências do Programa de Pós-graduação em Solos e Nutrição de Plantas, para obtenção do título de *Doctor Scientiae*.

APROVADA: 25 de abril de 2016.

Liovando Marciano da Costa

Gérson Rodrigues dos Santos

Antonio Batista Pereira

Carlos Ernesto G. R. Schaefer
(Coorientador)

Márcio Rocha Francelino
(Orientador)

Aos meus pais, irmão e família,

DEDICO

Agradecimentos

Em primeiro lugar, agradeço a Deus pela oportunidade de poder avançar mais uma etapa e seguir em frente com minha carreira profissional. Aos meus pais, principalmente, que mesmo distantes, sempre estiveram presentes dando-me apoio durante todos esses anos batalhando por um futuro melhor. Ao meu irmão, aos meus tios, tias e primos pelo apoio, pela ajuda, pelos conselhos, que foram de essencial importância. À minha namorada, Katia Maciel, pela paciência, conselhos e apoio.

Os professores Marcio Francelino e Carlos Ernesto Schaefer pela orientação, oportunidades de trabalho, auxílios e amizade e acolhimento em Viçosa durante esse período. Ao professor Eduardo Sá Mendonça pela indicação de vinda à UFV, ensinamentos, amizade e auxílios nos trabalhos. Ao professor Antonio Batista Pereira, pela imensa ajuda de campo, planejamento e companheirismo e alegria durante as operações na Antártica, que juntamente com o Adriano Schunnemam, sempre esteve presente para auxiliar tanto nos trabalhos de campo como os demais na UFV. Ao Daniel de Bortoli Teixeira pela parceria nos trabalhos e imensa ajuda estatística. Agradeço também ao Elias Neto e Mayara pela ajuda nos trabalhos de campo em 2014, Pedro Almeida na campanha de 2015, e pela amizade.

Agradeço aos demais professores da UFV, principalmente do departamento de solos, que de forma direta contribuíram para a conclusão deste trabalho durante a caminhada acadêmica. Às secretárias Claudinha e Luciana, pela presteza, paciência e auxílios no decorrer desses anos. Aos laboratoristas, que nos auxiliam no dia a dia nas análises de solo.

Ao programa Antártico Brasileiro, Marinha do Brasil, Ministério do Meio Ambiente e da Ciência e Tecnologia pelo apoio durante as operações Antárticas XXXII, XXXIII e XXXIV, onde foram realizados os trabalhos de campo da presente tese. Aos alpinistas Marcelo, Chico Petrone, Filipo, pelo apoio de campo. Ao Grupo Base Imperador, que no ano de 2015 desempenharam um papel fundamental no apoio aos trabalhos realizados na Península Keller.

Aos companheiros de república Luciano (vulgo Bahia), Elder (vulgo cabeça), aos amigos de longa data Luan (vulgo Fusão) e Paulo Cesar (vulgo Junim), pela amizade e pelo companheirismo durante esses anos. Aos amigos de Alegre que sempre estão presentes.

Aos membros da banca de qualificação e defesa (Liovando, Elpidio, Gérson) pela presteza na avaliação e na colaboração. A CAPES e CNPq pela concessão da bolsa de estudo no Brasil e pelo financiamento dos projetos de pesquisa.

A todos, o meu muito obrigado!

Biografia

ANDRÉ THOMAZINI, filho de Aldair dos Santos Thomazini e Nedis Aparecida Andreatta Thomazini, é natural da cidade de Baixo Guandu – ES. Iniciou sua carreira realizando curso de técnico em Agricultura na antiga Escola Agrotécnica Federal de Colatina (hoje IFES), concluindo o curso no ano de 2005. Em 2007 ingressou no curso de Agronomia no Centro de Ciências Agrárias da Universidade Federal do Espírito Santo, formando-se no ano de 2011. Em 2012, iniciou o curso de mestrado em Produção Vegetal na mesma instituição, com complementação na Universidade de Minnesota – EUA no ano de 2013, concluindo o curso no ano de 2014. Neste mesmo ano, ingressou no Doutorado no Programa de Pós-Graduação em Solos e Nutrição de Plantas da Universidade Federal de Viçosa, submetendo-se a defesa de tese em Abril de 2016.

Sumário

Resumo

THOMAZINI, André, D.Sc., Universidade Federal de Viçosa, abril de 2016. **Variabilidade espacial e temporal da dinâmica de CO_2 e atributos do solo na Antártica Marítima.** Orientador: Márcio Rocha Francelino. Coorientadores: Carlos Ernesto Gonçalves Reynaud Schaefer e Eduardo de Sá Mendonça.

A Antártica Marítima apresenta alta sensibilidade às mudanças climáticas, especialmente pelas alterações na temperatura do ar, que modificam a dinâmica do carbono e atributos do solo nos ecossistemas terrestres. Sendo assim, variáveis relacionadas ao solo (ou seja, carbono orgânico, temperatura do solo e umidade do solo), e o padrão de distribuição da vegetação, podem ser indicadores das mudanças climáticas. O objetivo deste trabalho foi investigar a relação espacial e temporal entre as trocas de carbono, o status de nutrientes do solo e seu desenvolvimento nos principais ecossistemas terrestres da Antártica Marítima. O estudo foi realizado na Península Keller e Coppermine, Ilha Rei George e Robert, respectivamente. Grids regulares foram instalados para avaliar a variabilidade espacial de atributos gerais do solo e troca de carbono em campos de liquens, musgos, liquens/musgos e locais de solo exposto, ao longo das áreas livres de gelo. Usando técnicas de geoestatística, a dependência espacial foi acessada através da modelagem do semivariograma e dimensão fractal. Amostras de solo foram coletadas em diferentes camadas para determinar alguns atributos gerais do solo. A respiração total do ecossistema, troca líquida do ecossistema e produção primária bruta foram determinadas medindo fluxos de CO_2 *in situ,* com um sistema automático de fechamento da câmara de medição (LI-COR Biosciences, Lincoln, NE, EUA), baseado em medições de curto e longo prazo.

Os resultados indicam uma alta capacidade dos tapetes de musgos (principalmente por *Sanionia uncinata*), para atuar como dreno de carbono, em locais onde a umidade do solo é elevada. Por outro lado, onde o guano é depositado, a temperatura do solo é elevada, levando a um aumento da mineralização da matéria orgânica, respiração do ecossistema, atuando como fonte de carbono para a atmosfera. A dependência espacial variou entre os locais, sendo que a deposição do guano e a cobertura vegetal governam a extensão da estrutura espacial. Os valores de dimensão fractal mostraram que há uma forte relação espacial entre o carbono orgânico e o alumínio. Os solos são caracterizados principalmente pelas altas quantidades de bases e incipiente formação de argila. Em zonas com influência ornitogênica fraca, o solo é ácido e os valores de alumínio trocável são elevados, associados a uma acidez potencial elevada. A proximidade do permafrost está reduzindo a temperatura do solo, e consequentemente o número de dias de degelo. No entanto, sob o aquecimento atual, este local tende a agir progressivamente como uma fonte de CO_2 para a atmosfera. Por outro lado, mais turfeiras podem ser formadas devido derretimento de neve/gelo, armazenamento grandes quantidades de carbono. O balanço entre o ganho e perda de CO_2 precisa ser mais pesquisado na Antártica Marítima, a fim de elucidar a dinâmica atual considerando outras áreas livres de gelo.

Abstract

THOMAZINI, André, D.Sc., Universidade Federal de Viçosa, April, 2016. **Spatial and temporal variability of CO_2 dynamic and soil attributes in Maritime Antarctica.** Adviser: Márcio Rocha Francelino. Co-advisers: Carlos Ernesto Gonçalves Reynaud Schaefer and Eduardo de Sá Mendonça.

Maritime Antarctica presents high sensitivity to climate change, especially by the alterations in air temperature, which modifies carbon dynamics and soil attributes in terrestrial ecosystems. Thus, variables related to soil (i.e. organic carbon, soil temperature and soil moisture), and vegetation distribution patterns, can represent climate change indicators. The objective of this work was to investigate the spatial and temporal relationship among carbon exchange, soil nutrient status and development in the main terrestrial ecosystems of Maritime Antarctica. The study was carried out at Keller and Coppermine Peninsula, in King George Island and Robert Island, respectively. Regular grids were installed to evaluate the spatial variability of general soil attributes and carbon exchange in lichens, mosses, lichens/mosses and bare soil sites along the ice-free areas. By using geostatistical techniques, spatial dependence was accessed through semivariogram and fractal dimension modeling. Soil was sampled at different soil layers to determine general soil attributes. Ecosystem respiration, net ecosystem exchange and gross primary production were determined by measuring CO_2 fluxes in situ with a closed automatic chamber system (LI-COR Biosciences, Lincoln, NE, USA), based on short and long-term measurements. Results indicate a high capacity of mosses carpets (especially by *Sanionia uncinata*) to act as a sink of carbon, where soil moisture is elevated. On the other hand, where guano is deposited, soil temperature is enhanced, leading to increase soil organic matter mineralization, ecosystem respiration, acting as a source of carbon to the atmosphere. Spatial

dependence strongly varied among sites, where guano deposition and vegetation coverage are reported to drive the extension of spatial structure. Fractal dimension values showed great spatial relationship between organic carbon and aluminum. Soils are mainly characterized by the high amounts of bases and weak clay formation. In zones with weak ornithogenic influence, soil is acid and values of exchangeable aluminum are high, associated with elevated potential acidity. The proximity of permafrost is leading to lower soil temperatures, reducing the number of thaw days. However, under current climate warming, this site will progressively act as a source of CO_2 to the atmosphere. On the other hand, peatlands could be formed due snow/ice melting, storing large amounts of carbon. The balance of uptake and release of CO_2 needs to be further researched in Maritime Antarctica, to elucidate the current dynamic for other different ice-free areas.

Introdução Geral

Nas últimas décadas, a elevação do dióxido de carbono (CO_2) na atmosfera, bem como seus fatores reguladores e consequências, vêm ganhando destaque na comunidade científica nacional e internacional. Atualmente, o nível de CO_2 atmosférico está acima de 403 ppm, segundo o portal de mudanças climáticas da NASA. Esses dados revelam uma constante preocupação mundial, uma vez que a série histórica indica um aumento contínuo da concentração de CO_2 atmosférico após a revolução industrial. O CO_2 é um gás importante para a vida humana, e que historicamente, regulou a existência e o surgimento de diversas espécies do reino vegetal. O carbono é o quarto elemento mais abundante do universo. No planeta Terra o carbono circula através dos oceanos, da atmosfera, da terra e do seu interior, num grande ciclo biogeoquímico. Os estoques de carbono terrestre, atmosférico e nos oceanos são estimados em 20.000, 750 e 40.000 Pg, respectivamente (Lal et al., 2004).

Os oceanos desempenham papel fundamental na ciclagem do carbono atmosférico, sendo o seu maior reservatório. Devido à grande capacidade de dissolução do CO_2, um processo contínuo de acidificação dos oceanos vem ocorrendo ao longo dos anos. Esse fato é agravado em regiões polares, uma vez que a capacidade de dissolução do CO_2 é aumentada em águas frias. Segundo o Painel Intergovernamental de Mudanças Climáticas, aproximadamente um terço do CO_2 produzido pela atividade humana ao longo de 200 anos foi absorvido até agora pelo mar, o que resultou em uma queda de 0.1 unidades no pH das águas marinhas. Isso acarretou um aumento de 26% na acidez marinha. Previsões indicam um aumento da ordem de 170%, baseado nos incrementos de CO_2 atmosférico, principalmente pela atividade humana em longo prazo (IPCC, 2007).

Na Antártica, as populações de Krill, bem como de outros organismos aquáticos, vem sendo reduzidas drasticamente nas últimas décadas, devido ao processo de acidificação do oceano. Isso reflete diretamente na cadeia alimentar, especialmente das numerosas colônias de pinguins, que se alimentam de Krill. Os pinguins por sua vez, desempenham papel fundamental na formação de solos e transferência de nutrientes (principalmente matéria orgânica e fósforo) dos oceanos para os ecossistemas terrestres (Doney et al., 2009). Com a escassez desse alimento, espera-se uma redução e/ou mudança de localização das populações de pinguins, refletindo diretamente na transferência de nutrientes dos oceanos para o solo, em longo prazo.

A transferência de carbono do solo para atmosfera via CO_2 é de suma importância no balanço de carbono, uma vez que os estoques (orgânico e inorgânico) no solo são estimados em 2500 Pg, sendo mais de 3 vezes superior ao compartimento atmosférico. Na Antártica, além de grandes quantidades de carbono estocado no permafrost e no solo devido às baixas temperaturas, o gelo e neve também armazenam CO_2 dentro de bolhas em seu interior. Esse CO_2 é liberado para a atmosfera à medida que a frente de degelo avança que por sua vez, vem ocorrendo com maior frequência nos últimos anos. Por outro lado, o CO_2 dentro da atmosfera do solo pode ser armazenado no permafrost durante o processo de "freezing". Apesar de participarem do processo de troca de CO_2, existe uma grande dificuldade de estimar essa troca pelo degelo e durante o processo de "freezing" (Thomazini et al., 2015).

As extensas comunidades vegetais de musgos e liquens, presentes nas áreas livres de gelo na Antártica, desempenham papel chave na troca de CO_2, onde este ciclo biológico está inteiramente interligado aos outros compartimentos que armazenam carbono, especialmente relacionado à transferência de nutrientes dos oceanos para as áreas livres de gelo pela fauna. Nos ecossistemas terrestres, os processos de fotossíntese e respiração são fundamentais no balanço de CO_2. Essa dinâmica é reportada como sendo altamente influenciada pela evolução do solo, temperatura e umidade, bem como da característica das comunidades vegetais, que colonizam determinadas porções da paisagem em função da disponibilidade de nutrientes e/ou umidade do solo, principalmente (Victoria et al., 2013). Entretanto, uma alta variabilidade nesses fatores ocorre na Antártica Marítima, dificultando a sua quantificação em grande escala. Essa variabilidade é aumentada, devido à grande sensibilidade dos ecossistemas terrestres às alterações ambientais.

Desde 2002, o grupo de pesquisas de ecossistemas terrestres da Antártica (TERRANTAR) do INCT da Criosfera do Departamento de Solos da Universidade Federal de Viçosa, vem desenvolvendo atividades na Antártica. No ano de 2010, os trabalhos relacionados à dinâmica de carbono, principalmente pela troca via CO_2, se intensificaram. Com isso, um grande banco de dados foi e está sendo gerado, auxiliando na modelagem e entendimento da participação dos diferentes ecossistemas terrestres da Antártica Marítima no ciclo biológico do carbono, atrelado a sua variabilidade espacial e temporal, bem como os fatores reguladores.

Diante do exposto, o presente trabalho teve como objetivo buscar entender o papel dos principais ecossistemas terrestres da Antártica Marítima na dinâmica de CO_2, bem como as variáveis relacionadas ao solo, temperatura, umidade e vegetação contribuem e influenciam, no espaço e no tempo, essa dinâmica, frente a um cenário de aquecimento global. Apesar do foco em uma escala pequena, esses dados irão contribuir para a compreensão da dinâmica atual de CO_2, bem como serem incorporados em modelos matemáticos para futuras previsões/mapeamento detalhados, em diferentes escalas de predição, amparados com as covariáveis ambientais.

Referências bibliográficas

Doney, S. C., Fabry, V. J., Feely, R. A. Kleypas, J. A. 2009. Ocean acidification: The other CO2 problem. Ann. Rev. Mar. Sci. 1, 169–192.

IPCC, 2007. Summary for policymakers, in Climate Change 2007: Impacts, Adaptation and Vulnerability, pp. 1–18, Cambridge Univ. Press, Cambridge, U. K.

Lal, R., 2004. Soil carbon sequestration to mitigate climate change. Geoderma 123, 1–22.

Thomazini, A., Mendonça, E.S., Teixeira, D.B., Almeida, I.C.C., La Scala, N., Canellas, L. P., Spokas, K.A., Milori, D.M.B.P. Turbay, C.V.G., Fernandes, R.B.A., Schaefer, C.E.G.R. 2015. CO_2 and N_2O emissions in a soil chronosequence at a glacier retreat zone in Maritime Antarctica. Sci. Total Environ. 521-522, 336–345.

Victoria, F.C., Alburqueque, M.P., Pereira, A.B., Simas, F.N.B., Spielmann, A.A., Schaefer, C.E.G.R., 2013. Characterization and mapping of plant communities at Hennequin Point. King George Island, Antarctica. Polar Res. 32, 19261.

CAPÍTULO 1

Geospatial variability of soil CO_2-C exchange in the main terrestrial ecosystems of Keller Peninsula, Maritime Antarctica

Abstract

THOMAZINI, André, D.Sc., Universidade Federal de Viçosa, April, 2016. **Geospatial variability of soil CO_2-C exchange in the main terrestrial ecosystems of Keller Peninsula, Maritime Antarctica.** Adviser: Márcio Rocha Francelino. Co-advisers: Carlos Ernesto Gonçalves Reynaud Schaefer and Eduardo de Sá Mendonça.

Soils and vegetation play an important role in the carbon exchange in maritime Antarctica but little is known on the spatial variability of carbon processes in Antarctic terrestrial environments. The objective of the current study was to investigate (i) the soil development and (ii) spatial variability of ecosystem respiration (ER), net ecosystem CO_2 exchange (NEE), gross primary production (GPP), soil temperature (ST) and soil moisture (SM) under four distinct vegetation types and a bare soil in Keller Peninsula, King George Island, Maritime Antarctica, as follows: site 1: moss-turf community; site 2: moss-carpet community; site 3: phanerogamic antarctic community; site 4: moss-carpet community (predominantly colonized by *Sanionia uncinata*); site 5: bare soil. Soils were sampled at different layers. A regular 40-point (5x8 m) grid, with a minimum separation distance of 1 m, installed at each site to quantify the spatial variability of carbon exchange, soil moisture and temperature.

Vegetation characteristics showed closer relation with soil development across the studied sites. ER reached 2.26 μmol CO_2 m^{-2} s^{-1} in site 3, where ST was higher (7.53ºC). A greater sink effect was revealed in site 4 (net uptake of 1.54 μmol CO_2 m^{-2} s^{-1}) associated with higher SM (0.32 m^3 m^{-3}). Spherical models were fitted to describe all experimental semivariograms. Results indicate that ST and SM are directly related to the spatial variability of CO_2 exchange. Heterogeneous vegetation patches showed smaller range values. Overall, poorly drained terrestrial ecosystems act as CO_2 sink. Conversely, where ER is more pronounced, they are associated with intense soil carbon mineralization. The formations of new ice-free areas, depending on the local soil drainage condition, have an important effect on CO_2 exchange. With increasing ice/snow melting, and resulting widespread waterlogging, increasing CO_2 sink in terrestrial ecosystems is expected for Maritime Antarctica.

Keywords: organic carbon, climate change, carbon exchange, polar environment, mapping, soil attributes

1. Introduction

Air temperature and precipitation rates are changing more rapidly in Maritime Antarctica than in other regions of the planet, with increasing rates in this region as a consequence of global climate changes (Convey et al., 2009; Turner et al., 2009). These transformations might cause several consequences in the terrestrial ecosystems, especially in soil formation and the spatial extent of expanding vegetation, due to their high sensitivity to climate changes (Simas et al., 2007; Mendonça et al., 2011; Convey et al., 2011; Cannone et al., 2012;

Thomazini et al., 2014; Zhu et al., 2014a; Zhu et al., 2014b). Thus, variables related to soil (i.e. organic carbon, soil temperature and soil moisture), and vegetation distribution patterns, can represent climate change indicators.

Vegetation and soil are key components to determine nutrient cycling dynamics, especially carbon exchange, in Maritime Antarctica (Cannone et al., 2012; Zhu et al., 2014a). How ecosystems act as a sink or source of carbon can be determined by the carbon cycling processes: ecosystem respiration (ER), net ecosystem CO_2 exchange (NEE) and gross primary production (GPP). These processes are highly influenced by soil temperature, soil moisture and permafrost melting (Cannone et al., 2012; Zhu et al., 2014a). Increasing soil temperature and permafrost melting may stimulate root respiration, decomposition of organic carbon and increase CO_2 emissions from soils (Mendonça et al., 2010; Carvalho et al., 2012; Thomazini et al., 2014). However, the effects of climate change on carbon exchange are still unclear in polar environments. Positive feedbacks may occur if warming accelerates soil carbon mineralization, and conversely, negative feedbacks if plant-derived carbon inputs exceed decomposition in the soil (Cannone et al., 2012).

The vegetation communities in ice-free areas of maritime Antarctica are restricted to mosses, lichens and algae. Only two vascular plants (*Colobanthus quitensis* (Kunth) Bartl. and *Deschampsia antarctica* Desv.) occur in maritime Antarctica (Convey et al., 2011). Vegetated sites might be influenced by animals' guano, forming soils named ornithogenic (Tatur et al., 1997). Ornithogenic soils are reported to be rich in carbon, nitrogen and nutrients (Simas et al., 2007; Francelino et al., 2011; Moura et al., 2012; Souza et al., 2014). However, most ice-free areas are not influenced by guano, being characterized by high stoniness and incipient soil development (Simas et al., 2007, Moura et al., 2012). In addition, some plant species are reported to occur in different types of soil according to chemical (i.e. phosphorus and carbon contents) and physical features (i.e. soil moisture), as well as landscape position (Francelino et al, 2011; Victoria et al., 2013). For these reasons, vegetation distribution is not regular, occurring mainly in patches with more than one species (Pereira and Putzke, 2013). Thus, to determine carbon exchanges and their driving factors focusing in conventional statistics may not represent adequately the spatial variability of carbon exchange in the vegetation patches. Therefore, through the application of spatial statistical analysis (geostatistical techniques), factors leading to current carbon dynamic can be properly determined, and assessed in a representative area.

Previous studies have evaluated soil CO_2 fluxes in McMurdo Dry Valleys of continental Antarctica (Parsons et al., 2004; Barrett et al., 2006; Ball et al., 2009; Cannone et al., 2012; Shanhun et al., 2012) and in the Arctic (Vogel et al., 2009; Huemmrich et al., 2010; Natali et al., 2011; Trucco et al., 2012). Recent studies of soil CO_2 fluxes have been carried out in Maritime Antarctica, focused only in carbon release (ER) (Mendonça et al., 2010; La Scala et al., 2010; Carvalho et al., 2012; Thomazini et al., 2014, Thomazini et al., 2015;). However, data of NEE, GPP (especially based on in situ measurements) and their driving factors regarding soil and vegetation characteristics are still scarce in Maritime Antarctica. Since it is becoming increasingly important to understand if terrestrial ecosystems in Antarctica act as a sink or source of C, the effects of climate change on the soil carbon exchange will depend on the synthesis of organic compounds from atmospheric CO_2 (GPP), the biotic conversion of organic carbon to CO_2 by all organisms in an ecosystem (ER) and the net carbon exchange between the ecosystem and the atmosphere (NEE).

Considering these assumptions, the objective of the present study was to investigate (i) the soil development and (ii) spatial variability of ER, NEE, GPP, ST and SM under four distinct vegetation types and a bared soil in Keller Peninsula, King George Island, Maritime Antarctica. We hypothesized that soil temperature, soil moisture as well as distinct vegetation communities affect carbon exchange in the terrestrial ecosystems of Maritime Antarctica.

2. Material and methods

2.1. Study area

The study was carried out at Keller Peninsula, Admiralty Bay, King George Island, South Shetland Islands (Fig. 1). Keller Peninsula comprises approximately 500 ha, being 4 x 2 km of length and width respectively (Francelino et al., 2011). According to the meteorological station located at Brazilian Commandant Ferraz station (62º4'33'' S, 58º23'46''W), mean air temperatures from 1986 to 2013 are reported to be +1.6 during the summer (December-March) and -5.3ºC during the winter (June-September) (INPE/CPTEC, 2015). Accordingly to the air temperatures probes installed in Keller Peninsula, mean air temperature ranged from 2.97 to 3.22ºC (08-17:00h) during the days of CO_2-C exchange measurement. Mean annual precipitation is about 400 mm. The altitude ranges from 0 to 340 m above the sea level (Francelino et al., 2011). Geology is predominantly basalt-andesites and pyritized andesite rocks. Overall, soils are not well-developed, occurring mainly Leptosols and Cryosols classes (Francelino et al., 2011). Permafrost tended to be absent in the coastal areas and sporadically appearing at mid-slope. Discontinuous permafrost at elevated sites may occur (Francelino et al., 2011).

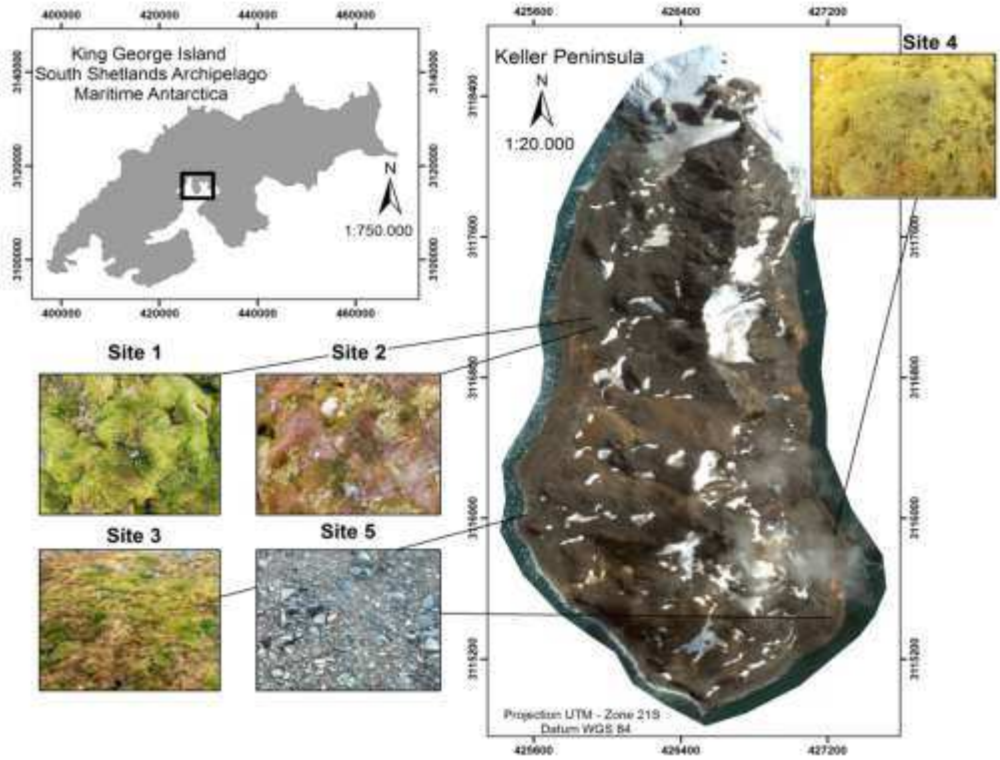

Fig. 1 Illustrative map of Keller peninsula and the terrestrial ecosystems studied. Site 1- moss-turf community; Site 2: moss-carpet community; Site 3: phanerogamic antarctic community; Site 4: moss-carpet community; Site 5: bare soil.

2.1.1 Investigated sites and grid establishment

In February 2015, five sites were selected, as illustrated in Fig. 1. These sites comprise the main vegetated terrestrial ecosystems and the most common bare soil types in Keller Peninsula. Also, these vegetated sites are characterized by occurring in small patches, typical of the Maritime Antarctica. To characterize the spatial variability, a regular 40-point 5x8 m grid with a minimum separation distance of 1 m was installed at each site to quantify ecosystem variables such as ER, NEE, GPP, ST and SM. Investigated sites consisted of the following:

Site 1 (moss-turf community): In Maritime Antarctica this vegetal community is formed by populations of mosses in which gametophytes are growing vertically from the substrate, such as *Chorisodontium aciplhyllum* (Hook. F et Wils.) Broth. This specie occurs on rock fragments where soil is absent. On the other hand, *Politrychaceae* develops under shallow soils. The plant community is called “Moss-turf community” at site 1, forming an association of *C. aciphylum* and *Sanionia uncinata* (Hedw.) Loeske. *D. antarctica* Desv. (*Poaceae*) and *C. quitensis* (Kunth) Bartl. (*Caryophyllaceae*) are represented by rare and small cushions. *Usnea antarctica* Du Rietz. grows on rock fragments. In some specific places, fruticose and crustose lichen grow under *C. aciphilum,* such as *Sphaeorophorus globosus* (Hudson) Vain and *Cornicularia aculeata* (Schreber) Acharius.

Site 2 (moss carpet community): In Maritime Antarctica this plant community is mainly characterized by populations of prostate mosses, such as *S. uncinata*, in the form of moss carpet. Generally, this specie occurs on shallow soils. Other mosses, such as *Syntrichia princeps* (De Not.) Mitt., are rare and represented by small populations. Populations of *D. antarctica* and *Polytrichastrum alpinum* (Hedw.) G.L. Smith, occurs in specific places with relatively deeper soils. *C. quitensis* is represented by rare and small cushions. Rock fragments are common under *U. antarctica*.

Site 3 (phanerogamic antarctic community): In this site, a plant community denominated ‘phanerogamic antarctic community” occurs growing on deeper soils, closer to the sea coast, normally characterized by *D. antarctica* and/or *C. quitensis*. Based on the floristic composition and vegetation dominance cover of these two species, tow formations can be described: "*D. antarctica* mosses association" and "*C. quitensis* mosses association". Site 3 is typically classified as "*Deschampsia* mosses association" since *D. antarctica* present the highest vegetation cover followed by *S. uncinata*. *C. quitensis* are represented by rare cespitose specimen distributed in the studied area, with some more significant populations on the community edge facing the sea. Other bryophytes occur, such as *S. princeps* and *P. alpinum*, the latter specie growing on ornithogenic spots.

Site 4 (moss carpet): The site is located on a marine terrace, characterized by coarse sediments and flat areas with water accumulation. The plant community is denominated "moss-carpet community", covering approximately a total area of 360x50 m, showing great variation on its floristic composition. There is no influence of guano, since there are no bird and penguin colonies. The vegetation is widely composed by *S. uncinata* on rocky soils. *C. quitensis* and *D. antarctica* are rare on deeper soils. Higher water table is related to populations of *Bryum orbiculatifolium* Card. et Broth., with occasional dispersed *S. princeps* and *Warstorfia sarmentosa* (Wahlenb.) Hedenäs.

Site 5 (bare soil): There is no vegetation cover at this site, with a stony soil, and no influence of marine animals or birds. The parent material is composed of basalt and andesite located at a scree slope.

2.2 Soil sampling

Soil was sampled in February 2015 to determine general soil properties, total soil organic carbon and total nitrogen at each investigated site. The soil sampling scheme was systematic using a sampling area divided into three experimental plots of 4 m^2 each. In each plot, three soil samples were taken at different layers (see Tables 1 and 2) according to the soil development. The soil samples were air dried, grounded and sieved through a 2-mm sieve to remove larger pieces of root material and the stony fraction. All soil samples were analyzed in the soil laboratory at the Universidade Federal de Viçosa, Minas Gerais, Brazil.

2.3. Soil general properties and total soil organic carbon

The pH was determined on a 1:2.5 soil: deionized water ratio; the potential acidity (H + Al) was extracted with $Ca(OAc)_2$ 0.5 mol L^{-1} buffered to pH 7.0, and quantified by titration with NaOH 0.0606 mol L^{-1}. Exchangeable Ca^{2+}, Mg^{2+} and Al^{3+} were extracted with 1 mol L^{-1} KCl and Na^+ and K^+ were extracted with Melich-1 (Embrapa, 1997). The element contents in the extracts were determined by atomic absorption (Ca^{2+}, Mg^{2+} and Al^{3+}), flame emission (Na^+ and K^+) and photocolorimetry (P). The effective cation exchange capacity (CEC_E) was calculated by sum of cations (Ca^{2+}, Mg^{2+}, Na^+, K^+ and Al^{3+}) and total cation exchange capacity (CTC_T) was estimated by the sum of bases and potential acidity. The soil texture analysis was performed by the pipette method (Embrapa, 1997). Total soil organic carbon was determined according to Walkley–Black method - wet oxidation with $K_2Cr_2O_7$ 0.167 mol L^{-1} in the presence of sulfuric acid with external heating (Yeomans and Bremner, 1988).

2.4 Soil CO_2-C exchange

Soil CO_2-C exchange measurements were carried out in February 2015, when positive air temperatures are registered and snow cover is reduced, representing the typical summer time carbon exchange of Maritime Antarctica. Soil CO_2-C exchange (μmol CO_2 m^{-2} s^{-1}) were measured to estimate ER, NEE, and GPP at the 40 grid points in the studied sites. A closed automatic chamber system was used in the measurements. CO_2-C exchange were measured using a CO_2 exchange system (LI-COR Biosciences, Lincoln, NE, USA) containing an infra-red gas analyzer (model LI-8100A), a multiplexer system (model LI-8150), one clear chamber (model LI-8100-104C), one opaque chamber (model LI-8100-104) and a laptop to collect data. This system operated at the same time during measurements and quantifies concentration through optical absorption spectroscopy. The system was calibrated at the factory using precision gases (CO_2 gas standards) at controlled temperatures.

PVC soil collars (20 cm diameter) were inserted into the soil prior measurements in each of the grid points, reaching a standard depth of 3 cm. Measurements occurred over the course of one day during daylight hours at each site. Soil CO_2-C emissions at each grid point were based on a single measurements over 1.5 min, during which time measurements were made of CO_2 concentrations inside the chamber at 3 s intervals. Measurements were carried out within one week, where climate conditions were equal in all of measurements performed at each site. A typical sequence included consecutive measurements under dark measurement (opaque chamber) followed by ambient light (clear chamber) at each grid point. At each site, soil CO_2-C emissions was measured using opaque and clear chamber to determine ER and NEE, respectively. Normally, ER values are always positive representing CO_2 release from the terrestrial ecosystems to the atmosphere. NEE is the net carbon gain or loss measured as CO_2 by a terrestrial ecosystem. This exchange is the balance of ecosystem carbon uptake by primary producers (GPP) and ecosystem respiration losses (ER) (autotrophic plus heterotrophic). NEE values may be both positive and negative. Negative values of NEE represent a carbon sink and positive values represent a carbon source. When NEE=0, the ecosystem is equilibrated. GPP was indirectly estimated as the difference between NEE and ER. We used the convention that positive values indicate net carbon release and negative values indicate carbon uptake by the terrestrial ecosystem studied for ER, NEE and GPP.

2.5 Soil temperature and soil moisture

ST and SM measurements were carried out at the same time of soil CO_2-C exchange at each grid point. The monitoring systems consist of soil temperature probes (Campbell L107E thermocouple, accuracy of ± 0.2°C) and soil moisture probes (CS656 water content reflectometer, accuracy of ± 2.5%). These probes were placed at 0-5 cm depths were PVC soil collar was inserted to determine the CO_2-C exchange. All probes were connected to a Campbell Scientific CR 1000 data logger, recording data at every 1 s interval during 1.5 min.

2.6 Spatial variability

The spatial variability was analyzed by descriptive statistics (mean, median, minimum, maximum, standard error of mean, coefficient of variation, skewness and kurtosis) and producing an experimental semivariogram to verify the occurrence of spatial dependence, based on the assumption of intrinsic stationary (Webster and Oliver, 1990). Isotropic and non-isotropic semivariograms were considered in this study. The semivariance estimation was determined by equation 1:

$$\hat{\gamma}(\mathrm{h}) = \frac{1}{2N(\mathrm{h})}\sum_{i=1}^{N(h)}[z(\mathrm{x}_i) - z(\mathrm{x}_i + \mathrm{h})]^2 \qquad (1)$$

where $\hat{\gamma}(\boldsymbol{h})$ is the semivariance at a separation distance of **h**; *N(**h**)* is the number of pairs separated by ***h***; $z(\boldsymbol{x}_i)$ is the value of variable *Z* at point ***xi*** and Z(**x**i + **h**) is the value of variable Z at point ***x***i + ***h***. The semivariogram graph can have a systematic behavior, which can be described by theoretical models (i.e. spherical, gaussian and exponential) (Isaaks and Srivastava, 1989). The theoretical model that best represented the relationship between experimental semivariance and distance ***h*** was adjusted by the following theoretical models (equations 2):

$$\begin{cases} Gaussian: \hat{\gamma}(\mathrm{h}) = C_0 + C_1\{1 - \exp[-3(h/a)^2]\}; 0 < h < d \\ Exponential: \hat{\gamma}(\mathrm{h}) = C_0 + C_1\{1 - \exp[-3(h/a)]\}; h > 0 \\ Spherical: \hat{\gamma}(\mathrm{h}) = C_0 + C_1\left[\frac{3}{2}\left(\frac{\mathrm{h}}{a}\right) - \frac{1}{2}\left(\frac{\mathrm{h}}{a}\right)^3\right]; if\ 0 < \mathrm{h} < a; \hat{\gamma}(\mathrm{h}) = C_0 + C_1; if\ \mathrm{h} \geq a \end{cases} \qquad (2)$$

where *d* is the maximum distance over which the semivariogram is defined; *a* is the range distance; C_0 is the nugget effect, $C_0 + C_1$ is the sill (Isaaks and Srivastava, 1989). The semivariance value increases with separation distance of the points (***h*** distance) until a distance that the sill ($C_0 + C_1$) remains constant. The nugget effect (C_0) is the value where the adjusted theoretical model crosses the y axis. The range distance (a) is the limit of the spatial dependence between points. The presence of a trend violates the intrinsic hypothesis. In this case, the semivariogram does not have a stable sill (Vieira et al., 2010). The trend removal technique was used as described in Vieira et al. (2010). The trend removal was done by fitting a trend surface to the original values by minimum least squares and then subtracting the value of the trend surface function from the original values. This constructed a new residual variable which was used to generate the experimental semivariogram having a sill (Vieira et al., 2010).

Cross-validation technique was considered for estimating the performance of the theoretical model chosen. The best model for fitting the experimental variograms was based on the coefficient of determination (R^2), root mean square error (RMSE) and residual sum of squares (RSS). The spatial dependence index (SDI) was determined by the ratio $C_1/(C_0 + C_1)$ classified by the following intervals: strong spatial dependence for SDI < 25%, moderate for 25% < SDI < 75% and low for SDI > 75% (Cambardella et al., 1994). The best adjust of the selected models were based on the smallest RMSE and RSS; and the highest R^2 (Isaaks and Srivastava, 1989). After having generated all the semivariogram models and the spatial dependence confirmed, values for each variable were estimated for non-sampled areas and maps of spatial distribution were generated using ordinary kriging interpolation method.

2.7 Data analysis

Data of general soil properties (n=3, each site and layer) and ER, NEE, GPP, ST and SM (n=40, each site) were interpreted in terms of general trends (mean and standard error of mean). Principal component analysis (PCA) was performed to explore general trends and to evaluate if terrestrial ecosystems studied could be separated according to their current dynamic of ER, NEE, GPP, ST and SM. Correlations of the soil CO_2 exchange components (ER, NEE and GPP) with ST and SM were tested using Pearson correlation analysis at 1% of significant level to find possible relationship between them. Descriptive statistical analyses and PCA were performed using the XLStat (XLStat, NY, USA, 2014) program. Spatial variability models were derived using GS+ software (Gamma Design Software, LLC, Plainwell, MI, USA, 1998) and kriging maps obtained with Surfer software (Golden Software Inc, Golden, CO, USA, 1995).

3. Results

3.1 Soil general properties and total soil organic carbon

Soil general properties were highly variable at the studied sites (Tables 1 and 2). As indicated in the description of the studied sites, site 1 does not have soil developed under the moss turf community, so that no data of soil attributes are available at this site. Most of the studied sites showed incipient soil development with depth (up to 20 cm). After 20 cm of depth, soil is rich in coarse materials (> 2 mm). However, higher soil development in depth was observed at site 3 (down to 30 cm). Overall, the soil is characterized by an abundance of coarse and fine sand with little clay contents in all studied sites. Soils are rich in phosphorus, exchangeable bases and eutrophic in all studied sites. In general, total soil organic carbon decreased with depth. Total soil organic carbon ranged from 7.71 to 79.06 g kg^{-1} in the site 5 and 4 at 0-5 cm depth, respectively. In general, total soil organic carbon among different sites followed the order: site 4>site 3> site 2> site 5.

Table 1. Soil chemical properties and total soil organic carbon of all the studied sites in Keller Peninsula

	pH	P	K	Na	Ca	Mg	Al	H+Al	BS	CEC_E	CEC_T	S	ISNa	C
		---------mg kg^{-1}-------			--------------------------cmol$_c$ kg^{-1}--------------------------							------%-----		g kg^{-1}
Layer (cm)							**Site 2**							
0-5	6.19	253.40	48.00	151.50	6.11	2.56	0.00	3.10	9.45	9.45	12.55	75.30	5.25	10.79
5-20	6.50	365.30	61.00	125.50	8.14	2.50	0.00	2.50	11.34	11.34	13.84	81.90	3.94	6.96
							Site 3							
0-5	5.68	244.30	61.00	164.50	10.87	3.17	0.00	4.30	14.91	14.91	19.21	77.60	3.72	28.94
5-20	5.94	265.70	46.00	145.50	11.02	3.33	0.00	3.60	15.10	15.10	18.70	80.70	3.38	21.23
20-30	6.66	319.30	46.00	136.50	9.96	3.17	0.00	3.80	13.84	13.84	17.64	78.50	3.36	7.71
							Site 4							
0-5	5.75	132.50	96.00	255.50	12.23	3.58	0.00	4.50	17.14	17.14	21.64	79.20	5.13	79.06
5-20	6.58	177.80	80.00	225.60	5.15	1.37	0.00	2.30	7.71	7.71	10.01	77.00	9.80	6.96
							Site 5							
0-5	6.59	236.70	96.00	176.40	10.03	6.66	0.00	2.30	17.70	17.70	20.00	88.50	3.83	7.71
5-20	6.58	347.00	106.00	179.40	14.66	5.91	0.00	1.20	21.62	21.62	22.82	94.70	3.42	5.80

pH: active acidity (H_2O); P: phosphorus; K: potassium; Na: sodium; Ca: calcium; Mg: magnesium; Al: aluminium; H+Al: potential acidity; BS: bases sum; CEC_E: effective cation exchange capacity; CEC_T: total cation exchange capacity; S: saturation of bases; ISNa: saturation of sodium; C: total organic carbon.

Table 2. Soil texture of the studied sites in Keller Peninsula

	Coarse sand	Fine sand	Silt	Clay	Class
	----------------------g kg^{-1}----------------------				
Layer (cm)			**Site 2**		
0-5	326.00	218.00	301.00	155.00	Sand Loam
5-20	277.00	168.00	346.00	209.00	Clay Loam
			Site 3		
0-5	538.00	176.00	142.00	144.00	Sand Loam
5-20	456.00	243.00	152.00	148.00	Sand Loam
20-30	572.00	187.00	94.00	147.00	Sand Loam
			Site 4		
0-5	822.00	16.00	24.00	137.00	Sand Loam
5-20	473.00	400.00	45.00	83.00	Sand
			Site 5		
0-5	279.00	111.00	351.00	259.00	Clay Loam
5-20	226.00	108.00	591.00	75.00	Silt Loam

Coarse sand (0.2-<2 mm), Fine sand (0.05-<0.2 mm), Silt (0.002-<0.05 mm), Clay (<0.002 mm).

3.2 Soil CO_2-C exchange

Descriptive statistics of ER, NEE, GPP, ST and SM in the studied sites are shown in Table 3. ER ranged from 0.08 to 2.26 µmol CO_2 m^{-2} s^{-1} in the studied sites. Mean ER was observed to be higher in site 3 (2.26 µmol CO_2 m^{-2} s^{-1}) compared with the others sites. This result is 9.41 times higher than the bare soil (site 5). The lowest mean ER was observed in site 4 (0.08 µmol CO_2 m^{-2} s^{-1}). Overall, mean ER tended to follow the order: site 3 > site 2 > site 1 > site 5 > site 4. Site 4 tended to present the highest CO_2 sink strength (net uptake of 1.54 µmol CO_2 m^{-2} s^{-1}) whereas the highest CO_2 source strength occurred in site 3 (net release of 0.47 µmol CO_2 m^{-2} s^{-1}) through NEE measurements. A small contribution to the CO_2 sink effect was observed in site 2 (net uptake of 0.08 µmol CO_2 m^{-2} s^{-1}). Site 3 showed relatively higher capacity of carbon sequestration from the atmosphere through GPP measurements (uptake of 1.79 µmol CO_2 m^{-2} s^{-1}). In site 5, where vegetation cover does not occur, the mean GPP is low (uptake of 0.12 µmol CO_2 m^{-2} s^{-1}). Overall, mean GPP among the different terrestrial ecosystems followed the order of uptake: site 3 > site 2 > site 1 > site 4 > site 5. Two principal components (PC1 and PC2) explained 42.20 and 33.23% of the variance in the total data set, respectively (Table 4). The studied sites were separated in the bi-plot diagram through PCA (Fig. 2). Well-separated sites included sites 4 and 5. NEE was highly weighted explaining 38.57% of the total variance in the PC1. In the PC2, 45.47% of the total variance was explained by GPP.

Table 3. Descriptive statistics of ecosystem respiration (ER), net ecosystem CO_2 exchange (NEE), gross primary production (GPP), soil temperature (ST) and soil moisture (SM) for all the studied sites in Keller Peninsula

	Mean	**Median**	**Min**	**Max**	**SE**	**CV**	**Skew**	**Kurt**
			ER (µmol CO_2 $m^{-2}s^{-1}$)					
Site 1	1.21	1.24	0.03	2.51	0.10	0.49	0.07	-0.47
Site 2	1.63	1.54	0.38	4.84	0.12	0.47	1.79	5.67
Site 3	2.26	2.22	1.04	3.85	0.09	0.26	0.28	0.23
Site 4	0.08	0.08	-0.21	1.00	0.07	0.52	-0.15	0.41
Site 5	0.24	0.14	0.03	1.23	0.04	1.10	2.38	5.24
			NEE (µmol CO_2 $m^{-2}s^{-1}$)					
Site 1	-0.32	-0.53	-1.95	1.55	0.14	2.65	0.37	-0.34
Site 2	-0.08	-0.07	-2.51	1.53	0.10	8.33	-1.06	3.96
Site 3	0.47	0.59	-3.20	2.37	0.17	2.27	-1.18	2.21
Site 4	-1.54	-1.58	-3.00	0.11	0.13	0.51	0.36	-0.65
Site 5	0.12	0.12	-0.10	0.45	0.01	0.67	1.02	5.98
			GPP (µmol CO_2 $m^{-2}s^{-1}$)					
Site 1	-1.53	-1.49	-2.84	-0.46	0.09	0.37	-0.03	-0.22
Site 2	-1.70	-1.50	-5.48	-0.41	0.14	0.53	-1.92	5.57
Site 3	-1.79	-1.57	-5.06	-0.15	0.17	0.60	-1.24	1.25
Site 4	-1.62	-1.69	-2.82	-0.42	0.10	0.37	0.16	-0.61
Site 5	-0.12	-0.02	-1.33	0.25	0.05	2.44	-2.52	6.98
			ST (ºC)					
Site 1	6.61	6.67	4.52	8.57	0.17	0.16	-0.23	-0.62
Site 2	5.99	6.30	3.95	7.43	0.15	0.15	-0.62	-0.77
Site 3	7.53	7.47	5.32	9.38	0.21	0.17	0.06	-1.51
Site 4	3.10	2.78	1.18	6.13	0.20	0.40	0.70	-0.30
Site 5	5.99	6.13	1.23	7.57	0.20	0.20	-1.74	4.35
			SM (m^3 m^{-3})					
Site 1	0.25	0.28	0.06	0.39	0.01	0.31	-0.56	-0.11
Site 2	0.17	0.18	0.01	0.30	0.01	0.46	-0.29	-0.88
Site 3	0.22	0.25	0.04	0.40	0.01	0.33	-0.23	-0.34
Site 4	0.32	0.32	0.07	0.46	0.01	0.29	-0.60	-0.27
Site 5	0.12	0.12	0.03	0.23	0.01	0.41	0.30	-0.61

n = 40; SE-standard error of mean; Min-minimum; Max-maximum; CV-coefficient of variation; Skew-skewness; Kurt-kurtosis. Negative values represent net uptake, Positive values represent net release.

Table 4. Results of the principal component analysis for the first two principal components (PC) for all the studied sites in Keller Peninsula

Principal components	PC1	PC2
Eigenvalue	2.10	1.66
Variability (%)	42.20	33.23
Cumulative (%)	42.20	75.44
% explained by each variable:		
ER	15.78	35.08
NEE	**38.57**	0.36
GPP	6.17	**45.47**
ST	25.68	4.72
SM	13.78	14.34

Boldface variables are considered highly weighted. Ecosystem respiration (ER), net ecosystem CO_2 exchange (NEE), gross primary production (GPP), soil temperature (ST) and soil moisture (SM).

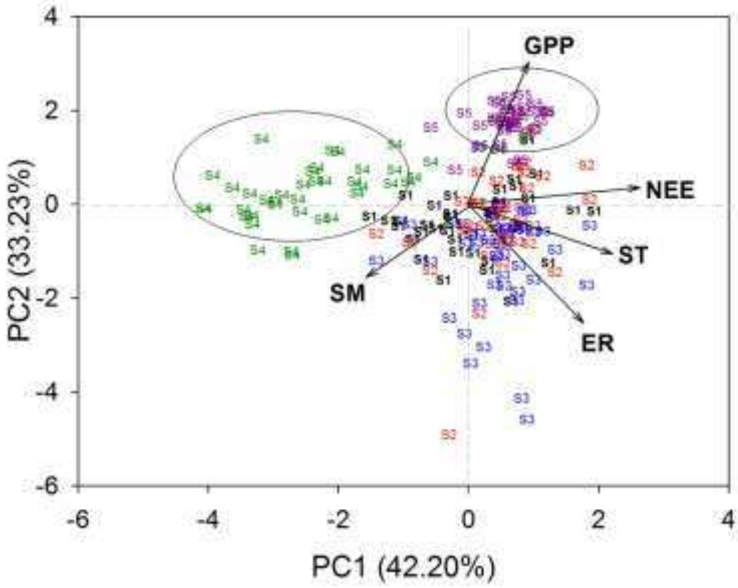

Fig. 2 Bi-plot diagram from the PCA of ecosystem respiration (ER), net ecosystem CO2 exchange (NEE), gross primary production (GPP), soil temperature (ST) and soil moisture (SM) for all the studied sites in Keller Peninsula. S1 (black) = all sampling points in the site 1; S2 (red) = all sampling points in the site 2; S3 (blue) = all sampling points in the site 3; S4 (green) = all sampling points in the site 5; S5 (purple) = all sampling points in the site 5.

3.3 Soil temperature and soil moisture

Mean ST and SM values in the studied sites are shown in Table 3. Mean ST appeared to be higher in site 3 and lower in site 4, compared with the other sites. Mean SM seemed to be higher in site 4, which is located in a marine terrace with ice-melting influence. The lowest mean SM was observed to occur on bare soil (site 5). Overall, when all data of soil CO_2 exchange, temperature and moisture were combined, Pearson correlation coefficients appeared to be low (Table 5). Despite this general trend, ST appeared to be weakly correlated (r=-0.26, p<0.01, Pearson correlation coefficient) with SM. There was a significant positive correlation (p<0.01, Pearson correlation coefficient) between ST with ER and NEE. SM was negatively correlated (p<0.01, Pearson correlation coefficient) with GPP.

Table 5. Pearson correlations among soil CO_2 exchange, soil temperature and soil moisture for all the studied sites in Keller Peninsula (n=200)

Variables	ER	NEE	GPP	ST	SM
ER	**1.00**				
p-value	**0**				
NEE	**0.54**	**1.00**			
p-value	**< 0.0001**	**0**			
GPP	**-0.46**	**0.50**	**1.00**		
p-value	**< 0.0001**	**< 0.0001**	**0**		
ST	**0.46**	**0.45**	0.00	**1.00**	
p-value	**< 0.0001**	**< 0.0001**	0.94	**0**	
SM	0.04	**-0.32**	**-0.39**	**-0.26**	**1.00**
p-value	0.53	**< 0.0001**	**< 0.0001**	**0.0002**	**0**

The bolded values are significant correlation coefficients. Ecosystem respiration (ER), net ecosystem CO_2 exchange (NEE), gross primary production (GPP), soil temperature (ST) and soil moisture (SM).

3.4 Spatial variability

Spatial variability patterns were best established using isotropic models in the studied sites (Table 6). Kriging maps are presented in Fig. 3. In the current study, spherical models fitted to all experimental semivariograms. Range values seemed to be higher in site 4 for all studied variables, excepted for GPP, which tend to be higher in site 2 (4.91 m). Lower range values appeared to occur in site 3 for ER and NEE (1.91 and 2.02 m, respectively). The local scale of the spatial variability (expressed by C_0 parameter) and the spatial variability structure (expressed by the C_1 parameter) was represented by the SDI, showing that there are no low SDI (>75%) in all the studied sites for all variables measured. In all studied sites, strong SDI (<25%) was observed to occur for ST, while moderate SDI (25% < SDI < 75%) tended to occur for SM. Strong SDI (<25%) were observed to occur in the sites 1, 3 and 5 for ER; sites 1, 2 and 4 for NEE, and sites 4 and 5 for GPP.

Table 6. Model type and parameters of the semivariograms fitted to the ecosystem respiration (ER), net ecosystem CO_2 exchange (NEE), gross primary production (GPP), soil temperature (ST) and soil moisture (SM) for all the studied sites in Keller Peninsula

		Model	C_0	$C_0 + C_1$	Range (m)	a	b	R^2	SDI (%)	RMSE	RSS
Site 1	ER	Sph.	0.007	0.337	2.57	0.04	0.954	0.78	2.08	0.442	3.63E-03
	NEE	Sph.	0.158	0.687	2.47	-0.04	0.991	0.99	23.00	0.659	2.25E-04
	GPP	Sph.	0.130	0.351	3.25	-0.67	0.574	0.69	37.04	0.548	5.00E-03
	ST	Sph.	0.062	0.676	2.55	0.03	0.771	0.62	9.17	0.751	0.0272
	SM	Sph.	0.0007	0.0025	2.33	0.001	0.916	0.71	28.00	0.046	1.28E-07
Site 2	ER	Sph.	0.115	0.341	2.26	0.14	0.889	0.47	33.72	0.499	5.41E-03
	NEE	Sph.	0.062	0.446	2.41	-0.08	0.453	0.80	13.90	0.648	4.72E-03
	GPP	Sph.	0.178	0.377	4.91	-0.12	0.927	0.91	47.21	0.520	1.55E-03
	ST	Sph.	0.066	0.407	2.14	-0.05	0.243	0.95	16.22	0.646	1.63E-04
	SM	Sph.	0.002	0.0045	2.95	0.001	0.419	0.84	44.44	0.068	2.86E-07
Site 3	ER	Sph.	0.080	0.353	1.91	-0.17	1.063	0.55	22.66	0.538	4.21E-03
	NEE	Sph.	0.160	0.499	2.02	-0.07	1.064	0.70	32.06	0.633	3.57E-03
	GPP	Sph.	0.200	0.471	2.59	-0.20	0.857	0.60	42.46	0.616	9.51E-03
	ST	Sph.	0.022	0.253	2.28	-0.01	0.559	0.96	8.70	0.463	1.99E-04
	SM	Sph.	0.002	0.005	3.61	0.05	0.773	0.93	40.00	0.065	2.32E-07
Site 4	ER	Sph.	0.112	0.186	3.53	0	0.851	0.77	60.22	0.371	3.94E-04
	NEE	Sph.	0.001	0.871	4.85	-0.17	0.886	0.96	0.11	0.516	2.33E-02
	GPP	Sph.	0.049	0.423	4.13	-0.20	0.87	0.89	11.58	0.453	5.69E-03
	ST	Sph.	0.001	1.518	3.50	-0.27	1.099	0.97	0.07	0.599	2.34E-02
	SM	Sph.	0.003	0.006	4.43	0.11	0.654	0.85	50.00	0.076	6.19E-07
Site 5	ER	Sph.	0.008	0.050	2.26	0.04	0.856	0.97	16.00	0.214	6.44E-06
	NEE	Sph.	0.001	0.0028	4.69	0	0.955	0.87	35.71	0.045	2.17E-07
	GPP	Sph.	0.0001	0.067	2.58	-0.05	0.608	0.90	0.15	0.258	8.34E-05
	ST	Sph.	0.070	0.424	3.36	0	0.923	0.83	16.51	0.501	6.70E-03
	SM	Sph.	0.0014	0.0025	3.86	0.06	0.463	0.86	56.00	0.049	1.02E-07

C_0: nugget effect; $C_0 + C_1$: sill; SDI: spatial dependence index ((C_0/($C_0 + C_1$)); RMSE: root mean square error; RSS: residual sum of squares

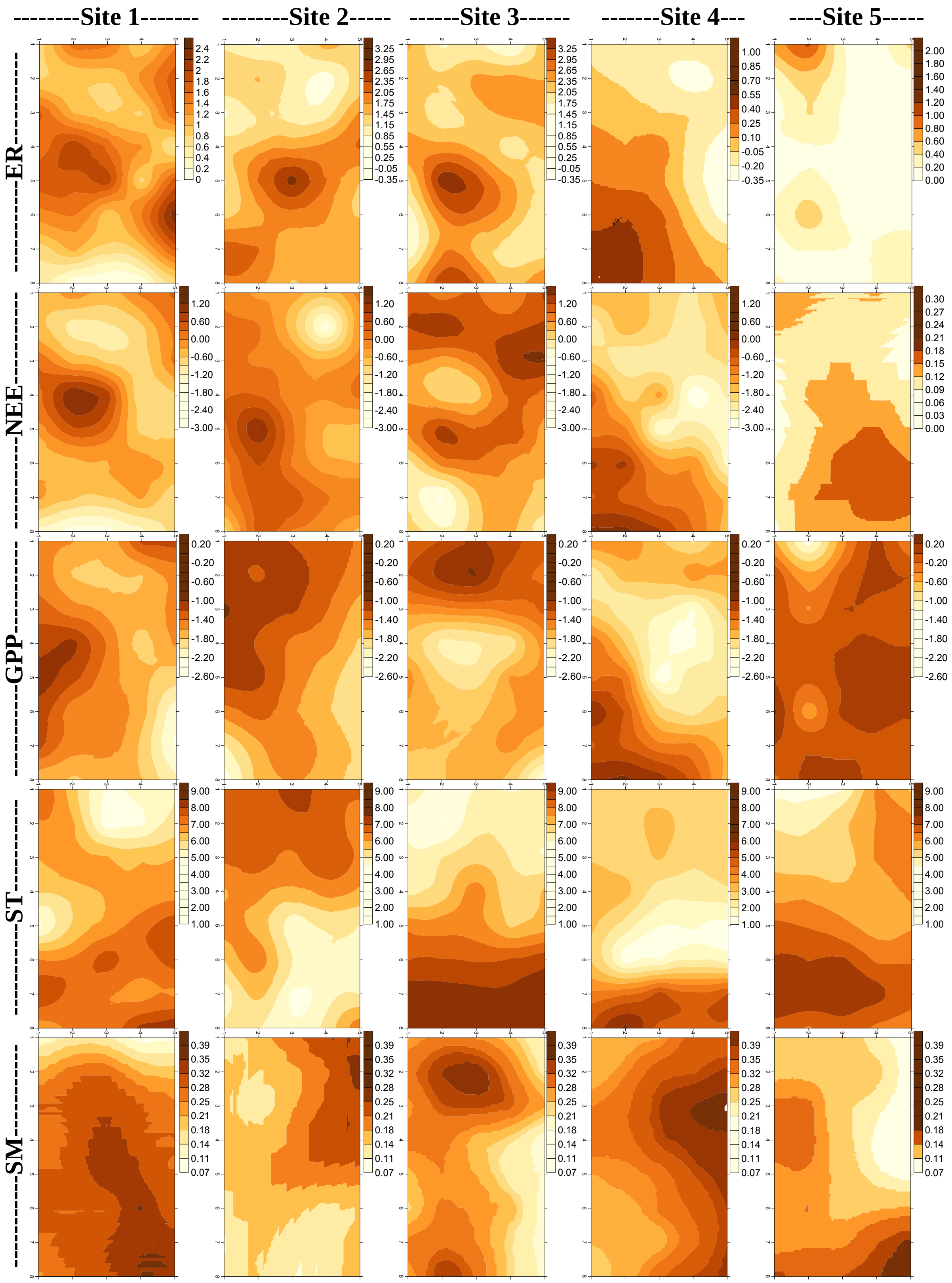

Fig. 3. Kriging maps of ecosystem respiration (ER), net ecosystem CO_2 exchange (NEE), gross primary production (GPP), soil temperature (ST) and soil moisture (SM) for all the studied sites in Keller Peninsula.

4. Discussion

Results suggest that different degrees of soil development are related to the characteristics of the different vegetation patches in the studied sites. When phanerogamic antarctic community occurs, soil development is enhanced, consistent with previous observations (Michel et al., 2006; Simas et al., 2007). On the other hand, in poorly drained soils (site 4), there is remarkable organic carbon storage at the soil surface (0-5 cm depth). These areas are preferentially covered by mosses (i.e. *S. uncinata*), highly responsible to greater soil organic carbon sink in terrestrial ecosystems of Maritime Antarctica. Zhu et al. (2014b) reported that total organic carbon contents ranged from 18.18 to 36.87% and from 1.08 to 1.25% in hydromorphic tundra and well-drained tundra soils, respectively. Higher carbon storage in poorly-drained soils is associated with peat formation (Zhu et al., 2014b).

CO_2-C exchange was strongly related to soil development and vegetation characteristics, directly affected by nutrient availability and organic biomass production. Results show that as the new ice-free soil becomes vegetated, ER tends to increase. This follow the order of vegetation colonization reported in the current work (site 4<site 1<site 2<site 3, Table 3), and can be explained by the combined contribution of plants (including roots) respiration processes (Thomazini et al., 2015).

La Scala et al. (2010) and Thomazini et al. (2015) reported that the presence of vegetation increased ER up to 514% and 440%, respectively. This difference is equivalent of 495.79 and 133.05 mg CO_2 m^{-2} h^{-1}, respectively. In this work, the difference (between sites 3 and 4) reach 345.31 mg CO_2 m^{-2} h^{-1} emitted, due to the contribution of vegetation cover. Low ER reported in site 4 (moss-turf community composed by *S. uncinata*) is explained by the higher SM (Table 3), which creates a hydromorphic environment that reduces the oxygen availability, ST and, consequently, mineralization processes of soil organic matter (Zhu et al., 2014b; Thomazini et al., 2014). This can be evidenced in the bi-plot diagram, where SM is more related to site 4 (Fig. 2). Mendonça et al. (2010) and La Scala et al. (2010) reported, at the same site, that mean ER was 1.06 and 1.36 μmol CO_2 m^{-2} s^{-1} or the equivalent of 167.90 and 215.42 mg CO_2 $m^{-2}h^{-1}$ in March 2009, respectively. This result is 13.25 and 17.00 times higher than values reported in this work, respectively. This is equivalent to a reduction of 0.98 and 1.28 μmol CO_2 m^{-2} s^{-1} or 155.23 and 202.75 mg CO_2 m^{-2} h^{-1} emitted to the atmosphere during this time, respectively. However, ST was 2.35 times higher in March 2009 (Mendonça et al., 2010). This result indicates that this site is colder and more saturated with water at the present, decreasing CO_2 emissions to the atmosphere, further accumulating greater organic carbon, previously discussed. Further research, especially focused in long-term measurements, is needed to confirm this statement.

In soils under phanerogamic antarctic community, elevated ER is observed (Table 3). It represents the most important carbon and nutrient reservoir in Maritime Antarctica, due to plant residue deposition, associated with greater diversity of soil microorganism, leading to increased autotrophic (plant and root) and heterotrophic components (microbial activity) of ecosystem respiration (Simas et al., 2007; Zhu et al., 2014a). In some cases, these sites are influenced by guano, which also leads to increasing ER (Zhu et al., 2014a). Possibly, the bird guano influence (both in soil respiration and soil development) contributed to an ER 1.38 times higher in site 3 compared with site 2, where similar soil and vegetation exist. This is an equivalent of 99.79 mg CO_2 $m^{-2}h^{-1}$

increase, comparing site 3 with site 2 (Table 3). This is in accordance with Zhu et al. (2014a), who reported significantly higher ER values at faunal-affected soils, compared to tundra under no faunal inputs. In addition, elevated ST drive and increase ER in Maritime Antarctica, consistent with the literature (Zhu et al., 2014a; Thomazini et al., 2015). Corroborating these statements, the bi-plot diagram from PCA, showed ST and ER more closely related in site 3 (Fig. 2), where higher ST was registered.

Results indicate a net gain of CO_2 at sites 1, 2 and 4, whereas a net loss at sites 3 and 5 was recorded (NEE, Table 3). These results suggest that the absence of vegetation cover (site 5) and advanced pedogenesis associated with intense carbon mineralization processes and ST (site 3) significantly decreased Antarctic tundra CO_2 sink strength. Thus, only at the phanerogamic antarctic community, a CO_2 source will be observed under vegetated conditions, due to high ER. In this work, a release of 0.44 μmol CO_2 m^{-2} s^{-1}, or the equivalent of 69.69 mg CO_2 $m^{-2}h^{-1}$, was recorded for phanerogamic antarctic community. Greater CO_2 sink strength was observed to occur at site 4, explained mainly by the moist and colder environment, which affects vegetation distribution, functioning and controls carbon mineralization processes that influence ER (as indicated by the low rates in this work). Also, CO_2 sink strength is apparently increasing over the years, as ER is decreasing at this site (Mendonça et al., 2010).

Zhu et al. (2014b) reported that hydromorphic tundra experienced a large net gain of CO_2 (uptake of 113.2 mg CO_2 $m^{-2}h^{-1}$) than well-drained area (uptake of 70.3 mg CO_2 $m^{-2}h^{-1}$). In this work, in similar hydromorphic tundra, a higher net uptake of 243.93 mg CO_2 $m^{-2}h^{-1}$ was reported, but a smaller CO_2 sink strength in a similar upland tundra occurred. The differences in the CO_2 sink strength are mainly attributed to the high variability of plant species, soil characteristics and seasonality. In continental Antarctica, Cannone et al. (2012) showed that most of the vegetation patches presented positive NEE values which are associated to elevated ER rates, possibly due to a drier environment compared to Maritime Antarctica. Also, these authors demonstrated that only *S. uncinata* patches presented GPP and NEE values close to zero. NEE is significantly positive and negatively correlated to ST and SM (Table 5), indicating that changes in ST and SM will clearly affect CO_2 cycle in Maritime Antarctica. Relationship between NEE with ST and SM is also demonstrated by Cannone et al. (2012), Zhu et al. (2014a) and Zhu et al., (2014b), however, the CO_2 sink strength needs to be further investigated in a future global warming scenario with alterations of ST and SM regimes and formation of new ice-free areas in the Maritime Antarctica.

Under vegetated conditions, slightly elevated GPP (up to 283.53 mg CO_2 m^{-2} h^{-1}) was observed, compared with bare soil (up to 19.00 mg CO_2 $m^{-2}h^{-1}$). The occurrence of higher plants and a great nutrient supply caused significant increases for GPP at site 3. Also, GPP showed a consistent trend to the highest means ER (Table 3). Despite their relatively small surface distribution, the productivity of the phanerogamic antarctic communities, especially those guano-affected, are higher than areas not affected by guano, due to a greater offer of nutrients (Zhu et al., 2014a). In fact, terrestrial productivity of Antarctic ecosystems is strongly limited by nutrient (i.e. nitrogen, phosphorus). Despite low rates of guano deposition, the photosynthesis and productivity rates will be more intensified in areas such as site 3, where a relatively larger surface is covered with vegetation (especially by *D. antarctica* and/or *C. quitensis*) and nutrients supply are originated from guano deposition from animals, and nutrient cycling by plants. Thus, these exert a great control in both ER and GPP in the terrestrial ecosystems of Maritime Antarctica.

In the current work, spatial changes in ST and SM appeared to be more related to the spatial variability of CO_2 exchange than the relationship reported by Mendonça et al. (2010) and La Scala et al. (2010) in Keller Peninsula. This is indicated by the similar range and models found in this work. These authors reported that spatial variability of ER was more related to the vegetation distribution than ST and SM. Despite the measurements carried out by these previous studies a few years ago, the differences are mainly instrumental (types of chamber/probes) and the lower number of investigated sites across the Peninsula. Our new results represent an adequate picture of vegetated and non-vegetated sites of Keller Peninsula. Also, we measured NEE and estimated GPP that may better explain this relationship.

Results show that isotropic models had the best performance to describe the spatial variability. It shows that there is no potential variability in different directions within the vegetation patches and bare soil according to the grid size utilized. This pattern was also demonstrated by Mendonça et al. (2010), La Scala et al. (2010) and Thomazini et al. (2014). These authors also demonstrated that most of the spatial variability models for ER and ST in Maritime Antarctica have been described by spherical and gaussian models. This indicates a high continuity of the studied variables, having no large changes at local scale (Isaaks and Srivastava, 1989). Results indicate a higher heterogeneity for ER and NEE in site 3 by the observed small range values. In the guano-affected site we find a greater diversity of plant species that may affect the spatial variability of ER and NEE. In this case, a more detailed grid (decreasing the space between points) would be necessary to better describe the spatial variability at site 3. On the other hand, most of the variables showed higher homogeneity at site 4 (greater range values), due the homogeneity of *S. uncinata* carpets. As showed in the current work, strong SDI were also observed by La Scala et al. (2010) and Mendonça et al. (2010) for ST in mosses and lichen carpets in Maritime Antarctica. With regard to SDI in mosses and lichen carpets, this parameter is highly variable due to seasonality or grid size, usually varying from weak to moderate (Mendonça et al., 2010).

Most previous studies showed that the combination of rising temperatures, increased precipitation and high nutrient inputs from marine animals might increase ER through the acceleration of mineralization rates in soil organic matter and decrease the CO_2 sink effect (Mendonça et al., 2010, Thomazini et al., 2014; Zhu et al. 2014a). However, as well-known, glaciers are subject to deglaciation due to the expected rising temperatures in Maritime Antarctica along the years. Hence, some areas will become saturated with water, especially those closer to the emerging coast which form newly exposed terraces. With time, these areas will become vegetated, predominantly colonized by mosses growing in a hydromorphic environment. Such environment is similar to site 4, in the present work. Therefore, a potential sink effect of CO_2 is expected in Maritime Antarctica, if new ice-free areas are originated. Nevertheless, the resulting glacio-isostatic uplift due to glacier retreat, eventually leads to drainage incisions and well-drained conditions, subjected to changes in its vegetation cover and greater pedogenesis. Some of these areas have potential to be colonized by other vegetation species (i.e. *D. antarctica* and *C. quitensis)* whereas other areas may lose the vegetation cover by erosion depending on soil type and topography. In this scenario, a net release of CO_2 may be expected, as reported by the results of NEE in sites 3 and 5. However, further research is needed to modeling these changes to better elucidate the current sink or source effect in ice-free areas of Maritime Antarctica.

5. Conclusions

This study provides the first measurements of net ecosystem exchange and gross primary production in Maritime Antarctica during the austral summer, considering an adequate spatial representation that have not been previously reported in the literature. CO_2 exchange was linked to vegetation and soil development, with close interplay between the two characteristics. Areas colonized by vascular plants are spatially more heterogeneous, showing low range values. In the current work, spatial variability of CO_2 exchange is related to soil temperature and soil moisture. A net loss of CO_2 that was observed in the sites predominantly colonized by vascular plants and without vegetation cover occurred due to higher mineralization processes associated with elevated soil temperature and absence of vegetation cover, respectively. In poorly drained areas a net gain of CO_2 is expected, storing more carbon over the years. As poorly drained areas become well drained, soil temperature tends to increase, vegetation characteristics are altered and the CO_2 sink strength decrease. Long-term and high-frequency measurements are needed to accurately quantify CO_2 exchange in terrestrial ecosystems of Maritime Antarctica.

Acknowledgments

We acknowledge CNPq (Conselho Nacional de Desenvolvimento Científico e Tecnológico) (556794/2009-5) and MCTI (Ministério da Ciência, Tecnologia e Inovação) for granting financial support. This work is a contribution of INCT- Criosfera TERRANTAR group.

References

Ball, B.A., Virginia, R.A, Barrett, J.E., Parsons, A.N., Wall, D.H., 2009. Interactions between physical and biotic factors influence CO_2 flux in Antarctic dry valley soils. Soil Biol. Biochem. 41, 1510-1517.

Barrett, J.E., Virginia, R.A., Parson, A.N., Wall, D.H., 2006. Soil carbon turnover in the McMurdo dry valleys, Antarctica. Soil Biol. Biochem. 38, 3065-3082.

Cambardella, C.A., Moorman, T.B., Novak, J.M., Parkin, T.B., Karlen, D.L., Turco, R.F. Konopka, A.E., 1994. Field-scale variability of soil properties in central Iowa soils. Soil Sci. Soc. Am. J. 67, 58, 1501–1511.

Cannone, N., Binelli, G., Worland, M.R., Convey, P., Guglielmin, M., 2012. CO_2 fluxes among different vegetation types during the growing season in Marguerite Bay (Antarctic Peninsula). Geoderma 189–190, 595–605.

Carvalho, J.V.S., Mendonça, E.S., La Scala, N., Reis, C., Reis, E.L., Schaefer, C.E.G.R., 2012. CO_2 losses and carbon quality of selected Maritime Antarctic soils. Antarct. Sci. 25, 11–18.

Convey, P., Hopkins, D.W., Roberts, S.J., Tyler, A.N., 2011. Global southern limit of flowering plants and moss peat accumulation. Polar Res. 30, 1–10.

Convey, P., Bindschadler, R.A., Di Prisco, G., Fahrbach, E., Gutt, J., Hodgson, D.A., Mayewski, P., Summerhayes, C.P., Turner, J., 2009. Antarctic climate change and the environment. Antarct. Sci. 21, 541-563.

Embrapa, 1997. Manual de Métodos de Análise de Solo. 2. ed. ver. atualiz. Centro Nacional de Pesquisa de Solos, Rio de Janeiro (212 pp. il., EMBRAPA/CNPS-RJ. Documentos, 1).

Francelino, M.R., Schaefer, C.E.G.R., Simas, F.N.B., Filho, E.I.F., Souza, J.J.L.L., Costa, L.M., 2011. Geomorphology and soils distribution under paraglacial conditions in an ice-free area of Admiralty Bay, King George Island, Antarctica. Catena, 85, 194–204.

Huemmrich, K.F., Kinoshita, G., Gamon, J.A., Houston, S., Kwon, H., Oechel, W.C., 2010. Tundra carbon balance under varying temperature and moisture regimes. J. Geophys. Res. Lett. 115, G00I02.

INPE (2009) Instituto Nacional de Pesquisas Espaciais-CPTEC <http://antartica.cptec.inpe.br/~antar/ weatherdata.shtml>.

Isaaks, E.H., Srivastava, R.M., 1989. An introduction to applied geostatistics. New York: Oxford University Press, 592 pp.

La Scala, N., Mendonça, E.S., Souza, J.V., Panosso, A.R., Simas, F.N.B., Schaefer, C.E.R.G., 2010. Spatial and temporal variability in soil CO_2 emissions and relation to soil temperature at King George Island, Maritime Antarctica. Polar Sci. 4, 479-487.

Mendonça, E.S., La Scala, N., Panosso, A.R., Simas, F.N.B., Schaefer, C.E.G.R., 2010. Spatial variability models of CO_2 emissions from soils colonized by grass (*Deschampsia antarctica)* and moss (*Sanionia uncinata*) in Admiralty Bay, King George Island. Antarc. Sci. 23, 27-33.

Moura, P.A., Francelino, M.R., Schaefer, C.E.G.R., Simas, F.N.B., Mendonça, B.A.F., 2012. Distribution and characterization of soils and landform relationships in Byers Peninsula, Livingston Island, Maritime Antarctica. Geomorphology, 155-156, 45–54.

Natali, S.M., Schuur, E.A.G., Trucco, C., Hicks Pries, C.E., Crummer, K.G., Baron Lopez, A.F., 2011. Effects of experimental warming of air, soil and permafrost on carbon balance in Alaskan tundra. Glob. Chang. Biol. 17(3), 1394–1407.

Parsons, A.N., Barrett, J.E., Wall, D.H., Virginia, R.A. 2004. Soil carbon dioxide flux in Antarctic Dry Valley ecosystems. Ecosystems, 7(3), 286–295.

Pereira, A.B., Putzke, J., 2013. The Brazilian research contribution to knowledge of the plant communities from Antarctic ice free areas. Anais da Academia Brasileira de Ciências (Impresso), 85, 923-935.

Shanhun, F.L., Almond, P.C., Clough, T.J., Smith, C.M.S., 2012 Abiotic processes dominate CO_2 fluxes in Antarctic soils. Soil Biol. Biochem. 53, 99–111.

Simas, F.N.B., Schaefer, C.E.G.R., Albuquerque Filho, M.R., Francelino, M.R., Fernandes Filho, E.I., Costa, L.M., 2007. Genesis, properties and classification of Cryosols from Admiralty Bay. Maritime Antarctica. Geoderma, 144, 116-122.

Souza, K.K.D., Schaefer, C.E.G.R., Simas, F.N.B., Spinola, D.N., De Paula, M.D., 2014. Soil formation in Seymour Island, Weddell Sea, Antarctica. Geomorphology, 225, 87-99.

Tatur, A., Myrcha, A., Niegodzisz, J., 1997. Formation of abandoned penguin rookery ecosystems in the Maritime Antarctic. Polar Biol. 17, 405–417.

Thomazini, A., Mendonça, E.S., Teixeira, D.B., Almeida, I.C.C., La Scala, N., Canellas, L. P., Spokas, K.A., Milori, D.M.B.P. Turbay, C.V.G., Fernandes, R.B.A., Schaefer, C.E.G.R. 2015. CO_2 and N_2O emissions in a soil chronosequence at a glacier retreat zone in Maritime Antarctica. Sci. Total Environ. 521-522, 336–345.

Thomazini, A., Teixeira, D.B., Turbay, C.V.G., La Scala Jr, N., Schaefer, C.E.G.R., Mendonça, E.S., 2014. Spatial variability of CO_2 emissions from newly exposed paraglacial soils at a glacier retreat zone on King George Island, Maritime Antarctica, Permafr. Periglac. Process. 25, 233–242.

Trucco, C., Schuur, E.A.G., Natali, S.M., Belshe, E.F., Bracho, R., Vogel, J., 2012. Seven-year trends of CO_2 exchange in a tundra ecosystem affected by long-term permafrost thaw. J. Geophys. Res. Lett. 117, G02031.

Turner, J., Bindschadler, R., Convey, P., 2009. Antarctic Climate Change and the Environment. Scientific Committee on Antarctic Research. Cambridge, p. 526.

Victoria, F.C., Alburqueque, M.P., Pereira, A.B., Simas, F.N.B., Spielmann, A.A., Schaefer, C.E.G.R., 2013. Characterization and mapping of plant communities at Hennequin Point. King George Island, Antarctica. Polar Res. 32, 19261.

Vieia, S.R., Carvalho, J.R.P., Ceddia, M.B., Gonzalez, A.P., 2010. Detrending non stationary data for geostatistical applications. Bragantia, 69, 1-8.

Vogel, J., Schuur, E.A.G., Trucco, C., Lee, H., 2009. Response of CO_2 exchange in a tussock tundra ecosystem to permafrost thaw and thermokarst development. J. Geophys. Res. Lett. 114, G04018.

Webster, R., Oliver, M.A., 1990. Statistical methods in soil and land resource survey. Oxford: Oxford University Press, p. 316.

Yeomans, J.C., Bremner, J.M., 1988. A rapid and precise method for routine determination of organic carbon in soil. Communications in Soil Science and Plant Analysis, **19,** 1467-1476.

Zhu, R., Bao, T., Wang, Q., Xu, H., Liu, Y. 2014a. Summertime CO_2 fluxes and ecosystem respiration from marine animal colony tundra in maritime Antarctica. Atmosp. Environ. 98, 190–201.

Zhu, R., Ma, D., Xu, H. 2014b. Summertime N_2O, CH_4 and CO_2 exchanges from a tundra marsh and an upland tundra in maritime Antarctica. Atmosp. Environ. 83, 269–281.

CAPÍTULO 2

Fractal dimension and spatial variability structure of soil attributes in a typical periglacial area of Keller Peninsula, Maritime Antarctica

Abstract

THOMAZINI, André, D.Sc., Universidade Federal de Viçosa, April, 2016. **Fractal dimension and spatial variability structure of soil attributes in a typical periglacial area of Keller Peninsula, Maritime Antarctica.** Adviser: Márcio Rocha Francelino. Co-advisers: Carlos Ernesto Gonçalves Reynaud Schaefer and Eduardo de Sá Mendonça.

Terrestrial ecosystems of Maritime Antarctica are characterized as a heterogeneous soil environments, although their detailed spatial variability structure remain little known. The objective of this study was to characterize, by means of applying a fractal dimension approach, the spatial variability structure of soil attributes in a typical periglacial area in Keller Peninsula, King George Island, Maritime Antarctica. General soil attributes and total organic carbon were determined, and a principal component analysis (PCA) was performed to select the most important soil attributes, according to their contribution to the total variance in the selected area. The spatial variability structure characterization of selected soil attributes was performed by deriving fractal dimension values (FD) from experimental semivariograms calculated at angles of 0, 45, 90 and 135º in a 133 point grid (50x50 m), with a minimum separation distance of 0.5 m. Scales of 0.5/5; 1/10; 2/20; 3/30; 4/40 and 5/50 m (separation distance/range) were considered in this study.

The most important soil attributes retained by the PCA were: exchangeable Al, total acidity (H+Al), bases sum (BS), total organic carbon (C), extractable Fe (Fe) and % Sand. Topologically significant FD values (FD < 3) were obtained for all calculated scales in average, indicating significant spatial variability structure for most soil attributes determined. Mean FD values were significantly lower ($p<0.05$) at a small scale (5 m) and large scales (40 and 50 m) in the 90º direction, which tended to present anisotropic pattern, especially for organic C and exchangeable Al. C and exchangeable Al presented spatial similarity expressed by the tendency observed in the fractogram as well as by significant correlation. According to the results, guano inputs, mosses and lichens colonization and local soil drainage, significantly affected the spatial variability structure of soil attributes, evidencing zones where soil is more or less heterogeneous. The FD approach provided a meaningful way to look at the pattern of pedogenesis and its spatial variation along ice-free periglacial areas.

Keywords: spatial dependence, polar environment, mapping, soil development

1. Introduction

Maritime Antarctica shows large variation on the vegetation distribution and soil attributes at short distances of its ice free areas, which are highly sensitive to changes, especially in function of variables related to the environment, such as soil temperature and moisture (Cannone et al., 2012, Thomazini et al., 2015). Heterogeneous terrestrial ecosystems occur throughout ice free areas of Maritime Antarctica (Thomazini et al., 2014), may increase as periglacial processes act (i.e. glacier melting, rising temperatures, colonization by animals and vegetation, guano deposition) (Mendonça et al., 2010; Thomazini et al., 2014). However, the characterization of the spatial variability structure and extension related to the soil attributes and its controlling factors is practically unknown in Maritime Antarctica.

Some geostatistical models have been applied to characterize the spatial variability structure in selected soil attributes, mainly related to soil CO_2 emissions, soil temperature and moisture (La Scala et al., 2010; Mendonça et al., 2010; Thomazini et al., 2014). These authors reported that only isotropic models were fitted to the experimental semivariogram, possibly, due a limitation on sampling and grid size. However, it is recognized that soil attributes can be described by anisotropic models, which shows that the spatial variability occurs in different directions and cannot be described by a single semivariogram (Isaaks and Srivastava, 1989). The anisotropy phenomena may occur because soil attributes are spatially distributed in a complex network that acts in several directions and at various scales, creating zones of tendencies (Panosso et al., 2012). Spatial anisotropy may occur in agricultural areas due to differences among land management, landform or drainage affecting soil attributes at different scales (La Scala et al., 2009; Panosso et al., 2012). In Maritime Antarctica, the irregular deposition of guano and the remarkable transition of vegetation in function of soil temperature and moisture might cause spatial anisotropy in soil attributes, according to the theory of anisotropy.

Although the spatial variability in soil attributes is widely documented by the semivariogram method, the fractal dimension (FD) can be considered a suitable tool to assess and quantify the spatial variability structure and complex autocorrelations for soil attributes at different scales (Vidal-Vázquez et al., 2010). The fractal dimension is capable of detecting the impacts of vegetation cover, drainage and biological influence on the spatial structure of soil attributes (Pérez et al., 2010). Bicalho et al. (2014) reported that the estimation of the scale regularity of an irregular behavior can be represented by the FD. Also, FD could be used to derive the homogeneous or heterogeneous features and the patterns of soil variability, especially in studying phenomena, such as soil attributes, that are scale dependent (Panosso et al., 2012).

Although tested, anisotropic models were not effectively proven to describe spatial variability structure of soil attributes in ice-free areas of Maritime Antarctica. For this reason, it is necessary to apply a detailed grid, with different separation distances in a large area to better capture the spatial structure and extension, considering the possibility of spatial anisotropy occurrence. Thereby, the objective of this study was to characterize, by means of applying a fractal dimension approach, the spatial variability structure of soil attributes in a typical periglacial area in Keller Peninsula, King George Island, Maritime Antarctica. This research hypothesized that guano deposition and resulting transitions on vegetation communities were the basic causes of spatial anisotropy in soil attributes.

2. Material and methods

2.1. Study area

The study was carried out at Keller Peninsula, Admiralty Bay, King George Island, South Shetland Islands (Fig. 1). Keller Peninsula comprises approximately 500 ha, being 4 x 2 km of length and width, respectively (Francelino et al., 2011). According to the meteorological station located at Brazilian Commandant Ferraz (62º4'33" S, 58º23'46"W), mean air temperatures from 1986 to 2013 are reported to be +1.6 during the summer (December-March) and -5.3ºC during the winter (June-September) (INPE/CPTEC, 2015). Mean annual precipitation is about 400 mm. The altitude varies from 0 to 340 m above the sea level (Francelino et al., 2011). Geology is predominantly basalt-andesites and pyritized andesites rocks. Overall, soils are weakly developed, occurring mainly Leptosols and Cryosols classes (Francelino et al., 2011). Permafrost tended to be absent in the coastal areas and sporadically appearing at mid-slope (higher than 35 m). Discontinuous permafrost can be observed at elevated sites (Francelino et al., 2011).

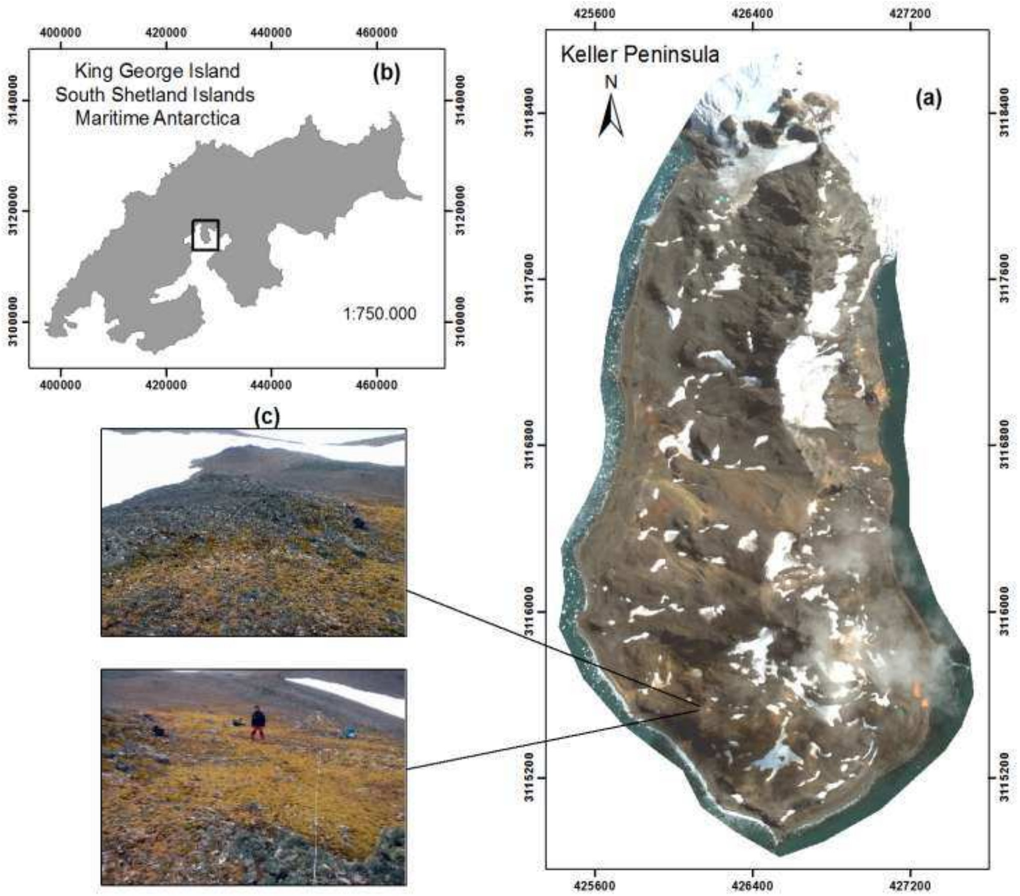

Fig. 1 Illustrative map of Keller peninsula (a, b) and the studied area (c).

2.1.1 Grid establishment

The studied area is typically periglacial, located on the southwest face of Keller Peninsula (62°5'9.03"S and 58°24'49.03"W). It is a small stepped plateau at 96 meters above sea level, slope 3^{o}-5^{o}, covered by rock fragments of different sizes coming from short-range transport of weathered materials. This rock fragments comes from small rock outcrops of andesite and basalt, interbedded with volcanic ash. To characterize spatial variability in different directions, a 133-point 50 m x 50 m grid was installed (Fig. 2). The separation distance was 0.5, 1, 2.5, 5 and 10 m between sampling points, oriented in different directions (0, 45, 90 and 135º) (Fig 2). Skuas (*Stercorarius maccormicki*) nests occur at a slightly elevated portion of the grid on the west side. This portion is delimited by a small rock outcrop line. In this section (beginning of directions 45, 90 and 135º), a vegetation community classified as "Fruticose lichens community" occur. This vegetation community is mainly characterized by the presence of lichens growing on rock fragments, as *Usnea antarctica* Du Rietz. and *Usnea aurantiaco-atra* (Jacq.) Bory. Between rock blocks and outcrops populations of mosses occur. With deeper, well drained soils *Polytrichastum alpinum* (Hedwig) G. L. Smith grows, whereas in areas with abundance of rock fragments and incipient soil development only *Sanionia uncinata*, *Syntrichia saxicola* (Card.) R.H. Zander grows. This vegetation characteristic is also observed to occur in the end of the direction 0º.

In the lower part of the selected area, a vegetation community of "moss-carpet" occurs. More relevant populations are: *S. uncinata*, Syntrichia saxicola (Card.) R.H. Zander, *Chorisodontium aciphyllum* (Hook. f. & Wilson) Broth. and

Warnstorfia sarmentosa (Wahlenb.) Hedenas. In the middle of the area, a denser vegetation cover of mosses occurs, dominated by *S. uncinata*. The east side of the studied area is represented by less dense moss carpets. Towards the eastern side, vegetation cover tends to disappear and bare soil with small rock fragments is dominant. Bare soils correspond to the last points in the directions 45, 90 and 135º.

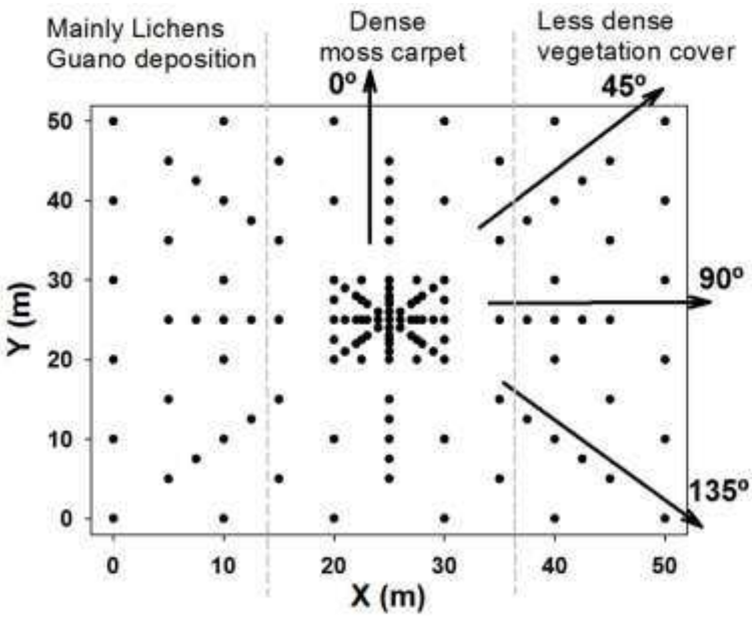

Fig 2. Representation of the sampling grid installed in the selected area with the associated vegetation cover.

2.2 Soil sampling

Soil was sampled in February 2015 to determine soil general attributes and total soil organic carbon. Three disturbed soil samples were taken at 0-10 cm depth from all 133 grid points. The soil samples were air dried, grounded and sieved through a 2-mm mesh to remove the stone fraction and larger pieces of organic material. All soil samples were analyzed in the soil laboratory at the Federal University of Viçosa, Minas Gerais, Brazil.

2.3. General soil attributes and total soil organic carbon

The stoniness and rockiness were estimated by sieving of the >2mm fraction. The particle size distribution (sand, silt, and clay) was performed by the pipette method (Embrapa, 1997). The pH was determined on a 1:2.5 soil: deionized water ratio; the potential acidity (H + Al) was extracted with $Ca(OAc)_2$ 0.5 mol L^{-1} buffered to pH 7.0, and quantified by titration with NaOH 0.0606 mol L^{-1}. Exchangeable Ca^{2+}, Mg^{2+} and Al^{3+} were extracted with 1 mol L^{-1} KCl and Na^{+} and K^{+} were extracted with Mehlich-1 (Embrapa, 1997). The element content in the extracts were determined by atomic absorption (Ca^{2+}, Mg^{2+} and Al^{3+}), flame emission (Na^{+} and K^{+}) and photocolorimetry (P). The effective cation exchange capacity (CEC_E) was calculated by sum of cations (Ca^{2+}, Mg^{2+}, Na^{+}, K^{+} and Al^{3+}). Total cation exchange capacity (CTC_T) was estimated by the sum of bases and potential acidity. Microelements (Fe^{2+}, Zn^{2+}, Mn^{2+} and Cu^{2+}) were extracted with 0.05 mol L^{-1} HC1 + 0.025 mol L^{-1} H_2SO_4, and determined using inductively coupled spectroscop. Total soil organic carbon was determined by wet oxidation with $K_2Cr_2O_7$ 0.167 mol L^{-1} in the presence of sulfuric acid with external heating (Yeomans and Bremner, 1988).

2.4 Spatial dependence structure

The spatial dependence structure was determined by means of a fractal dimension. Fractal dimension was calculated by the experimental semivariogram method (Webster and Oliver, 1990; Vidal Vázquez et al., 2005).

The semivariance of points separated at distance ***h*** was determined by the equation 1:

$$\hat{\gamma}(\mathrm{h}) = \frac{1}{2N(\mathrm{h})}\sum_{i=1}^{N(h)}[z(\mathrm{x}_i) - z(\mathrm{x}_i + \mathrm{h})]^2 \qquad (1)$$

where $\hat{\gamma}(\boldsymbol{h})$ is the semivariance at a separation distance of ***h***; *N(**h**)* is the number of pairs separated by ***h;*** $z(\boldsymbol{x}_i)$ is the value of variable *Z* at point *xi* and Z(**x**i + **h**) is the value of variable Z at point ***x***i + ***h***. The semivariance of all determined variables was calculated for all directions (0, 45, 90 and 135º). The fractal surface structure was described by the power law relation in the equation 2:

$$|\boldsymbol{z}(\boldsymbol{x}) - \boldsymbol{z}\,(\boldsymbol{x} + \boldsymbol{h})| \;\propto\; \boldsymbol{h}^{\boldsymbol{H}} \qquad (2)$$

where **z** is the value of the attribute at **x** location, **h** is the separation distance and **H** is the fractal codimension or Hölder exponent (Huang and Bradford, 1992). Comparing the equations (1) and (2), we can derive the expression to denote a fractal characteristic at a given scale as given in the equation 3:

$$\widehat{\boldsymbol{\gamma}} \propto \boldsymbol{h}^{2\boldsymbol{H}}\; or\; \log[\widehat{\boldsymbol{\gamma}}(\boldsymbol{h})] \propto \boldsymbol{2H}\log[\boldsymbol{h}] \qquad (3)$$

According to equation (3), the slope of the variogram on the log–log scale is equal to **2H**. The **H** exponent can then be obtained by means of a linear regression taken in this log–log graph as represented in the equation 4 (Perfect and Kay, 1995):

$$\boldsymbol{H} = \lim_{\boldsymbol{h} \to 0} \frac{\log[\hat{\gamma}(\boldsymbol{h})]}{2\log[\boldsymbol{h}]} \tag{4}$$

If 0 < H ≤ 1, the fractal codimension is defined as represented in the equation 5:

$$\boldsymbol{H} = \boldsymbol{d} - \boldsymbol{FD} \tag{5}$$

where **FD** is the fractal dimension and **d** is the Euclidian dimension of the system in which the fractal distribution has been described. The Euclidian dimension assumes values of 1, 2 and 3 for lines, surfaces and volumes, respectively. Hence, for a distribution of a soil attribute, the Euclidian dimension assume value **d** = 3. Thus, the fractal dimension is demonstrated by the equation 6:

$$\boldsymbol{FD} = 3 - \boldsymbol{H} \tag{6}$$

When **H** = 0, the value of **FD** is equal to 3, which represents the lack of spatial dependence structure. It represents that there is no relationship between the way the attribute varies in determined space and the distance between grid points. In this case, there is no fractal dimension, and the methodology does not apply. However, when 0 < **H** < 3, the fractal dimension assume values that characterize the presence of spatial dependence structure, explaining the spatial dependence of the soil attribute studied in function of **h** (Palmer, 1988). The spatial variability could be considered without topological significance when FD≥3, or with topological significance when FD<3 (Bicalho et al., 2014).

Fractograms were derived from variograms to describe the spatial variability at different scales. In this study, scales of 0.5/5; 1/10; 2/20; 3/30; 4/40 and 5/50 m (separation distance/range) were considered for each direction.

2.5 Data analysis

Soil attributes were first analyzed by applying descriptive statistics (mean, standard error of mean, coefficient of variation). The one-way analysis of variance was performed to assess differences in the mean values of soil attributes at each grid direction (0, 45, 90, 135º). A principal component analysis (PCA) was performed in order to identify highly weighted soil variables in each principal component (PC). Principal component either with eigenvalue >1 (Kaiser criterion, Kaiser, 1960) or significant correlation (p<0.05, Pearson's rank correlation) between the PC and soil variables were selected. A bidimensional representation (bi-plot diagram) was elaborated with the first two PCs. An analysis of variance was applied on the scores of each principal component, in order to test the effect of direction on the PCs. Differences between the directions were tested with the Tukey multicomparison test of means (p<0.05). Pearson's correlation coefficient (p<0.05) was performed between fractograms of soil variables in order to identify similarity of the spatial variability structure. Descriptive statistical analyses and PCA were performed using the XLStat (XLStat, NY, USA, 2014) program. Spatial variability and the fractal dimension were determined using a program developed by Vivas-Miranda (2000).

3. Results

3.1 General soil attributes and total soil organic carbon

Soil general attributes in the different directions are presented in Table 1. No statistical significance ($p>0.05$) was observed for the mean soil physical attributes among the different directions in the studied area. Soil physical attributes indicate an area with low clay contents and high stoniness and rockiness at the surface 0-10 cm layer. In addition, high amounts of exchangeable nutrients were recorded for all directions. P and exchangeable Al were significantly higher ($p<0.05$) at 90º direction. Mean values of Ca were significantly higher ($p<0.05$) in the 0 and 135º directions. Significantly lower ($p<0.05$) C contents were recorded in the 0º direction. Overall, sum of bases tented to be higher in the 0 and 135º directions. The coefficient off variation (CV) values ranged from 4 to 113%. Mean values of CV tended to be smaller in the 0º direction (24%). Mean CV values was observed to be smaller for Sand (9%) and greater for exchangeable Al and C (83 and 76%, respectively), considering all directions

Table 1. Descriptive statistics of soil general attributes and total soil organic carbon (0-10 cm) of the different directions in the studied area

	--------------------0º---------------------					--------------------45º---------------------					--------------------90º--------------------					---------------------135º---------------------				
	Min	Max	Mean	CV	Error	Min	Max	Mean	CV	Error	Min	Max	Mean	CV	Error	Min	Max	Mean	CV	Error
> 2 mm ($g\ kg^{-1}$)	472.53	740.00	605.20a	0.13	18.07	343.75	787.50	590.20a	0.17	20.37	336.73	856.50	609.41a	0.21	27.41	277.23	847.06	590.78a	0.21	24.93
Sand ($g\ kg^{-1}$)	450.00	628.00	550.90a	0.08	10.10	446.00	623.00	559.92a	0.09	10.09	459.00	690.00	555.39a	0.08	9.34	473.00	725.00	567.60a	0.11	12.80
Silt ($g\ kg^{-1}$)	139.00	263.00	195.70a	0.18	8.14	151.00	329.00	198.32a	0.23	9.38	152.00	304.00	204.04a	0.19	8.22	116.00	268.00	200.20a	0.17	7.11
Clay ($g\ kg^{-1}$)	230.00	289.00	253.45a	0.06	3.21	205.00	287.00	241.88a	0.09	4.53	158.00	289.00	240.61a	0.13	6.75	153.00	275.00	232.12a	0.17	8.00
pH	4.84	5.67	5.25a	0.04	0.05	4.84	6.13	5.31a	0.06	0.07	4.02	5.98	5.25a	0.09	0.10	4.50	5.99	5.40a	0.07	0.08
P ($mg\ kg^{-1}$)	12.90	667.80	189.30b	0.99	43.17	9.10	791.30	189.0b	0.85	32.66	78.80	619.80	261.94a	0.57	29.90	65.60	694.10	244.00b	0.59	31.52
P-rem ($mg\ L^{-1}$)	11.00	31.10	20.69a	0.24	1.13	2.70	33.10	19.30a	0.37	1.46	6.50	34.30	17.23a	0.43	1.58	11.90	35.60	21.79a	0.35	1.58
K ($cmol_c\ kg^{-1}$)	0.11	0.33	0.22a	0.29	0.01	0.11	0.34	0.20a	0.31	0.01	0.11	0.25	0.19a	0.19	0.01	0.11	0.31	0.22a	0.27	0.01
Na ($cmol_c\ kg^{-1}$)	0.01	0.67	0.43a	0.34	0.03	0.01	0.64	0.39a	0.34	0.03	0.01	0.53	0.39a	0.31	0.03	0.01	0.69	0.45a	0.34	0.03
Ca ($cmol_c\ kg^{-1}$)	6.92	15.62	10.78ac	0.22	0.54	1.91	14.47	8.91b	0.30	0.54	3.50	17.07	8.74bc	0.36	0.68	4.45	25.66	11.73a	0.40	0.96
Mg ($cmol_c\ kg^{-1}$)	3.74	10.57	7.92b	0.21	0.38	1.44	11.37	7.03a	0.30	0.44	1.41	11.18	6.30a	0.39	0.53	2.20	11.09	6.95b	0.37	0.52
Al ($cmol_c\ kg^{-1}$)	0.60	2.30	1.21a	0.42	0.12	0.00	8.10	1.95b	0.99	0.39	0.00	7.40	2.46a	0.90	0.47	0.00	5.50	1.43a	1.01	0.30
H+Al ($cmol_c\ kg^{-1}$)	4.10	8.10	5.87a	0.19	0.26	2.60	20.80	6.87a	0.55	0.77	1.00	18.80	7.43a	0.55	0.86	1.50	13.70	5.93a	0.48	0.58
BS ($cmol_c\ kg^{-1}$)	13.53	23.73	19.35a	0.17	0.76	3.69	26.43	16.53c	0.27	0.90	5.44	23.51	15.63bc	0.30	1.00	7.22	28.66	19.35a	0.24	0.96
CEC_E ($cmol_c\ kg^{-1}$)	14.57	24.43	20.56a	0.16	0.76	11.79	27.23	18.48a	0.20	0.75	12.84	24.66	18.09a	0.17	0.67	12.72	28.66	20.79a	0.19	0.80
CEC_T ($cmol_c\ kg^{-1}$)	19.07	29.13	25.22a	0.15	0.88	17.16	32.33	23.40a	0.15	0.71	18.00	30.56	23.06a	0.12	0.60	19.73	31.26	25.28a	0.12	0.63
S (%)	66.60	83.20	76.55a	0.05	0.89	15.10	88.70	70.79a	0.22	3.11	24.60	95.50	67.61a	0.26	3.73	34.50	95.00	75.83a	0.17	2.66
C ($g\ kg^{-1}$)	3.07	26.74	10.81c	0.53	1.32	4.58	100.17	17.36a	1.13	3.99	4.47	45.82	16.87ab	0.72	2.59	4.47	53.48	14.66b	0.68	2.03
Cu ($cmol_c\ kg^{-1}$)	2.33	4.88	3.75a	0.16	0.14	1.60	5.63	3.71a	0.23	0.18	2.51	6.20	3.90a	0.23	0.19	2.63	7.16	3.93a	0.23	0.18
Mn ($cmol_c\ kg^{-1}$)	45.30	129.60	82.16a	0.26	4.85	18.00	169.20	70.04a	0.49	7.05	25.20	126.10	71.70a	0.40	6.06	39.30	167.70	74.36a	0.43	6.47
Fe ($cmol_c\ kg^{-1}$)	58.40	169.30	103.43a	0.21	5.10	65.50	225.30	109.31a	0.32	7.19	60.70	281.00	119.67a	0.41	10.35	50.10	176.80	100.70a	0.28	5.85
Zn ($cmol_c\ kg^{-1}$)	1.60	3.85	2.51a	0.22	0.13	1.33	3.76	2.11a	0.29	0.13	1.31	4.26	2.18a	0.36	0.17	1.63	3.58	2.18a	0.25	0.11

Means followed by the same letters in rows are equal (Tukey; $p < 0.05$); Min: minimum; Max: maximum; CV:coefficient of variation; >2mm: stoniness and rockiness; pH: active acidity (H_2O); P: phosphorus; P-rem: remaining phosphorus; K: potassium; Na: sodium; Ca: calcium; Mg: magnesium; Al: exchangeable aluminium; H+Al: total acidity; BS: bases sum; CEC_E: effective cation exchange capacity; CEC_T: total cation exchange capacity; S: saturation of bases; C: total organic carbon; Cu: copper; Mn: manganese; Fe: Iron; Zn: Zinc.

3.2 Principal component analysis

The results of the principal component analysis are presented in Table 2. The first six principal components had their eigenvalues greater than 1 (Kaiser, 1960). However, in this study, only the PC1 and 2 were considered to describe the spatial variability structure in the selected area, because no correlation between the principal components and variables were observed in PC3, 4, 5 and 6. PC1 and 2 explained 31.41 and 15.74% of the total variance in the data set, respectively (Table 2). PC1 was positively correlated with S and BS, and negatively correlated with exchangeable Al, H+Al, C and Fe. PC2 was positively correlated with Sand. Selected soil variables are also considered highly weighted, explaining 58.9 and 13.7% in the PC1 and 2, respectively. These two groups (PC1 and PC2) were also well-separated in the bi-plot diagram (Fig 3).

No clear differences between directions (0, 45, 90 and 135º) and soil variables can be observed in the bi-plot diagram. For this reason, we described the spatial variability structure only for exchangeable Al, H+Al, BS, S, C, Fe and Sand, which were the most important soil variables retained in the PCA. The analysis of variance of the PC1 and 2 showed that only in PC1, the direction was a significant factor (F= 2.977; p<0.036), indicating that the relationships between soil attributes were not the same in all grid directions. However, no statistical significance (p<0.05) among directions were detected by the criteria applied by the multicomparison test.

Table 2. Results of the principal component analysis for the first six principal components (PCs) for the studied soil attributes in Keller Peninsula

Principal components	PC1	PC2	PC3	PC4	PC5	PC6
Eigenvalue	6.91	3.46	2.60	1.87	1.68	1.46
Variability (%)	31.41	15.74	11.84	8.51	7.64	6.65
Cumulative (%)	31.41	47.14	58.98	67.49	75.13	81.79
	Correlations (p<0.05)					
> 2 mm (g kg^{-1})	0.43	0.26	-0.14	-0.34	-0.17	0.43
Sand (g kg^{-1})	-0.20	**0.79**	0.10	-0.31	0.33	-0.08
Silt (g kg^{-1})	0.02	-0.69	-0.27	0.43	-0.15	-0.29
Clay (g kg^{-1})	0.31	-0.46	0.19	-0.02	-0.37	0.53
pH	0.51	0.05	-0.31	0.57	0.04	-0.14
P (mg kg^{-1})	0.06	0.26	-0.63	-0.25	0.33	-0.31
P-rem (mg L^{-1})	0.58	0.50	-0.20	-0.33	0.31	0.08
K ($cmol_c$ kg^{-1})	-0.18	-0.41	0.30	0.17	0.76	0.17
Na ($cmol_c$ kg^{-1})	-0.04	-0.44	0.30	0.28	0.69	0.19
Ca ($cmol_c$ kg^{-1})	0.82	-0.01	0.11	0.02	0.06	-0.38
Mg ($cmol_c$ kg^{-1})	0.59	-0.19	0.39	-0.28	-0.09	0.25
Al ($cmol_c$ kg^{-1})	**-0.82**	-0.12	0.09	-0.15	-0.10	-0.36
H+Al ($cmol_c$ kg^{-1})	**-0.88**	-0.19	0.25	-0.25	-0.08	-0.15
BS ($cmol_c$ kg^{-1})	**0.92**	-0.12	0.30	-0.11	0.03	-0.16
CEC_E ($cmol_c$ kg^{-1})	0.77	-0.21	0.41	-0.21	-0.01	-0.37
CEC_T ($cmol_c$ kg^{-1})	0.41	-0.34	0.63	-0.39	-0.03	-0.36
S (%)	**0.96**	0.10	-0.10	0.16	0.07	0.09
C (g kg^{-1})	**-0.60**	0.00	0.29	-0.19	0.18	0.18
Cu ($cmol_c$ kg^{-1})	0.18	-0.55	-0.57	-0.39	0.02	-0.09
Mn ($cmol_c$ kg^{-1})	0.23	-0.59	-0.47	-0.32	0.16	0.14
Fe ($cmol_c$ kg^{-1})	**-0.70**	-0.31	-0.03	-0.24	-0.04	-0.04
Zn ($cmol_c$ kg^{-1})	0.05	-0.60	-0.46	-0.36	0.14	0.07
Analysis of variance						
F	2.977	0.539				
P	0.036	0.657				

>2mm: stoniness and rockiness; pH: active acidity (H_2O); P: phosphorus; P-rem: remaining phosphorus; K: potassium; Na: sodium; Ca: calcium; Mg: magnesium; Al: aluminium; H+Al: potential acidity; BS: bases sum; CECE: effective cation exchange capacity; CECT: total cation exchange capacity; S: saturation of bases; C: total organic carbon; Cu: copper; Mn: manganese; Fe: Iron; Zn: Zinc.

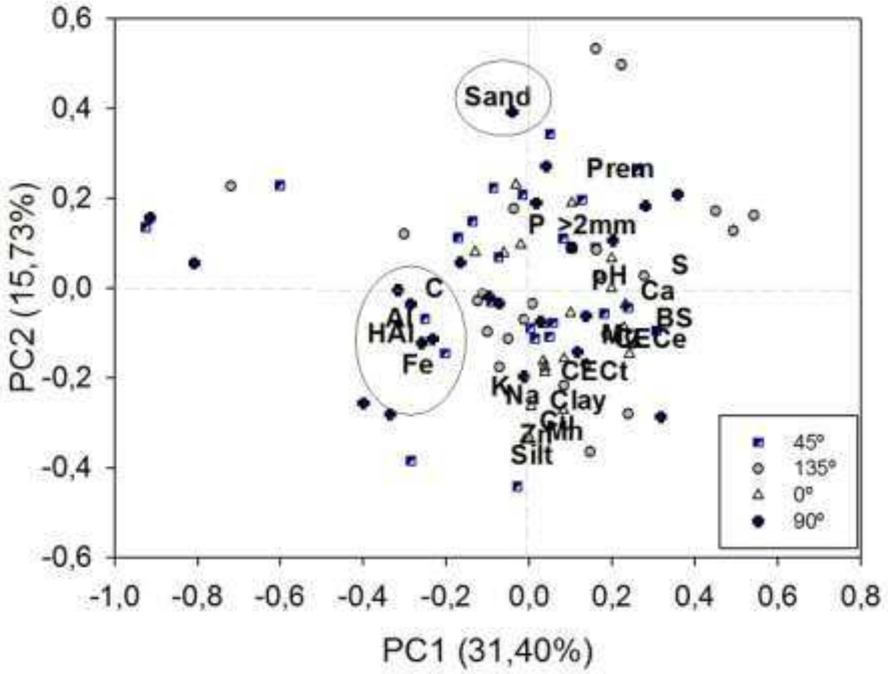

Fig 3. Bi-plot diagram from the PCA of soil general attributes and total soil organic carbon of the selected area in Keller Peninsula. >2mm: stoniness and rockiness; pH: active acidity (H_2O); P: phosphorus; P-rem: remaining phosphorus; K: potassium; Na: sodium; Ca: calcium; Mg: magnesium; Al: aluminium; H+Al: total acidity; BS: bases sum; CECe: effective cation exchange capacity; CECt: total cation exchange capacity; S: bases saturation; C: total organic carbon; Cu: copper; Mn: manganese; Fe: Iron; Zn: Zinc.

3.3 Spatial dependence structure

Mean FD values derived from the slope of the experimental semivariograms at different scales and directions are presented in the Table 3. Topologically significant FD values (FD < 3) were obtained for all calculated scales (0.5/5; 1/10; 2/20; 3/30; 4/40 and 5/50) in the studied area, presenting heterogeneous spatial variability structure in average. In the 90º direction, mean FD values were significantly lower (p<0.05) at a small scale (5 m) and large scales (40 and 50 m) compared to the other directions. No significant differences (p>0.05) were observed to occur in the scales from 10 to 30 m for all directions, considering the mean FD values of all soil attributes determined.

The fractogram, which is the bidimensional representation of FD values derived from different scales for the selected soil variables, are shown in Fig 4. FD values were highly variable on the majority selected soil variables, according to the considered scales. Topological significance (FD<3) were observed to occur for most directions. The FD values of Al ranged from 2.42 to 3.13 at a scale of 5 m. Also, there is a tendency of FD values of Al to increase with scale in the 90º direction. On the other hand, Al FD values tended to decreased as scale increase in the 0, 45 and 135º directions.

Overall, FD values of H+Al tended to decrease with increasing scale. Exceptions included the 90º direction at a scale of 5 m. H+Al FD values varied from 2.62 over a large scale (40 m) to 3.23 over a small scale (5 m). The same spatial pattern was observed for S. The spatial pattern for BS showed that there is a decrease of FD values with increase in scale. However, all FD values of BS showed a well-structured spatial variability for all scales and directions. Lower BS FD values were obtained in the 90º direction. According to the fractogram, the spatial variation of C FD values was not the same for all directions. Less-structured spatial variability was observed at smaller scales (up to 20 m) in the 0º direction and larger scales (after 30 m) in the 135º direction. The FD values of C ranged from 2.46 (90º direction) to 3.32 (0º direction) at a scale of 5 m. There is no clear pattern in the spatial structure of Fe, showing well-structured spatial variability for all considered scales. Most of the directions had topological significance (FD<3) for Sand. A more structured spatial pattern was recorded at scales from 20 to 50 m in all directions. However, FD values of Sand tended to be less-structured in the 45º direction at a scale of 5 m.

Similar spatial pattern was recorded for Al and C in the 90º direction, being more well-structures spatially at small scales. This result is also supported by significant correlation between the fractogram of C and Al ($r = 0.93$, $p<0.001$, Pearson's correlation coefficient). The different spatial patterns observed in the fractogram for directions and scales, especially in the 90º direction, indicating anisotropy in the spatial variability structure of the selected soil variables. Anisotropy was more evidenced for C and Al, according to the evident variation in the spatial pattern (mostly in the 0 and 90º direction), demonstrated in the fractogram.

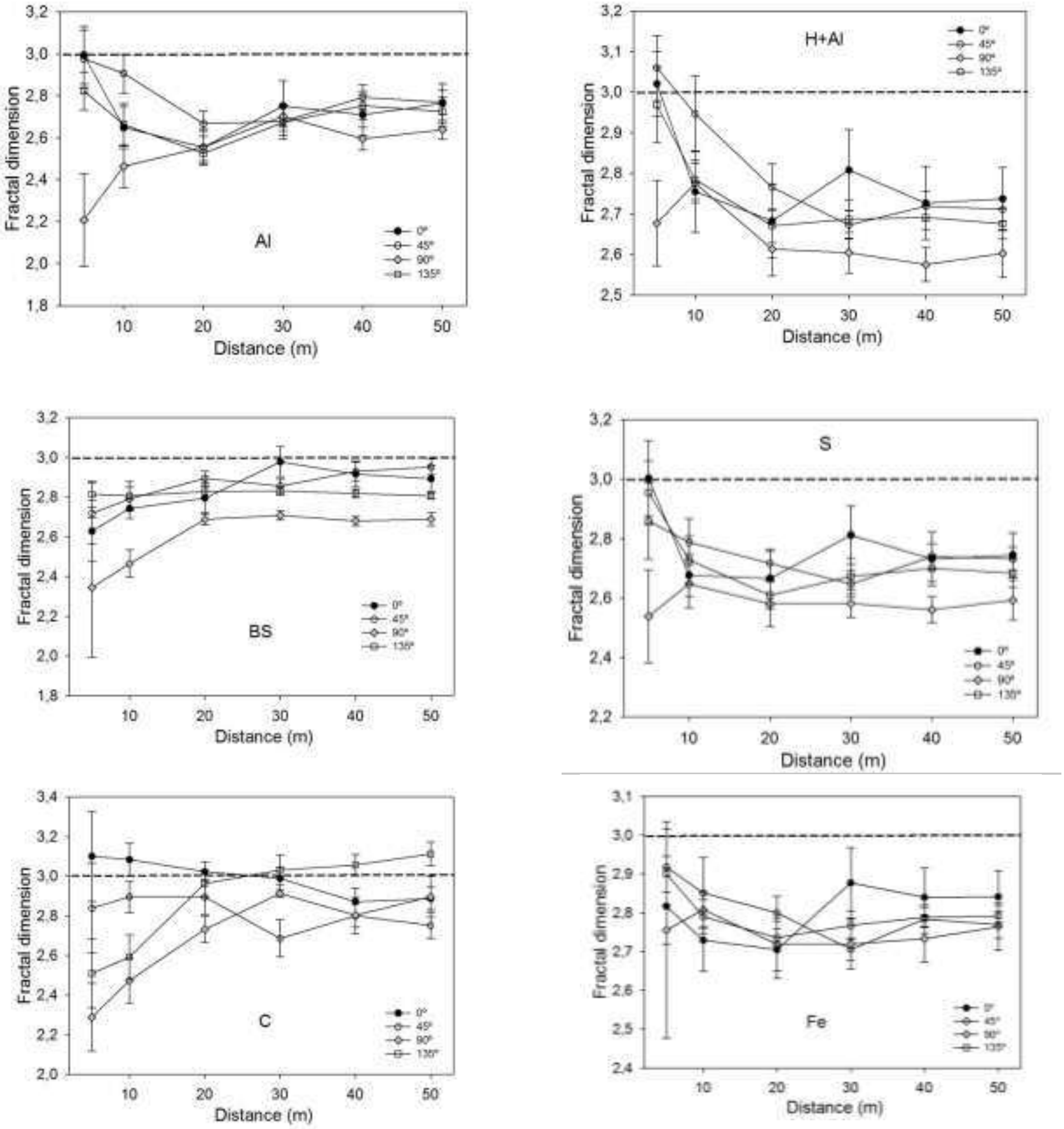

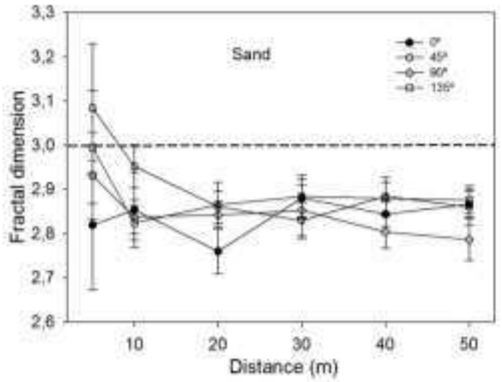

Fig. 4. Fractograms of selected soil attributes (trough PCA) calculated from semivariograms at different scales (5, 10, 20, 30, 40 and 50 m) and directions (0, 45, 90 and 135º). Al: exchangeable aluminum; H+Al: total acidity; BS: bases sum; S: saturation of bases; C: total organic carbon; Fe: Iron.

Table 3. Mean FD values of soil attributes at different scales and directions in the studied grid

	Distance (m)					
Direction	**5**	**10**	**20**	**30**	**40**	**50**
0º	2.97 a	2.86 a	2.84 a	2.93 a	2.93 a	2.93 a
45º	2.94 a	2.87 a	2.88 a	2.86 a	2.90 a	2.90 a
90º	2.78 b	2.74 a	2.79 a	2.80 a	2.79 b	2.81 b
135º	2.96 a	2.87 a	2.87 a	2.87 a	2.87 a	2.89 a

Means followed by the same letters in columns are equal (Tukey; $p < 0.05$).

4. Discussion

The gradient of vegetation imposed by guano deposition and local soil drainage, strongly influenced soil general attributes and total soil organic carbon across the area. On the west side of the grid, the first sampled points (0-10 m) in the 45, 90 and 135º directions are more subjected to guano deposition by Skuas, especially in the 90º direction. Also, the west side is predominantly colonized by *Usnea* sp. growing on rock fragments, indicating a well-drained site. Despite being not a typical guano-influenced area (such as penguin colonies), the cumulative low contents of guano that has been deposited over the years, significantly altered the soil nutrient status in different directions (Table 1).

With heavy guano deposition soil pH is lowered, as reported by Michel et al (2006) and Simas et al. (2007). In this work, soil pH values were higher than reported by these authors in areas strongly influenced by penguin's colonies. This result is more evident in the 0º direction, which is less influenced by guano. In this 0º direction, there is a tendency of low P, C and Mg contents in average. In addition, wetter environment is observed in the 0º direction, as indicated by the presence of mosses communities (especially *Sanionia uncinata*), which are associated with poorly-drained soils (Simas et al., 2008; Victoria et al., 2013).

Overall, the selected area is a typical periglacial landscape with incipient clay development, abundance of rock fragments on the soil surface and high exchangeable bases. The CV values of soil attributes are a first indicator of spatial variability (Bicalho et al., 2014). Initially, results suggest a great variation on Al and C contents in the entire area, according to the CV values presented in Table 1. On the other hand, small variation was recorded for % Sand, indicating a more uniform pattern in the entire area.

Results suggest a great importance of Al, H+Al, S, BS, C, Fe and Sand to describe the spatial variability structure in the selected area, explaining more than 47% of the total variance in the data set of 22 measured soil variables. Explained variance observed for the two first components in this work is reported to be suitable, when including a large number of soil attributes that are typically highly variable, as soil attributes, in a data set (Anderson and Gribble, 1998). In our study, PC1 was mainly related to soil chemical attributes (26.5% of the total variance explained by BS and S). On the other hand, PC2 was more related with soil physical attributes (18.22% of the total variance explained by % Sand).

Overall, these results indicate an importance of the nutrient exchangeable bases availability and sand contents to explain the relationship between guano deposition, vegetation and local soil drainage on the spatial variability of soil development in periglacial environments. Despite being characterized by the high amounts of exchangeable bases, values can strongly vary according to the landscape position in periglacial environments of Maritime Antarctica (Michel et al., 2006), which is observed in this work. Amounts of bases are also associated with the level of clay formation (Simas et al., 2007). Chemical weathering of primary minerals leads to the increase of exchangeable bases on the soil solution, reducing sand and increasing clay contents, with an advance in pedogenesis (Simas et al., 2007). These processes are highly influenced by seabird droppings, nutrient cycling from vegetation, soil temperature and moisture (Michel et al., 2006; Souza et al., 2014). If pedogenetic processes are favored in a given part of the landscape, this may cause strong tendency on the spatial variability structure of soil variables (Panosso et al., 2012), especially in Maritime Antarctica, where environmental dynamic is marked.

The differentiation on the level of soil formation along the grid was clearly evident according to the FD values used to assess spatial patterns. Most of the FD values obtained for the selected soil variables had topological significance, indicating differences in the spatial pattern of pedogenesis. In these cases, FD values are associated with greater angles of the logarithm of semivariance as a function of the logarithm of distance, indicating existent of spatial dependence (Vidal-Vázquez et al., 2010; Panosso et al., 2012; Bicalho et al., 2014). A few soil attributes had FD values higher than 3 at determined scales, indicating that the slope of the straight line regression was small, with no spatial dependence, reaching to a pure nugget effect (Vidal-Vázquez et al., 2010).

Despite being not applied in Maritime Antarctica yet, FD method have been proved to describe the influence of microrelief (Vidal-Vázquez et al., 2010), soil management and carbon dynamic (La Scala et al., 2009; Bicalho et al., 2014) on the spatial variability of soil attributes in others environments. These authors have reported FD values highly variable, in general showing spatial dependence structure (topological significance), especially in the direction of drainage and management at small scales (0-20 m). This further indicates that particular processes (such as nutrient input or soil drainage) have great influence on the spatial variability of soil attributes, creating zones more or less heterogeneous on the soil, as reported in the current work.

Greater differences in the spatial structure were detected in the 90º direction, when comparing FD values among other directions. Overall, according to the fractogram, results suggest a tendency on the 90º direction, showing different spatial pattern compared to the others directions. This observation may indicate presence of anisotropic pattern, which could not be characterized by a unique FD value for different scales or directions (Panosso et al., 2012). Anisotropic may exist due several factors, such as formation and management of soils, type of tillage and slope (La Scala et al., 2009; Vidal-Vázquez et al., 2010; Panosso et al., 2012; Bicalho et al., 2014). However, it must be interpreted carefully, since FD values can be influenced by scale, type of soil, location and orientation of the sampling grid (Panosso et al., 2012).

In the 90º direction, guano is more concentrated in the first sampled points (0-10 m). The middle (10-30 m) is fully covered by *Sanionia uncinata* and the end (30-50 m) almost without vegetation cover. In the end and the first samples points of 0, 45 and 135º directions, is possible to observe some dispersed patches of vegetation and low or no guano input compared to 90º direction, respectively. Thus, environmental variables had positive contribution on the differentiation of zones in terms of homogeneity/heterogeneity along the area. This result indicates that weathering is irregular, affecting the spatial variability of soil attributes. For this reason, the spatial structure is overall more developed along the 90º direction, contributing to the anisotropic tendency and lower FD values.

The most evident similarity on the spatial pattern was observed for C and Al contents in the 90º direction, both FD values increasing with increase in scale. Relationship between soil C and Al contents is documented for Maritime Antarctica (Michel et al., 2006). However, our results also indicate a spatial relationship (same pattern) between C and Al along directions, with similar characteristics as those reported in this study, for the 90º direction. It can be identified by the significant correlation between the fractogram of C and Al ($r=0.93$, $p<0.001$, Pearson's correlation coefficient). Thus, both guano input and colonization of *Usnea* sp. in a well-drained zone contributed to the high spatial dependence and spatial correlation of C and Al contents at small scales (0-20 m) in Maritime Antarctica. The high variability of soil attributes (without topological significance) in periglacial environments could be related to the decrease in spatial dependence, strongly varying in short distances. There results suggest that through FD modeling is possible to find different spatial patterns for the most important soil attributes in Keller peninsula, evidencing different levels of soil development in function of guano input, colonization by mosses and lichens, and also the variation of soil drainage imposed by landscape dynamics.

5. Conclusions

In a typical periglacial area of Maritime Antarctica, soil attributes presented significant spatial variability structure, characterized by means of fractal dimension derived from experimental variograms, evidencing spatial dependence at small, medium and large scales along the selected area. Through the application of a robust and detailed grid, anisotropic tendency was assessed, especially for organic carbon and exchangeable Al. Significant spatial variability structure (with topological significance) is more evident in the

90º direction, induced by the well-defined zones of guano input, colonization by vegetation and drainage. Also, a spatial correlation (similarity) between organic carbon and exchangeable Al occurs in the 90º direction. The fractal dimension method used to describe the spatial variability structure of soil attributes was proved to be efficient, helping to a better understanding of pedogenesis, and its controlling factors, in a typical ice-free area of Maritime Antarctica.

Acknowledgments

We acknowledge CNPq (Conselho Nacional de Desenvolvimento Científico e Tecnológico) (556794/2009-5) and MCTI (Ministério da Ciência, Tecnologia e Inovação) for granting financial support. This work is a contribution of INCT- Criosfera TERRANTAR group.

References

Anderson, M.J., Gribble, N.A., 1998. Partitioning the variation among spatial, temporal and environmental components in a multivariate data set. Aust. J. Ecol. 23, 158–167

Bicalho, E.S., Panosso, A.R., Teixeira, D.D.B., Miranda, J.G.V., Pereira, G.T., La Scala, N. 2014. Spatial variability structure of soil CO_2 emission and soil attributes in a sugarcane area. Agric. Ecosys. Environ. 189, 206–215.

Cannone, N., Binelli, G., Worland, M.R., Convey, P., Guglielmin, M., 2012. CO_2 fluxes among different vegetation types during the growing season in Marguerite Bay (Antarctic Peninsula). Geoderma 189–190, 595–605.

Embrapa, 1997. Manual de Métodos de Análise de Solo. 2. ed. ver. atualiz. Centro Nacional de Pesquisa de Solos, Rio de Janeiro (212 pp. il., EMBRAPA/CNPS-RJ. Documentos, 1).

Francelino, M.R., Schaefer, C.E.G.R., Simas, F.N.B., Filho, E.I.F., Souza, J.J.L.L., Costa, L.M., 2011. Geomorphology and soils distribution under paraglacial conditions in an ice-free area of Admiralty Bay, King George Island, Antarctica. Catena, 85, 194–204.

Huang, C.H., Bradford, J.M., 1992. Applications of a laser scanner to quantify soil microtopography. Soil Sci. Soc. Am. J. 56, 14–21.

INPE (2009) Instituto Nacional de Pesquisas Espaciais-CPTEC <http://antartica.cptec.inpe.br/~antar/ weatherdata.shtml>.

Isaaks, E.H., Srivastava, R.M., 1989. An introduction to applied geostatistics. New York: Oxford University Press, 592 pp.

Kaiser, H.F., 1960. The application of electronic computers to factor analysis. Educ. Psychol. Meas. 20, 141–151

La Scala, N., Panosso, A.R., Pereira, G.T., Gonzalez, A.P., Miranda, J.G.V., 2009. Fractal dimension and anisotropy of soil CO_2 emission in an agricultural field during fallow. Int. Agrophys. 23, 353–358.

La Scala, N., Mendonça, E.S., Souza, J.V., Panosso, A.R., Simas, F.N.B., Schaefer, C.E.R.G., 2010. Spatial and temporal variability in soil CO_2 emissions and relation to soil temperature at King George Island, Maritime Antarctica. Polar Sci. 4, 479-487.

Mendonça, E.S., La Scala, N., Panosso, A.R., Simas, F.N.B., Schaefer, C.E.G.R., 2010. Spatial variability models of CO_2 emissions from soils colonized by grass (*Deschampsia antarctica)* and moss (*Sanionia uncinata*) in Admiralty Bay, King George Island. Antarc. Sci. 23, 27-33.

Michel, R.F.M., Schaefer, C.E.G.R., Dias, L., Simas, F.N.B., Benites, V., Mendonca, E.S., 2006. Ornithogenic gelisols (cryosols) from Maritime Antarctica: pedogenesis, vegetation and carbon studies. Soil Sci. Soc. Am. J. 70, 1370–1376.

Palmer, M.W., 1988. Fractal geometry: a tool for describing spatial patterns of plant communities. Vegetation 75, 91–102.

Panosso, A.R., Perillo, L.I., Ferraudo, A.S., Pereira, G.T., Miranda, J.G.V., La Scala, N., 2012. Fractal dimension and anisotropy of soil CO_2 emission in a mechanically harvested sugarcane production area. Soil Tillage Res. 124, 8–16.

Pérez, L.D., Millán, H., González-Posada, M., 2010. Spatial complexity of soil plow layer penetrometer resistance as influenced by sugarcane harvesting: a prefractal approach. Soil Tillage Res. 110, 77–86.

Perfect, E., Kay, B.D., 1995. Applications of fractals in soil and tillage research: a review. Soil Tillage Res. 36, 1–20.

Simas, F.N.B., Schaefer, C.E.G.R., Albuquerque Filho, M.R., Francelino, M.R., Fernandes Filho, E.I., Costa, L.M., 2007. Genesis, properties and classification of Cryosols from Admiralty Bay, Maritime Antarctica. Geoderma 144, 116–122.

Simas, F.N.B., Schaefer, C.E.G.R., Albuquerque-Filho, M.R., Francelino, M.R., Fernandes Filho, E.I., Costa, L.M., 2008. Genesis, properties and classification of Cryosols from Admiralty Bay, Maritime Antarctica. Geoderma 144, 116–122.

Souza, K.K.D., Schaefer, C.E.G.R., Simas, F.N.B., Spinola, D.N., De Paula, M.D., 2014. Soil formation in Seymour Island, Weddell Sea, Antarctica. Geomorphology 225, 87–99.

Thomazini, A., Mendonça, E.S., Teixeira, D.B., Almeida, I.C.C., La Scala, N., Canellas, L. P., Spokas, K.A., Milori, D.M.B.P. Turbay, C.V.G., Fernandes, R.B.A., Schaefer, C.E.G.R. 2015. CO_2 and N_2O emissions in a soil chronosequence at a glacier retreat zone in Maritime Antarctica. Sci. Total Environ. 521-522, 336–345.

Thomazini, A., Teixeira, D.B., Turbay, C.V.G., La Scala Jr, N., Schaefer, C.E.G. R., Mendonça, E.S., 2014. Spatial variability of CO2 emissions from newly exposed paraglacial soils at a glacier retreat zone on KingGeorge Island,Maritime Antarctica. Permafr. Periglac. Process. 25, 233–242.

Victoria, F.C., Alburqueque, M.P., Pereira, A.B., Simas, F.N.B., Spielmann, A.A., Schaefer, C.E.G.R., 2013. Characterization and mapping of plant communities at Hennequin Point. King George Island, Antarctica. Polar Res. 32, 19261.

Vidal Vázquez, E., Miranda, J.G.V., Paz González, A., 2005. Characterizing anisotropy and heterogeneity of soil surface microtopography using fractal models. Ecol. Modell. 182, 337–353.

Vidal Vázquez, E., Vieira, S.R., De Maria, I.C., Paz González, A., 2010. Fractal dimension and geostatistical parameters for soil microrelief as a function of cumulative precipitation. Sci. Agric. 67, 78–83.

Vivas-Miranda, J.G., 2000. Analisis fractal del microrrelieve del suelo. Ph.D. Thesis. Universidad de La Coruna, Coruna.

Webster, R. Oliver, M.A. 1990. Statistical methods in soil and land resource survey. Oxford: Oxford University Press, 316 pp.

Yeomans, J.C., Bremner, J.M., 1988. A rapid and precise method for routine determination of organic carbon in soil. Communications in Soil Science and Plant Analyses, New York 19, pp. 1467–1476.

CAPÍTULO 3

Mapping and modeling the spatial variability of soil attributes in a typical periglacial area of Keller Peninsula, Maritime Antarctica

Abstract

THOMAZINI, André, D.Sc., Universidade Federal de Viçosa, April, 2016. **Mapping and modeling the spatial variability of soil attributes in a typical periglacial area of Keller Peninsula, Maritime Antarctica.** Adviser: Márcio Rocha Francelino. Co-advisers: Carlos Ernesto Gonçalves Reynaud Schaefer and Eduardo de Sá Mendonça.

In Maritime Antarctica, guano deposition, organic matter and vegetation, associated with soil drainage conditions, are the main drivers of soil development. However, the spatial variability extension of soil attributes remains little documented. The objective of this study was modeling the spatial variability of selected soil attributes in a guano-influenced area of Keller Peninsula, King George Island, Maritime Antarctica. A representative heterogeneous area was selected in February 2015, where a large variation on the spatial distribution of vegetation and guano occur, in a typical periglacial landscape. A 133-point 50x50 m grid with a minimum separation distance of 0.5 m was installed, in which sections were delimited according to guano influence and vegetation cover. Soil was sampled (0-10 cm) at each point of the grid, in order to map and model the spatial variability of general soil attributes. Principal component analysis (PCA) was used to select the most important soil attributes.

Further, experimental semivariograms were calculated and thematic kriging maps obtained.

Soil attributes significantly ($p<0.05$) varied across the sections. Bases contents and physical soil attributes (sand and silt) were the most important variables selected through PCA. In zones where guano is deposited, soil acidification occurs, controlling the availability of nutrients. In this section, high exchangeable Al contents and potential acidity were observed, associated with elevated amounts of organic matter and phosphorus. Thus, spatial variability of soil attributes vary strongly at short distances, mainly in function of guano deposition and vegetation cover transitions. Results reported in this study can be also observed to occur in other similar periglacial landscapes.

Keywords: Ordinary kriging, periglacial landscapes, spatial analysis

1. Introduction

There has been growing scientific attention for studying Maritime Antarctica in the past decades, especially focused in terrestrial environment changes (i.e. soil and vegetation), under a regional warming trend. Following climate warming, new ice-free areas have been formed (Turner et al.., 2009) being subjected to increasing chemical and biological influence, mainly in the austral summer period (Simas et al., 2007). Thereby, soil and vegetation change continuously across the landscape, and can be used as a climate change indicator (Thomazini et al., 2015). Despite many recent advances on soil formation and vegetation studies in Maritime Antarctica (Simas et al., 2008; Pereira and Putzke, 2013; Victoria et al., 2013; Putzke et al. 2015), modeling and mapping of such variables, as well as its spatial dependence, are still scarce in Maritime Antarctica.

Plant species in Maritime Antarctica are characterized by strong relationship with soil attributes, bird's colonies and conditions (i.e. water content). Overall, vegetation communities are patchy on soil or rock surface (Victoria et al., 2013). Exceptionally, extensive areas normally waterlogging on hydromorphic environments, are colonized by large moss fields, mainly by *Sanionia uncinata* (Hedw.) Loeske. (Pereira and Putzke, 2013). Also, in areas with greater nutrients abundance, *Deschampsia antarctica* Desv. (*Poaceae*) and *Colobanthus quitensis* (Kunth) Bartl. (*Caryophyllaceae*) may occur, associated or not with, such as *Prasiola crispa* (Lightfoot) Menegh., *Bryum* spp., *Polytrichastrum alpinum* G.L. Smith, *Usnea antarctica* Du Rietz, and *Politrichum juniperinum* Hedw., growing in well-drained areas.

Similarly, soil types and attributes vary significantly across the landscape, as a function of weathering degree, parent material, or external chemical and biological influence (i. e. colonization by birds or nutrient cycling from vegetation) (Simas et al., 2007; Schaefer et al., 2008; Simas et al., 2008; Souza et al., 2014). Notably, fresh guano input from birds has a marked importance on the soil-forming process in Antarctica, through the ornithogenic process that enhances nutrients pools (Tatur and Barczuk 1985; Simas et al., 2007). Ornithogenic soils are characterized by low pH and base saturation, very high phosphorus (Mehlich-1), exchangeable Al and total organic carbon contents, and usually greater depths (Simas et al., 2007). However, there is a lack of information on the spatial dependence and relationship among soil attributes-vegetation in Maritime Antarctica, being practically not documented yet.

The spatial dependence of soil attributes can be determined by an accurate sampling and spatial modeling method to better describe the phenomena, since most of this dependence is uncertain due to the heterogeneity of the environmental variables that occur in terrestrial ecosystems of Maritime Antarctica (Mendonça et al., 2010; Thomazini et al., 2014). The extension of chemical and biological influence on soil development can be determined by using geoestatistical techniques, to model and map different ice-free areas at different scales (Isaaks and Srivastava, 1989). The spatial variability, based on geostatistical analysis, has been successfully applied to characterize several physical, chemical, and biological attributes of soils in this region (Teixeira et al., 2011; Thomazini et al., 2014). Modeling experimental semivariogram and performing thematic maps by interpolation techniques in geostatistical analysis enable more accurate estimations of the studied soil attribute and its spatial dependence structure across the area (Webster and Oliver, 1990, Teixeira et al., 2011), allowing assumptions of the main controlling factors of soil development in this area.

Recent studies have reported the spatial variability of some environmental variables, such as soil CO_2 emissions and temperature in Maritime Antarctica (Mendonça et al., 2010; La Scala et al., 2010; Thomazini et al., 2014). These authors elaborated thematic maps using ordinary kriging in typical ice-free areas, mainly characterized by small vegetation patches and bare soils. However, general soil attributes of guano-influenced areas and vegetation transition have not been mapped yet. Therefore, to asses this spatial variability in such a representative area, detailed grid should be used to allow the recognition of the variability range. We hypothesized that changes in vegetation distribution and guano deposition affect spatial variability of soil attributes in Maritime Antarctica, being important to better understand soil-forming process using geostatistical techniques. The aim of this study was modeling the spatial variability of selected soil attributes in a guano-influenced area of Keller Peninsula, King George Island, Maritime Antarctica.

2. Material and methods

2.1. Study area

The study was carried out at Keller Peninsula in Admiralty Bay, located at King George Island, which is the largest island in the South Shetland Islands (Fig. 1). Keller Peninsula comprises approximately 500 ha, being 4 x 2 km of length and width respectively (Francelino et al., 2011). According to the meteorological station located at Brazilian Commandant Ferraz (62º4'33" S, 58º23'46"W), mean air temperatures from 1986 to 2013 are reported to be +1.6 during the summer (December-March) and -5.3ºC during the winter (June-September) (INPE/CPTEC, 2015). Mean annual precipitation is about 400 mm and the altitude varies from 0 to 340 m above the sea level (Francelino et al., 2011).

Permafrost tended to be absent in the coastal areas and sporadically appearing at mid-slope (higher than 35 m). In addition, discontinuous permafrost can be observed at elevated sites (Francelino et al., 2011). Geology is dominated by Upper Jurassic basalts, basalt–andesites, and pyritized andesites rocks (Hawkes, 1961). Also, deposition of volcanic ash coming from the Deception volcano is reported in King George Island (Blume et al., 2004).

Overall, soils are weakly developed, occurring mainly Leptosols and Cryosols classes (Francelino et al., 2011).

The selected area is typical periglacial area, located on the southwest face of Keller Peninsula (62°5'9.03"S and 58°24'49.03"W). It is a small stepped plateau, located at 96 meters above sea level, with a slope of 3^{o}-5^{o}, covered by rock fragments of different sizes coming from the transport in short distances of the weathered materials. Rock fragments come from small rock outcrops of andesite and basalt surrounding the plateau. The plateau is enriched by volcanic tuffs. According to the World Reference Base for Soil Resources (WRB) classification system, the most common soil type is classified as Skeletic/Gelic Regosol in the selected area (Albuquerque-Filho, 2005). Skuas (*Stercorarius maccormicki*) nesting occur on the west side, occasioning irregular guano deposition on this side.

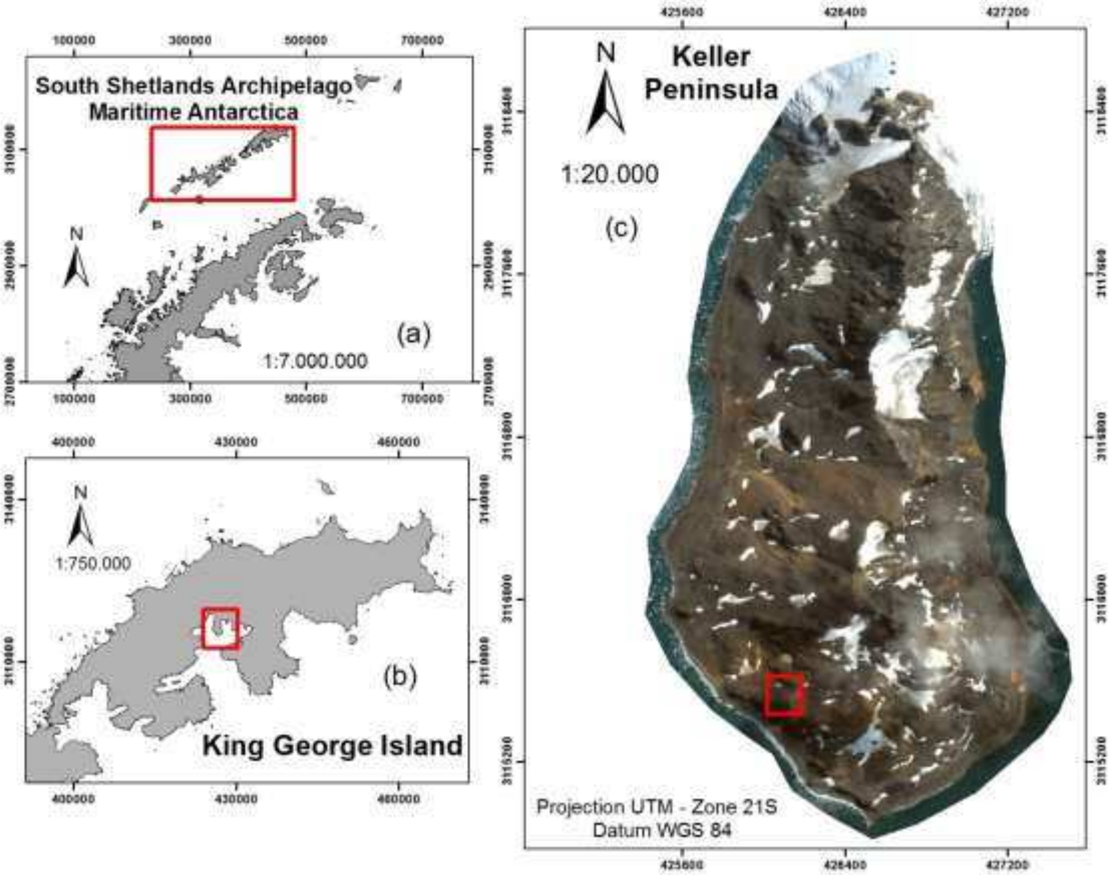

Fig 1. Illustrative map of South Shetlands Archipelago (a), where King George Island is localized, (b) and the selected study area in Keller Peninsula (c).

2.1.1 Grid establishment

To characterize the spatial variability of soil attributes in different directions, a 133-point 50 m x 50 m grid was installed (Fig. 2). The separation distance was 0.5, 1, 2.5, 5 and 10 m between sampling points, oriented in different directions (0, 45, 90 and 135º). Based on the main vegetation coverage and frequency of species that occur in the selected area, three sections were separated as represented in Fig 2.

Section 1: A slightly elevated site within the selected area, which is fringed by a small linear rock outcrop (Fig 2b). In this section, a vegetation community classified as “Fruticose lichens community” occur, mainly characterized by the presence of lichens (*Usnea antarctica* Du Rietz. and *Usnea aurantiaco-atra* (Jacq.) Bory.) growing on rock fragments. In rock fractures and micro depressions, mosses also occur, especially *Polytrichastum alpinum* (Hedwig) G. L. Smith growing in well-drained parts. Areas with incipient soil development only *Sanionia uncinata*, *Syntrichia saxicola* (Card.) R.H. Zander grows. Skuas nesting occur in this site, mainly in the middle of this section. Similar characteristic is also observed to occur in the end of the direction 0º.

Section 2: This section is located in the middle of the selected area. Vegetation community is classified as “moss-carpet community”. More relevant individuals are: *S. uncinata*, *Syntrichia saxicola*, *Chorisodontium aciphyllum* (Hook. f. and Wilson) Broth. and *Warnstorfia sarmentosa* (Wahlenb.) Hedenas. In the middle of this section, a more dense vegetation cover of mosses occurs, in which *S. uncinata* is predominant, growing in a poorly drained zone (Victoria et al., 2013; Putzke et al., 2015).

Section 3: Located on the east side of the studied area, this section is represented by a less dense mosses carpet, closer to the section 3 (Fig 2d). Towards the eastern side, vegetation coverage tends to disappear and bare soil is dominant. Small rock fragments can be observed in the soil surface without *Usnea* sp. colonization, with occasional visible erosive processes on the soil surface. Uncovered soils correspond to the last points in the directions 45, 90 and 135º.

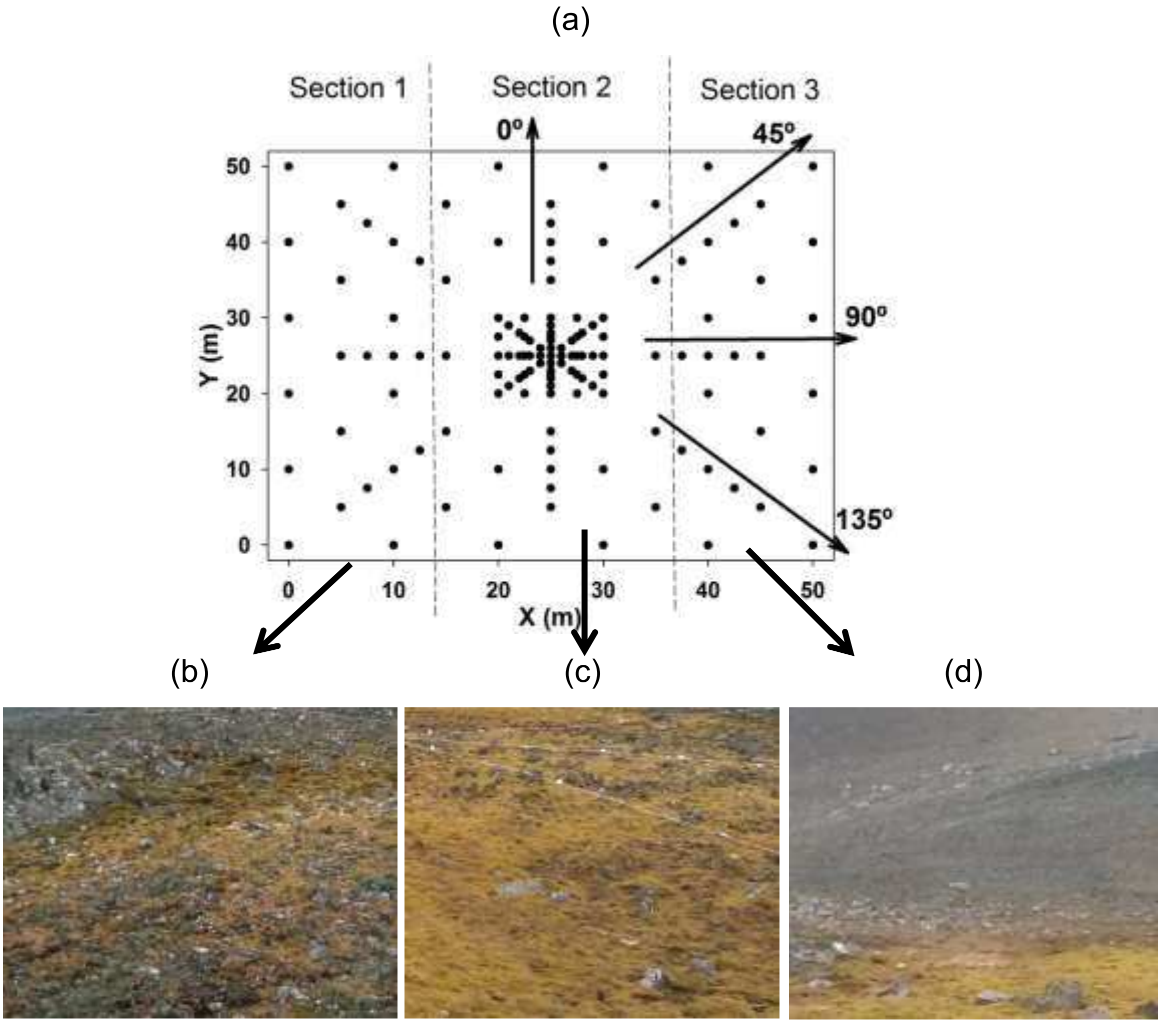

Fig. 2. Representation of the sampling grid installed (a) and delimited sections 1 (b), 2 (c) and 3 (d) in the selected area of Keller Peninsula.

2.2 Soil sampling

Soil was sampled in February 2015 to determine general soil attributes. Disturbed soil samples were taken at 0-10 cm depth from all 133 grid points in the selected area. Soil samples were air dried, grounded and sieved through a 2-mm mesh to remove the stone fraction and larger pieces of organic material. All soil samples were analyzed in the soil laboratory at the Universidade Federal de Viçosa, Minas Gerais, Brazil.

2.3. General soil attributes

In this study, 22 soil attributes were determined. The stoniness and rockiness were estimated by sieving of the >2mm fraction. The particle size distribution (sand, silt, and clay) was performed by the pipette method (Embrapa, 1997). The pH was determined on a 1:2.5 soil: deionized water ratio; the potential acidity (H + Al) was extracted with $Ca(OAc)_2$ 0.5 mol L^{-1} buffered to pH 7.0, and quantified by titration with NaOH 0.0606 mol L^{-1}. Exchangeable Ca^{2+}, Mg^{2+} and Al^{3+} were extracted with 1 mol L^{-1} KCl and Na^{+} and K^{+} were extracted with Mehlich-1 (Embrapa, 1997). The element content in the extracts were determined by atomic absorption (Ca^{2+}, Mg^{2+} and Al^{3+}), flame emission (Na^{+} and K^{+}) and photocolorimetry (P). The effective cation exchange capacity (CEC_E) was calculated by sum of cations (Ca^{2+}, Mg^{2+}, Na^{+}, K^{+} and Al^{3+}). Total cation exchange capacity (CTC_T) was estimated by the sum of bases and potential acidity.

Microelements (Fe^{2+}, Zn^{2+}, Mn^{2+} and Cu^{2+}) were extracted with 0.05 mol L^{-1} HC1 + 0.025 mol L^{-1} H_2SO_4, and determined using inductively coupled spectroscop. Total soil organic carbon was determined by wet oxidation with $K_2Cr_2O_7$ 0.167 mol L^{-1} in the presence of sulfuric acid with external heating (Yeomans and Bremner 1988). The remaining phosphorus was obtained after shaking a $CaCl_2$ 10 mmol L^{-1} solution containing of 60 mg L^{-1} of phosphorus with 5 g of soil during one hour. The remaining phosphorus in the solution gives an idea of the phosphorus adsorption capacity on the soil sample.

2.4 Spatial dependence analysis

General soil attributes were analyzed by geostatistic analysis in order to verify the occurrence of spatial dependence. The spatial dependence was verified by fitting theorical models to experimental semivariograms, based on the assumption of intrinsic stationary (Webster and Oliver, 1990). Isotropic and non-isotropic semivariograms were considered in this study when analyzing the spatial dependence of soil attributes. The semivariance estimation was determined by the equation 1:

$$\hat{\gamma}(\mathrm{h}) = \frac{1}{2N(\mathrm{h})} \sum_{i=1}^{N(h)} [z(\mathrm{x}_i) - z(\mathrm{x}_i + \mathrm{h})]^2 \qquad (1)$$

where $\hat{\gamma}(\boldsymbol{h})$ is the semivariance at a separation distance of ***h***; *N(**h**)* is the number of pairs separated by ***h;*** $z(\mathbf{x}_i)$ is the value of variable *Z* at point ***xi*** and Z(**x**i + **h**) is the value of variable Z at point ***x***i + ***h***. Theoretical models (i.e. spherical, gaussian and exponential) were used to describe the behavior of the semivariogram, which best represented the relationship between experimental semivariance and distance ***h*** (Isaaks and Srivatava 1989). In this study, the theoretical models were considered as shown in the equations 2:

$$\begin{cases} Gaussian: \hat{\gamma}(\mathrm{h}) = C_0 + C_1\{1 - \exp[-3(h/a)^2]\}; 0 < h < d \\ Exponential: \hat{\gamma}(\mathrm{h}) = C_0 + C_1\{1 - \exp[-3(h/a)]\}, h > 0 \\ Spherical: \hat{\gamma}(\mathrm{h}) = C_0 + C_1\left[\frac{3}{2}\left(\frac{\mathrm{h}}{a}\right) - \frac{1}{2}\left(\frac{\mathrm{h}}{a}\right)^3\right]; if\ 0 < \mathrm{h} < a; \hat{\gamma}(\mathrm{h}) = C_0 + C_1; if\ \mathrm{h} \geq a \end{cases} \qquad (2)$$

where *d* is the maximum distance over which the semivariogram is defined; *a* is the range distance; C_0 is the nugget effect, C_0 + C_1 is the sill (Isaaks and Srivastava, 1989). The semivariance value increases with separation distance of the points (***h*** distance) until a distance that the sill (C_0 + C_1) remains constant. The nugget effect (C_0) or y-intercept from the model, is the value where the adjusted theoretical model crosses the y axis. Also, nugget effect is considered the sampling error. The range distance (*a*) is the limit of the spatial dependence between points, where beyond that distance, the variable is spatially independent. When semivariance curve is flat rather than increasing trend, indicates insignificant spatial dependence, or that the data are randomly distributed in space (Isaaks and Srivastava, 1989).

The best adjust of the selected models were based on the smallest residual sum of squares (RSS) and the highest coefficient of determination (R^2). Cross-validation technique was also considered for estimating the performance of the theoretical model chosen, when estimating values in non-sampled points by using experimental data. The performance was based on the regression coefficient (better fit when closer to one), the y-intercept (better fit when closer to zero) and root mean square error (RMSE). The lower the RMSE is, the greater is the accuracy of estimate (Isaaks and Srivastava, 1989). The spatial dependence index (SDI) was determined by the ratio $C_1/(C_0 + C_1)$ classified by the following intervals: strong spatial dependence for SDI < 25%, moderate for 25% < SDI < 75% and low for SDI > 75% (Cambardella et al., 1994).

After having generated all the semivariogram models and the spatial dependence confirmed, values for each variable were estimated for non-sampled areas and thematic maps were generated using ordinary kriging interpolation method. This geostatistical interpolation method uses a linear impartial estimator with minimum variance, based on the property values of the closest neighbors, and takes into account the spatial variability structure found for the variable (Webster and Oliver, 1990).

2.5 Data analysis

General soil attributes were first analyzed by descriptive statistics (mean, minimum, maximum, coefficient of variation and standard error of mean) at each section. In order to verify differences on soil attributes among the delimited sections, one-way analysis of variance and Tukey multicomparison test of means ($p<0.05$) were performed. The 22 soil attributes determined were subjected to principal component analysis (PCA), in order to select the most significant soil variables that best represent the soil functions/characteristics in the studied area. In this study, only the first two principal components were selected at each section. For a given principal component, only soil attributes with high percentage explained were retained for geostatistic analysis. Highly weighted soil attributes were defined as absolute values within 10% of the highest, selecting a maximum of three soil attributes at each principal component.

Pearson correlation analysis ($p<0.05$) was performed among the soil attributes retained in the PCA. Descriptive statistical analyses and PCA were performed using the XLStat (XLStat, NY, USA, 2014) program. Spatial variability models were derived using GS+ software (Gamma Design Software, LLC, Plainwell, MI, USA, 1998) and kriging maps obtained using the software package ArcGIS Desktop 10.1 (Environmental Systems Research Institute, Redlands CA, USA).

3. Results

3.1. General soil attributes

General soil attributes in the three delimited sections are presented in Table 1. Overall, soil is characterized by high stoniness at soil surface in the three sections. Statistical difference ($p<0.05$) was observed for the mean soil physical and chemical attributes among the three different sections in the studied area. Mean values of sand, phosphorus and exchangeable Al were significantly higher ($p<0.05$) in section 1, whereas no statistical significance ($p>0.05$) was observed for mean values of silt, remaining phosphorus, total cation exchange capacity and copper. Mean values of clay, bases sum and effective cation exchange capacity were significantly lower ($p<0.05$) in section 1.

There is a statistical difference ($p<0.05$) among the three delimited sections for mean values of potential acidity and total organic carbon, as follow: section 1 > section 2 > section 3. On the other hand, the opposite was observed to occur for mean values of calcium and saturation of bases (section 1 < section 2 < section 3). Mean values of pH were significantly higher ($p<0.05$) in section 3, whereas mean values of potassium and sodium were significantly lower ($p<0.05$) in section 3. The coefficient of variation (CV) values ranged from 5 to 95%. Mean values of CV tended to be smaller in section 2 (32%) and greater in section 1.

Table 1. Descriptive statistics of soil attributes for the three delimited sections in the studied area of Keller Peninsula

	Section 1					Section 2					Section 3				
	Mean	Min	Max	CV	Error	Mean	Min	Max	CV	Error	Mean	Min	Max	CV	Error
> 2 mm (g kg^{-1})	527.50 b	234.23	744.44	0.22	21.76	567.61 ab	307.69	847.06	0.21	13.59	620.76 a	325.44	856.50	0.21	25.07
Sand (g kg^{-1})	577.86 a	344.00	725.00	0.13	14.50	540.80 b	434.00	628.00	0.08	4.92	547.86 b	459.00	622.00	0.08	7.95
Silt (g kg^{-1})	214.00 a	116.00	348.00	0.25	10.22	205.12 a	139.00	326.00	0.19	4.47	212.31 a	163.00	291.00	0.16	6.35
Clay (g kg^{-1})	208.07 b	153.00	308.00	0.17	6.85	254.17 a	156.00	289.00	0.08	2.42	239.72 a	205.00	275.00	0.08	3.62
pH	5.26 b	4.02	6.13	0.09	0.09	5.35 b	4.80	6.83	0.07	0.04	5.64 a	5.14	6.21	0.05	0.06
P (mg kg^{-1})	403.38 a	164.40	791.30	0.38	28.67	171.77 c	3.90	852.50	0.95	19.04	276.77 b	25.30	733.80	0.54	28.35
P-rem (mg L^{-1})	17.48 a	2.70	39.80	0.59	1.94	18.84 a	5.40	35.00	0.37	0.80	21.44 a	3.80	34.40	0.38	1.56
K ($cmol_c$ kg^{-1})	0.22 a	0.13	0.30	0.21	0.01	0.23 a	0.11	0.34	0.23	0.01	0.15 b	0.10	0.21	0.19	0.01
Na ($cmol_c$ kg^{-1})	0.42 a	0.22	0.62	0.23	0.02	0.47 a	0.01	0.69	0.23	0.01	0.31 b	0.18	0.46	0.24	0.01
Ca ($cmol_c$ kg^{-1})	7.41 c	1.91	11.90	0.37	0.52	10.42 b	6.45	17.52	0.24	0.29	13.23 a	5.85	28.46	0.49	1.24
Mg ($cmol_c$ kg^{-1})	5.65 bd	0.74	9.15	0.40	0.42	7.22 ac	3.74	12.17	0.29	0.25	6.16 cd	2.41	9.76	0.35	0.40
Al ($cmol_c$ kg^{-1})	3.27 a	0.00	8.10	0.79	0.49	1.41 b	0.00	4.30	0.60	0.10	1.15 b	0.00	3.40	0.98	0.21
H+Al ($cmol_c$ kg^{-1})	8.97 a	1.50	20.80	0.55	0.93	6.18 b	0.80	11.40	0.30	0.22	4.22 c	1.00	8.90	0.57	0.46
BS ($cmol_c$ kg^{-1})	13.70 b	3.26	21.37	0.35	0.90	18.34 a	11.84	28.02	0.20	0.43	19.85 a	10.96	32.58	0.28	1.06
CEC_E ($cmol_c$ kg^{-1})	16.97 b	8.16	21.91	0.19	0.60	19.75 a	14.57	28.62	0.17	0.39	21.00 a	13.96	32.58	0.24	0.97
CEC_T ($cmol_c$ kg^{-1})	22.67 a	17.16	25.46	0.09	0.37	24.52 a	17.57	33.62	0.14	0.40	24.06 a	18.00	34.38	0.20	0.89
S (%)	60.69 c	15.10	93.40	0.35	4.02	74.47 b	50.90	96.60	0.11	0.96	81.54 a	56.00	95.50	0.13	2.06
C (g kg^{-1})	20.79 a	5.22	100.17	0.95	3.74	14.43 b	3.07	53.48	0.63	1.06	7.28 c	2.20	18.56	0.46	0.63
Cu ($cmol_c$ kg^{-1})	4.02 a	1.60	7.16	0.27	0.21	4.04 a	2.33	9.09	0.28	0.13	3.88 a	2.28	6.29	0.25	0.18
Mn ($cmol_c$ kg^{-1})	69.45 cd	15.30	169.20	0.51	6.66	78.17 ac	35.00	176.40	0.36	3.29	57.08 bd	25.20	173.00	0.52	5.65
Fe ($cmol_c$ kg^{-1})	117.53 ac	50.10	281.00	0.50	11.04	107.59 cd	58.40	169.30	0.22	2.80	93.93 bd	62.20	157.90	0.28	4.91
Zn ($cmol_c$ kg^{-1})	2.27 cd	1.31	4.26	0.31	0.13	2.31 ac	1.31	3.85	0.26	0.07	1.89 bd	1.18	3.54	0.28	0.10

Means followed by the same letters in rows are equal (Tukey; $p < 0.05$); Min: minimum; Max: maximum; CV: coefficient of variation; Error: standard error of mean; >2mm: stoniness and rockiness; pH: active acidity (H2O); P: phosphorus; P-rem: remaining phosphorus; K: potassium; Na: sodium; Ca: calcium; Mg: magnesium; Al: aluminium; H+Al: potential acidity; BS: bases sum; CECE: effective cation exchange capacity; CECT: total cation exchange capacity; S: saturation of bases; C: total organic carbon; Cu: copper; Mn: manganese; Fe: Iron; Zn: Zinc.

3.2 Principal component and correlation analysis

Results of the principal component analysis are shown in Table 2. The two principal components explained 61.78, 44.07 and 54.55% of the total variance in the data set for section 1, 2 and 3, respectively. According to the Kaiser criterion (Kaiser, 1960), all eigenvalues were higher than 1.00, being indicated to explain the total variance in the entire data set for each section. In section 1, three soil attributes were selected in the PC1: potential acidity, bases sum and saturation of bases. Also, in the PC2, sand and silt were considered highly weighted soil attributes. Calcium, saturation of bases, pH and magnesium were selected in the PC1 e PC2 in section 2. In section 3, remaining phosphorus was selected in the PC1 and iron in the PC2. Thus, ten soil attributes were considered highly weighted and selected to model the spatial dependence, as follow: sand, silt, pH, exchangeable Ca^{2+} and Mg^{2+} potential acidity, bases sum, saturation of bases, remaining phosphorus and soluble iron.

Table 3 present the pearson correlation matrix for the selected soil attributes through principal component analysis. Significant correlation coefficients (p<0.05) were obtained for 73% (33 significant correlations) of the total possible correlations among the selected soil variables. However, only 12% of the significant correlations had values greater than 0.80, being: positive correlations between calcium with bases sum (r=0.89; p<0.05) and bases sum with saturation of bases (r= 0.82; p<0.05), and negative correlations between sand with silt (r= -0.82; p<0.05) and potential acidity with saturation of bases (r= -0.97; p<0.05).

Table 2. Results of the principal component analysis for the first two principal components (PCs) for each section in Keller Peninsula

Principal components	---Section 1--- PC1	PC2	---Section 2--- PC1	PC2	---Section 3--- PC1	PC2
Eigenvalue	9.81	3.77	6.26	3.44	7.35	4.65
Variability (%)	44.60	17.17	28.44	15.63	33.40	21.14
Cumulative (%)	44.60	61.78	28.44	44.07	33.40	54.55
			% explained			
> 2 mm (g kg^{-1})	1.51	1.61	2.11	1.68	0.32	6.97
Sand (g kg^{-1})	0.75	**17.21**	0.05	5.41	0.61	9.51
Silt (g kg^{-1})	1.31	**16.15**	0.37	11.66	0.62	5.94
Clay (g kg^{-1})	0.02	7.70	0.48	2.43	0.12	6.07
pH	6.56	0.28	0.72	**13.85**	9.12	0.01
P (mg kg^{-1})	3.71	3.03	2.41	3.48	3.78	1.48
P-rem (mg L^{-1})	3.17	12.29	7.43	0.10	4.69	**11.45**
K ($cmol_c$ kg^{-1})	1.08	1.24	0.04	0.35	0.96	1.86
Na ($cmol_c$ kg^{-1})	3.77	0.01	0.03	0.22	0.21	2.85
Ca ($cmol_c$ kg^{-1})	8.31	0.66	**12.52**	0.00	**10.65**	0.04
Mg ($cmol_c$ kg^{-1})	8.66	0.22	3.08	**13.69**	1.85	1.10
Al ($cmol_c$ kg^{-1})	5.99	4.35	7.85	1.33	8.37	4.15
H+Al ($cmol_c$ kg^{-1})	**9.03***	1.85	8.87	4.37	8.93	5.34
BS ($cmol_c$ kg^{-1})	**9.65**	0.06	11.81	4.20	**10.72**	0.43
CEC_E ($cmol_c$ kg^{-1})	7.15	1.79	9.21	6.33	8.86	1.37
CEC_T ($cmol_c$ kg^{-1})	0.00	7.95	4.30	11.27	5.63	3.84
S (%)	**9.64**	0.98	**13.80**	0.39	**11.49**	2.22
C (g kg^{-1})	5.44	0.96	3.43	0.78	0.88	3.16
Cu ($cmol_c$ kg^{-1})	1.71	8.70	5.36	8.32	2.15	9.50
Mn ($cmol_c$ kg^{-1})	3.53	4.63	0.84	3.72	5.65	4.33
Fe ($cmol_c$ kg^{-1})	7.90	0.01	4.50	1.85	0.21	**13.39**
Zn ($cmol_c$ kg^{-1})	1.14	8.33	0.81	4.56	4.17	4.99

*Boldface values are considered highly weighted. >2mm: stoniness and rockiness; pH: active acidity (H_2O); P: phosphorus; P-rem: remaining phosphorus; K: potassium; Na: sodium; Ca: calcium; Mg: magnesium; Al: aluminium; H+Al: potential acidity; BS: bases sum; CEC_E: effective cation exchange capacity; CEC_T: total cation exchange capacity; S: saturation of bases; C: total organic carbon; Cu: copper; Mn: manganese; Fe: Iron; Zn: Zinc.

Table 3. Pearson correlation matrix among the selected soil attributes in the principal component analysis

	Sand	Silt	pH	Ca	Mg	H+Al	BS	S	Prem	Fe
Sand										
Silt	**-0.82**									
pH	**-0.24**	**0.34**								
Ca	-0.15	0.11	**0.50**							
Mg	**-0.18**	0.01	0.01	0.04						
H+Al	0.15	-0.11	**-0.65**	**-0.65**	**-0.26**					
BS	**-0.21**	0.11	**0.44**	**0.89**	**0.50**	**-0.68**				
S	**-0.19**	0.12	**0.63**	**0.75**	**0.39**	**-0.97**	**0.82**			
Prem	**0.27**	**-0.26**	**0.23**	**0.45**	0.12	**-0.65**	**0.45**	**0.63**		
Fe	0.02	-0.01	**-0.38**	**-0.34**	**-0.36**	**0.67**	**-0.46**	**-0.67**	**-0.52**	

The bolded values are significant correlation coefficients (p<0.05); P-rem: remaining phosphorus; Ca: calcium; Mg: magnesium; H+Al: potential acidity; BS: bases sum; S: saturation of bases; Fe: Iron.

3.3 Spatial dependence analysis

Model type, estimated parameters and cross-validation of experimental semivariograms obtained for the selected soil attributes are presented in Table 4. All the selected soil attributes showed spatial dependence structure according to the modeled experimental semivariograms (Table 4 and Fig 3). Spatial dependence patterns were best established using isotropic models for all the soil attributes. Exponential models were fitted to sand, silt, magnesium and bases sum; Spherical models to pH and remaining phosphorus; and Gaussian models to calcium, potential acidity, saturation of bases and iron. Range values varied from 11.7 m to 37.17 m for magnesium and remaining phosphorus, respectively. Also, pH and saturation of bases had range values greater than 30 m. On the other hand, range value lower than 15 m was observed to occur for base sum, magnesium and iron. Spatial dependence index (SDI) ranged from 67.5 to 88.30% for sand and bases sum, respectively, showing that there are no strong spatial dependence for the selected soil attributes (SDI < 25%). All coefficient of determination of the models were greater than 0.79, reaching to 0.94 for potential acidity.

Thematic maps obtained by ordinary kriging are presented in Fig. 4. Results show a tendency of silt accumulation on the lower part of the selected area, whereas sand contents tended to be higher on the upper zone of the selected area (especially in the upper part of section 1). The obtained thematic maps from ordinary kriging showed strong spatial relationship among pH, remaining phosphorus, calcium, potential acidity, bases sum, saturation of bases and iron. In zones where pH tended to be lower, values of remaining phosphorus, calcium, bases sum and saturation of bases are reduced. On the other hand, in zones where the environment if less acid, values of potential acidity and iron tended to be more elevated.

Table 4. Model type and parameters of the experimental semivariograms fitted to the selected soil attributes

	Model	C_0	$C_0 + C_1$	Range (m)	SDI (%)	RSS	R^2	a	b	RMSE
Sand	Exponential	824.00	2535.00	26.43	67.50	81.8 E04	0.79	0.74	139.68	0.171
Silt	Exponential	416.00	1808.00	17.73	77.00	32.69E03	0.84	0.35	134.56	0.190
pH	Spherical	0.04	0.17	34.74	77.00	4.57E-03	0.87	0.76	1.26	0.130
Prem	Spherical	16.40	61.89	37.17	73.50	275.00	0.92	0.98	0.31	0.149
Ca	Gaussian	2.11	6.95	25.21	69.10	3.79	0.93	0.61	3.51	0.169
Mg	Exponential	0.62	5.05	11.70	87.70	1.83	0.87	1.05	-0.33	0.107
H+Al	Gaussian	1.87	12.28	18.35	84.10	10.91	0.95	0.91	0.56	0.070
BS	Exponential	3.29	21.18	14.22	88.30	37.50	0.87	1.02	-0.28	0.103
S	Gaussian	38.30	152.50	33.23	73.45	116.00	0.94	0.95	3.05	0.120
Fe	Gaussian	175.00	1431.00	13.76	87.80	18.4E03	0.93	0.66	36.10	0.100

C_0: nugget effect; C_0 + C_1: sill; SDI: spatial dependence index; RSS: residual sum of squares; RMSE: root mean square error; P-rem: remaining phosphorus; Ca: calcium; Mg: magnesium; H+Al: potential acidity; BS: bases sum; S: saturation of bases; Fe: Iron.

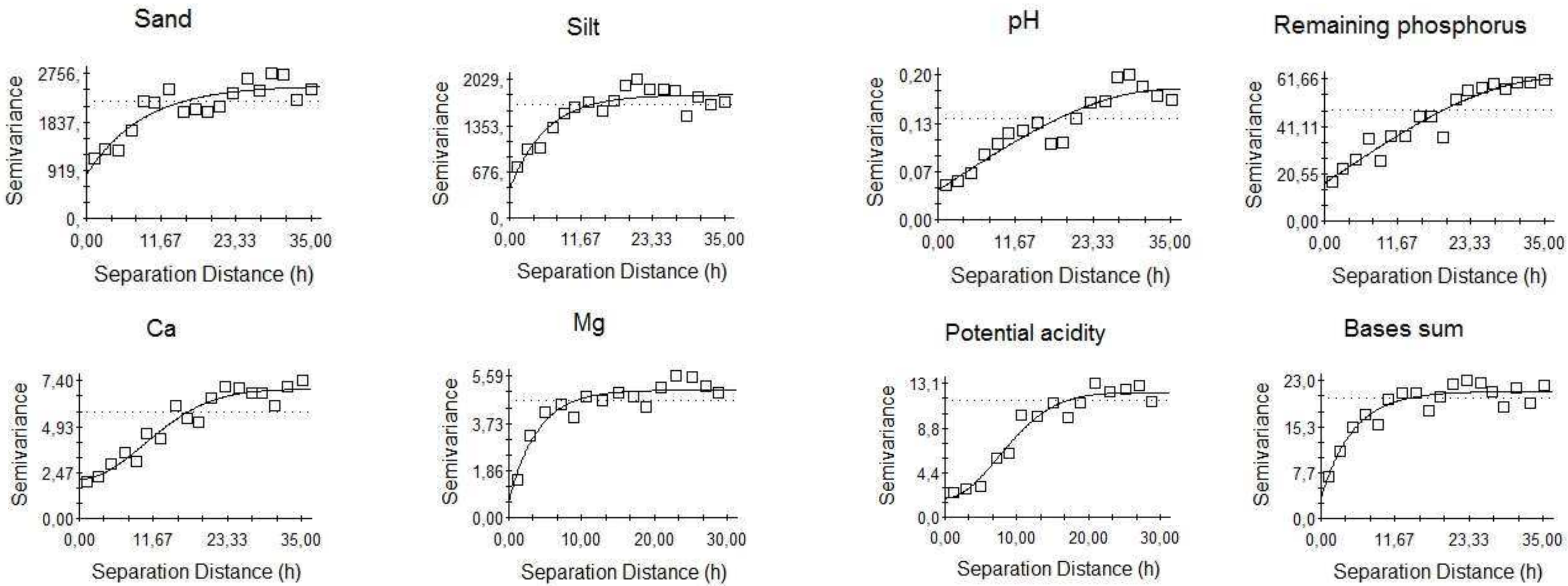

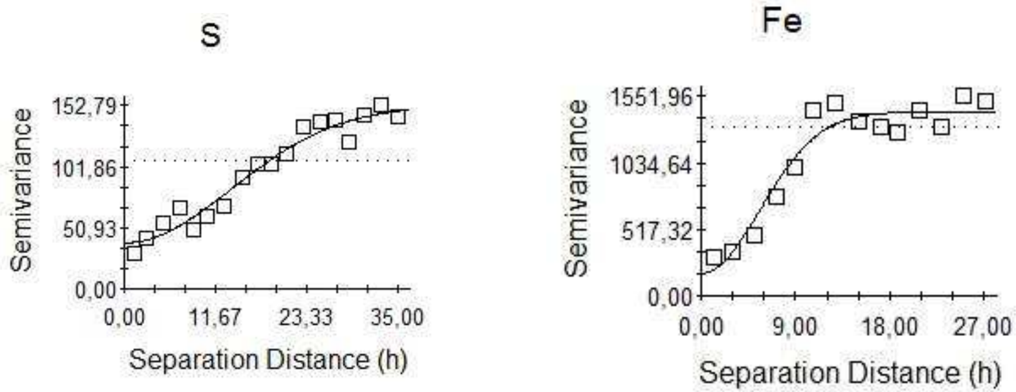

Fig. 3. Experimental semivariograms fitted to sand, silt, pH, remaining phosphorus (Prem), exchangeable Ca and Mg, potential acidity (H+Al), bases sum, saturation of bases (S) and extracted Iron (Fe) in the studied area of Keller Peninsula.

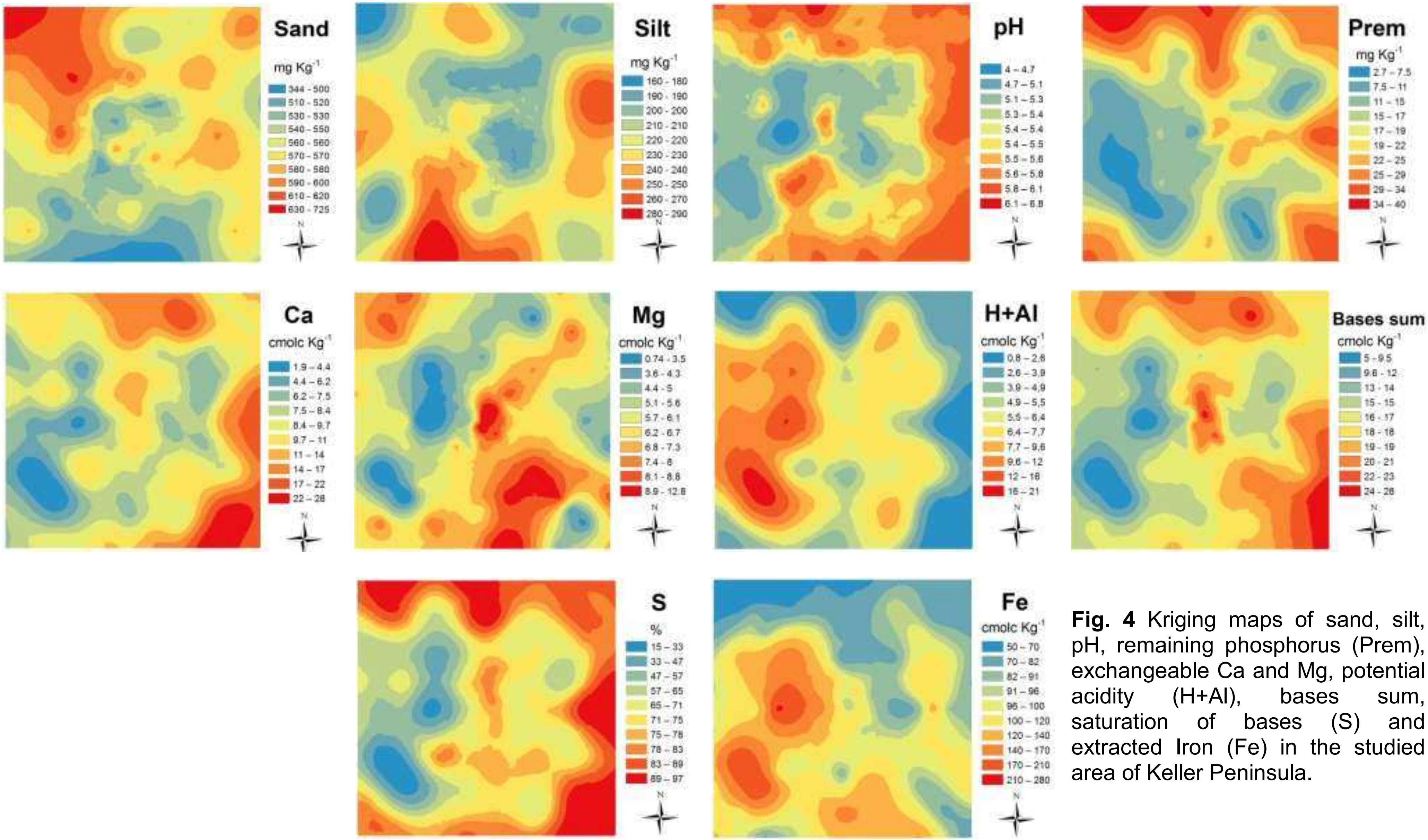

Fig. 4 Kriging maps of sand, silt, pH, remaining phosphorus (Prem), exchangeable Ca and Mg, potential acidity (H+Al), bases sum, saturation of bases (S) and extracted Iron (Fe) in the studied area of Keller Peninsula.

4. Discussion

Selected soil attributes trough principal component analysis are mainly related to the remarkable soil nutrients availability, increased acid by guano mineralization and advanced mineral weathering in periglacial zones of Maritime Antarctica, compared to other regions of Antarctica. This characteristics has widely been documented in the literature (Michel et al., 2006; Simas et al., 2007, Simas et al., 2008, Schaefer et al., 2008, Francelino et al., 2011, Moura et al., 2012, Souza et al., 2014), but not selected and mapped by both multivariate analysis and geostatistic, respectively. The coefficient of variation may indicate the initial evaluation of heterogeneity or homogeneity of soil attributes in a survey. However, it may not be efficient when applied individually, in which real spatial variation could be masked. In this case, the geostatistic associated with multivariate analysis are recommended (Teixeira et al., 2011).

In the current study, Exponential, Spherical and Gaussian models were selected to describe the spatial variability, which has already been proved to be efficient for describe spatial dependence of soil attributes (Mendonça et al., 2010, La Scala et al., 2010; Teixeira et al., 2011; Thomazini et al., 2014). The low and moderate spatial dependence reported are related to the high variability of soil attributes in short distances in periglacial zones of Maritime Antarctica (Thomazini et al., 2015) and due extrinsic factors, such as input of nutrients and organic matter (i.e. guano) and fast modification of the vegetation on the landscape, which typically occur in Maritime Antarctica (Francelino et al., 2011).

The selected typical periglacial area of Keller Peninsula presented differences on soil attributes along the delimited sections, mainly in function of the variables related to the environment, such as guano deposition coupled with high amounts of organic matter, drainage and vegetation communities' predominance. Therefore, a differentiated soil development can be observed along the delimited sections, as indicated in the thematic kriging maps of soil attributes (Fig 4). Schaefer et al. (2008) and Simas et al. (2008) reported that soils in Maritime Antarctica can be weak or strongly influenced by guano, being classified as 'soils under weak ornithogenic influence' and 'ornithogenic soils'. In the current study, part of the soils in the selected area are classified as 'soils under weak ornithogenic influence', since Skua nests occur sparsely with limited guano deposition, especially in the middle of the section 1. In this section soils can be classified as ornithogenic since in some sampled points, values of phosphorus reached to 852.5 mg kg^{-1} (Simas et al., 2008).

In Maritime Antarctica, mean values of phosphorus were reported to be almost nine times higher in ornithogenic than non-ornithogenic soils (Moura et al., 2012). Possibly, a more pronounced influence of birds occurred in the past in the studied area, since is possible to observe abandoned Skua nests in the area. Despite being weakly influenced, deposition of guano associated with high amounts of organic matter had strong influence on the soil development and vegetation colonization in the selected area, as indicated by the results in Table 1.

Keller Peninsula is highly subjected to active periglacial erosion, with a marked influence of solifluction (Francelino et al., 2011), which can modify soil physical and chemical attributes. It can be confirmed by the pattern observed for silt and sand on the thematic kriging maps in Fig 4. In the current study, greater clay contents were detected in the middle of the selected area (section 1) compared to the other sections, despite of the low range of values typically found in this region (Simas et al., 2008). In ornithogenic soils, phosphatization enhances clay formation more than other soil forming processes (Pereira et al., 2013). However, results suggest that clay is being transported and accumulated in areas where guano is less at 0-10 cm depth. In addition, cryoturbation in Maritime Antarctica is higher than in other regions in Antarctica, which can increase soil nutrients with depth (Schaefer et al., 2008; Pereira et al., 2013). Since only 0-10 cm layer was sampled, further research is needed to confirm this.

Results reported by Albuquerque-Filho (2005) showed that mean values of phosphorus increased with depth at the same areas. This emphasizes and confirms greater phosphorus availability with depth, promoted by cryoturbation and possibly, by dense populations of birds in the past. Also, these results indicate that spatial variability of soil attributes can present different pattern in deep soil layers, which can be further confirmed.

Results suggest that the deposition of guano increased the organic matter contents more than dense moss carpets (section 2). Moss carpets are reported to create organic soil layers (Simas et al., 2007), representing the most important atmospheric CO_2 sink in Maritime Antarctica in some cases (Thomazini et al., 2015). Results are in accordance with Michel et al. (2006) and Simas et al. (2007), showing that soils under ornithogenic influence have high exchangeable Al saturation in the topsoil, as demonstrated in the section 1, evidencing that organic matter is associated with exchangeable Al. Pereira et al. (2013) also reported that greater mineralization rates of guano, contribute to increased soil acidification and exchangeable Al contents in the soil. In section

1, soil chemical weathering is more pronounced and soils present chemical and mineralogical characteristics highly influenced by chemical reactions (Simas et al., 2006), which appear to more influencing soil attributes at section 3. This result is in agreement with Simas et al. (2007), who reported that chemical attributes of soils at Keller Peninsula are consistent with the geochemistry of the basaltic parent rock, when guano influence is reduced.

Moura et al. (2012) stated that calcium contents are reduced under ornithogenic influence, being up to seven times lower. In this study, calcium contents were almost two times lower in section 1 compared to sections 2 and 3, indicating a similar trend. Due to the extremely acid reaction during ornithogenesis ($pH<2.0$), apatite forms of reduced availability may also be partially dissolved, leading to lower Ca availability (Simas et al., 2007). High correlation was observed between exchangeable Ca and bases sum ($r=0.89$), suggests that calcium contents strongly contributed to the bases sum in these soils. This can be further confirmed by the similarity among isolines in the thematic kriging maps of calcium and bases sum. Soils are mostly eutrophic with potential acidity generally lower than those stated by Pereira et al. (2013). In some cases, the oxidation of nitrogen and sulfur compounds from guano and organic matter may enhance potential acidity, forming dystrophic soils even with elevated bases sum (Simas et al., 2007; Pereira et al., 2013). Due to relatively lower guano impact, this is not so marked in the studied soils.

Additionally, a strong spatial relationship was observed between potential acidity and saturation of bases, indicated by the well-defined inverse similarity on the themathic kriging maps. Overall, soil is more developed under ornithogenic influence in Maritime Antarctica (Simas et al., 2007; Schaefer et al., 2008). For this reason, we expected soil more developed in section 1.

Hence, values of remaining phosphorus were closely related to the soil development, and tended to be lower in section 1, especially in the middle of this section. Possibly, distinct soil mineralogy in this section account for the above mentioned results.

Guano is rich in nutrients, especially nitrogen and phosphorus, which reacts with the soil matrix and produces some strong acids (i.e. H_2SO_4 and HNO_3) during guano mineralization, reducing values of pH and contributing to increased soil acidification (Schaefer et al., 2008, Moura et al., 2012). In the current study, a gradient of variation of pH values can be observed in Fig 4. Where guano is deposited the soil is more acid, notably in the middle of the section 1. As the influence of guano decrease, pH values increase reducing soil acidification, towards the section 3. Moura et al. (2012), reported that mean values of 4.7 for pH, reaching to 3.4, in the ornithogenic soils in Maritime Antarctica, being the most developed soils, showing the lowest pH.

Results suggest a strong relationship between guano deposition, conjugated with high amounts of organic matter and vegetation cover with soil attributes, in which, pH is the main soil attribute governing the availability of most selected soil attributes. As shown in Fig 4, in zones where soil is less acid, values of remaining phosphorus, calcium, bases sum and saturation of bases tended to be elevated, especially towards the section 3. On the other hand, values of potential acidity and iron were lower in more acid zones, especially towards the section 1. Hence, these patterns can be extrapolated to other similar areas in Maritime Antarctica, since the selected area comprises the main terrestrial ecosystems and processes/influences that the soil can be subjected in this environment. However, supplementary studies need to be developed, as little is known and documented regarding the spatial variability and mapping of soil attributes in Maritime Antarctica.

5. Conclusions

In a typical periglacial area in Maritime Antarctica, the input of guano coupled with high amounts of organic matter, and the remarkable transition of vegetation cover, strongly influence the soil development and nutrients assembly. Typically, soils are mainly characterized by the high amounts of bases and weak clay formation. In zones with weak ornithogenic influence, soil is acid and values of exchangeable aluminum are high, associated with elevated potential acidity and increased iron availability. Moreover, pH is governing the availability of bases, especially calcium. On the other hand, in zones where there is no guano deposition, soil nutrient status is closely related to the parent material. Also, spatial variability of soil attributed strongly varies in short distances due the high heterogeneity imposed by the environment and landscape conditions. Furthermore, this study shows the possibilities of using geostatistic to characterize and map soil attributes in periglacial areas of Maritime Antarctica. This preliminary study by using a detailed grid, revealed an efficient approach to describe the spatial variability at small and medium scales. Hence, further research using other scales need to be applied to increase the knowledge of spatial variability of soil attributes in periglacial zones.

Acknowledgments

We acknowledge CNPq (Conselho Nacional de Desenvolvimento Científico e Tecnológico) (556794/2009-5) and MCTI (Ministério da Ciência, Tecnologia e Inovação) for granting financial support. This work is a contribution of INCT-Criosfera TERRANTAR group.

References

Albuquerque-Filho, M. R. Geoquímica de solos da Península Keller, Ilha Rei George, Antártica, como subsídio ao monitoramento ambiental. 129p. Tese (Doutorado em Solos e Nutrição de Plantas) – Universidade Federal de Viçosa, 2005.

Blume, H.P., Chen, J., Kalk, E., Kuhn, D., 2004. Mineralogy and weathering of Antarctic Cryosols. In: Kimble, J.M. (Ed.), Cryosols: Permafrost Affected Soils. Springer-Ver- lag, Berlin, pp. 415–426.

Cambardella, C.A., Moorman, T.B., Novak, J.M., Parkin, T.B., Karlen, D.L., Turco, R.F. Konopka, A.E., 1994. Field-scale variability of soil properties in central Iowa soils. Soil Sci. Soc. Am. J. 67, 58, 1501–1511.

Embrapa, 1997. Manual de Métodos de Análise de Solo. 2. ed. ver. atualiz. Centro Nacional de Pesquisa de Solos, Rio de Janeiro (212 pp. il., EMBRAPA/CNPS-RJ. Documentos, 1).

Francelino, M.R., Schaefer, C.E.G.R., Simas, F.N.B., Filho, E.I.F., Souza, J.J.L.L., Costa, L.M., 2011. Geomorphology and soils distribution under paraglacial conditions in an ice-free area of Admiralty Bay, King George Island, Antarctica. Catena, 85, 194–204.

Hawkes, D.D., 1961. The geology of the South Shetland Islands: I, The petrology of King George Island. Falkland Islands Dependencies Survey, 26. 28 pp.

INPE, 2015 Instituto Nacional de Pesquisas Espaciais-CPTEC <http://antartica.cptec.inpe.br/~antar/ weatherdata.shtml>.

Isaaks, E.H., Srivastava, R.M., 1989. An introduction to applied geostatistics. New York: Oxford University Press, 592 pp.

Kaiser, H.F., 1960. The application of electronic computers to factor analysis. Educ. Psychol. Meas. 20, 141–151

La Scala, N., Mendonça, E.S., Souza, J.V., Panosso, A.R., Simas, F.N.B., Schaefer, C.E.R.G., 2010. Spatial and temporal variability in soil CO_2 emissions and relation to soil temperature at King George Island, Maritime Antarctica. Polar Sci. 4, 479-487.

Mendonça, E.S., La Scala, N., Panosso, A.R., Simas, F.N.B., Schaefer, C.E.G.R., 2010. Spatial variability models of CO_2 emissions from soils colonized by grass (*Deschampsia antarctica)* and moss (*Sanionia uncinata*) in Admiralty Bay, King George Island. Antarc. Sci. 23, 27-33.

Michel, R.F.M., Schaefer, C.E.G.R., Dias, L., Simas, F.N.B., Benites, V., Mendonca, E.S., 2006. Ornithogenic gelisols (cryosols) from Maritime Antarctica: pedogenesis, vegetation and carbon studies. Soil Sci. Soc. Am. J. 70, 1370–1376.

Moura, P.A., Francelino, M.R., Schaefer, C.E.G.R., Simas, F.N.B., Mendonça, B.A.F., 2012. Distribution and characterization of soils and landform relationships in Byers Peninsula, Livingston Island, Maritime Antarctica. Geomorphology, 155-156, 45–54.

Pereira, T.T.C., Schaefer, C.E.G.R., Ker, J. C., Almeida, C.C., Almeida, I.C.C., Pereira, A. B., 2013. Genesis, mineralogy and ecological significance of ornithogenic soils from a semi-desert polar landscape at Hope Bay, Antarctic Peninsula. Geoderma, 209-210, 98–109.

Pereira, A.B., Putzke, J., 2013. The Brazilian research contribution to knowledge of the plant communities from Antarctic ice free areas. Anais da Academia Brasileira de Ciências (Impresso), 85, 923-935.

Putzke, J.; Athanásio, C.G.; Albuquerque, M.P.; Victoria, F.C. & Pereira, A.B. 2015. Comparative study of moss diversity in South Shetland Islands and in the Antarctic Peninsula. Revista Chilena de Historia Natural, 88: 01-06, 2015.

Schaefer, C.E.G.R., Simas, F.N.B., Gilkes, R.J., Mathison, C., Costa, L.M., Albuquerque, M.A., 2008. Micromorphology and microchemistry of selected Cryosols from Maritime Antarctica. Geoderma 144, 104–115.

Simas, F.N., Schaefer, C.E.R.G., Melo, V.F., Guerra, M.B.B., Saunder, M., Gilkes, R.J., 2006. Clay-sized minerals in permafrost-affected soils (cryosols) from King George Island, Antarctica. Clays Clay Miner. 54, 723–738.

Simas, F.N.B., Schaefer, C.E.G.R., Albuquerque Filho, M.R., Francelino, M.R., Fernandes Filho, E.I., Costa, L.M., 2007. Genesis, properties and classification of Cryosols from Admiralty Bay, Maritime Antarctica. Geoderma 144, 116–122.

Simas, F.N.B., Schaefer, C.E.G.R., Albuquerque-Filho, M.R., Francelino, M.R., Fernandes Filho, E.I., Costa, L.M., 2008. Genesis, properties and classification of Cryosols from Admiralty Bay, Maritime Antarctica. Geoderma 144, 116–122.

Souza, K.K.D., Schaefer, C.E.G.R., Simas, F.N.B., Spinola, D.N., De Paula, M.D., 2014. Soil formation in Seymour Island, Weddell Sea, Antarctica. Geomorphology 225, 87–99.

Tatur, A., Barczuk, A., 1985. Ornithogenic phosphates on King George Island, maritime Antarctic. In: Siegfried, W.R., Condy, P.R., Laws, R.M. (Eds.), Antarctic Nutrient Cycles and FoodWebs. Springer–Verlag, Berlin, pp. 163–169.

Teixeira, D.D.B., Panosso, A.R., Cerri, C.E.P., Pereira, G.T., La Scala, N., 2011. Soil CO_2 emission estimated by different interpolation techniques. Plant Soil 345, 187–194.

Thomazini, A., Mendonça, E.S., Teixeira, D.B., Almeida, I.C.C., La Scala, N., Canellas, L. P., Spokas, K.A., Milori, D.M.B.P. Turbay, C.V.G., Fernandes, R.B.A., Schaefer, C.E.G.R. 2015. CO_2 and N_2O emissions in a soil chronosequence at a glacier retreat zone in Maritime Antarctica. Sci. Total Environ. 521-522, 336–345.

Thomazini, A., Teixeira, D.B., Turbay, C.V.G., La Scala Jr, N., Schaefer, C.E.G. R., Mendonça, E.S., 2014. Spatial variability of CO2 emissions from newly exposed paraglacial soils at a glacier retreat zone on King George Island, Maritime Antarctica. Permafr. Periglac. Process. 25, 233–242.

Turner, J., Bindschadler, R., Convey, P., 2009. Antarctic Climate Change and the Environment. Scientific Committee on Antarctic Research, Cambridge, p. 526.

Victoria, F.C., Alburqueque, M.P., Pereira, A.B., Simas, F.N.B., Spielmann, A.A., Schaefer, C.E.G.R., 2013. Characterization and mapping of plant communities at Hennequin Point. King George Island, Antarctica. Polar Res. 32, 19261.

Webster, R. Oliver, M.A. 1990. Statistical methods in soil and land resource survey. Oxford: Oxford University Press, 316 pp.

Yeomans, J.C., Bremner, J.M., 1988. A rapid and precisemethod for routine determination of organic carbon in soil. Communications in Soil Science and Plant Analyses, New York 19, pp. 1467–1476.

CAPÍTULO 4

Long-term net ecosystem exchange from two typical vegetation communities in olivine-basalt soils from Coppermine Peninsula, Maritime Antarctica

Abstract

THOMAZINI, André, D.Sc., Universidade Federal de Viçosa, April, 2016. **Long-term net ecosystem exchange from two typical vegetation communities in olivine-basalt soils from Coppermine Peninsula, Maritime Antarctica.** Adviser: Márcio Rocha Francelino. Co-advisers: Carlos Ernesto Gonçalves Reynaud Schaefer and Eduardo de Sá Mendonça.

Climate warming is greatly affecting terrestrial ecosystems of Maritime Antarctica, especially due the alterations in soil temperature and moisture, which strongly alter carbon dynamics. Hence, the contribution of terrestrial ecosystems to act as a sink or source of CO_2 is still unclear. The objective of this study was to evaluate net ecosystem exchange (NEE), soil temperature and moisture based on long-term *in situ* measurements from two typical vegetation communities in Coppermine Peninsula, Robert Island, Maritime Antarctica. A moss site (hereafter Site 1) and a moss/lichen site (hereafter Site 2) were selected on February 2014. Soil temperature and moisture were monitored from February 2014 to January 2016. NEE was measured in situ on January 2016. Soil was sampled at 0-5 and 5-20 cm depth. Significant differences on soil attributes, NEE, soil temperature and moisture occur when comparing both sites. Site 1 is mainly characterized by the hydromorphic environment, where soil temperature is less varied than Site 1, showing greater number of isothermal days where thaw is more pronounced. On the other hand, strong variations in soil temperature occurred in Site 2, where freeze is more evident and permafrost is contributing to reduce soil temperature in the sampled depth. Both sites act as a carbon sink, with major potential recorded in Site 1, reaching an uptake of 704.39 g CO_2 m^{-2} during the monitored period. Under increasing climate warming, well-drained mixed community Site 2 will progressively act as a source of CO_2 to the atmosphere. The exchange of CO_2 is Maritime Antarctica is highly controlled by the type of vegetation, soil temperature and moisture regimes. Extensive moss carpets represent the major sites of carbon sink in Maritime Antarctica. Further research is needed to investigate the potential of mosses/lichens communities to act as a sink of CO_2 without permafrost influence.

Keywords: climate warming, greenhouse gas emission, carbon dioxide, temporal analysis

1. Introduction

Antarctica is undergoing several changes due climate change, especially due the increase in air temperature. Turner et al. (2014) reported that since 1950s, mean air temperatures have raised significantly on the Antarctic Peninsula (up to 2.8ºC), where the influence of temperature is more pronounced than in any other region of the planet. In the last decades, some records represented the highest temperature ever recorded on the Antarctic continent (+17.5ºC at Esperanza Station) (Turner et al., 2014). These changes are severely taking place along the Antarctic Peninsula reaching to Maritime Antarctica, where in lower latitudes the effects of increase in air temperature may cause several changes on the terrestrial environments (Newsham et al., 2015). Plants colonization/growing, glacier and permafrost melting, soil development and exchange of carbon are reported to be highly affected by climate change in Antarctica (Clarke et al., 2012; Almeida et al., 2014; Newsham et al., 2015; Thomazini et al., 2015), being possible to use them as proxy of climate change.

Despite being characterized by lower temperatures even during the austral summer, a large number of mosses, lichens and algae occur in Maritime Antarctica. In ice-free areas, bryophytes are represented by 110, liverworts 22 and lichen 360 species, approximately (Pereira and Putzke, 2013). Native flowering plants are represented by only two species: *Deschampsia antarctica* Desv. (Poaceae) and *Colobanthus quitensis* (Kunth) Bartl (Caryophyllaceae). *Poa annua* L. (Poaceae) is an introduced flowering plant introduced, coming from Europe, and initially observed on the vicinity of Arctowski research station on King George Island (Pereira and Putzke, 2013). The distribution of plant communities has an irregular pattern across the landscape, being directly associated with water regime, nutrients availability and deposition of guano (Victoria et al., 2013). Species of *Usnea antartica* and *Cladonia* spp. generally occur in places with large number of rock fragments on the soil surface, where soil is well-drained and moderately to weakly developed. On the other hand, mosses patches (especially represented by *Sanionia uncinata* (Hedw.) Loeske.) grow on marine terraces and poorly-drained zones, where soil is only incipiently developed. *Politrichum* sp and *Bryum* spp., also may grow on marine terraces; however, other mosses, like these mosses preferably occur on soil with lower water contents. The flowerings plants are characterized by occur on well-developed soils, rich in nutrients and/or ornithogenic areas (Simas et al., 2007, Victoria et al., 2013).

The vegetation species distribution in Maritime Antarctica is highly heterogeneous on the landscape, being governed mainly by water regime and soil characteristics. Is well-known that periglacial zones constantly undergo changes, intensified in the last decades due climate change (Turner et al., 2014). Notably, glacier melting has been occurring due increases in air temperature, which promote appearance of new hydromorphic areas, while landscape has been uplifted due glacier retreat (Tatur et al. 1997). For this reason, vegetation communities are also frequently changing its constitution, size and position on the landscape (Victoria et al., 2013). In addition, birds (such as Skuas and Penguins), have also been changing its colonization in ice-free areas over the years (Turner et al., 2014). Since vegetation patches and guano deposition by birds play an important function on the nutrient cycling in Maritime Antarctica, the prospects of nutrient cycling under these modifications on the landscape remain still unknown, especially about carbon exchange to the atmosphere.

In the last decade, several studied were carried out in Maritime Antarctica regarding soil CO_2 emissions (Mendonça et al., 2010; La Scala et al., 2010; Carvalho et al., 2012; Thomazini et al., 2014, Thomazini et al., 2015), in which soil temperature and moisture, associated with the type of vegetation, were the most important controlling factors that significantly affect carbon emission. However, most of them were based on total ecosystem respiration, which is the sum of all respiration occurring by the living organisms (Luo and Zhou, 2006). In this case, the currently carbon exchange that might contribute or not to the nutrient cycling and climate change, is hardly interpreted. By using only ecosystem respiration, poorly and well-drained areas can have similar amounts of carbon released to the atmosphere, depending on the type of vegetation community. However, little is known about the capacity of carbon sequestration of these ecosystems. For this reason, is important to evaluate the currently NEE, especially based on long-term *in situ* measurements and their driving factors (such as soil temperature and moisture) to better contribute to the knowledge of carbon exchange under fast climate changing in Maritime Antarctica. Despite being documented (Zhu et al., 2014), NEE and its relationship with soil temperature and moisture are still unknown in Maritime Antarctica, especially focused on long-term *in situ* measurements. The objective of this study was to evaluate NEE, soil temperature and moisture based on long-term *in situ* measurements from two typical vegetation communities in Coppermine Peninsula, Robert Island, Maritime Antarctica. We hypothesized that as vegetation communities becoming more humid, their capacity of sequester carbon from the atmosphere significantly increase over the time.

2. Material e Methods

2.1 Study area

The study was carried out at Coppermine Peninsula (62°23'S, 59°42'W), on the west side of Robert Island (Fig. 1). Robert Island is located between Nelson and Greenwich Islands, both parts of South Shetland Islands. The geology of the Coppermine Peninsula is mainly composed by olivine, olivine-basaltic, rare andesite-basaltic and agglomerates interspersed with andesite-basalt and andesite-lava (Machado et al., 2005). Coppermine peninsula is mainly featured by the ecological importance of the extensive mosses carpets in this portion of the Island. Mosses patches can reach to cover 1.5 ha, representing one of the most important bryophytes communities in Maritime Antarctica (Bustamante et al., 1987).

Wetter areas are colonized by *Sanionia uncinata, Calliergidium austrostramineum* and *Calliergon sarmentosum*. In areas less hydromorphic, species of *Polytrichastrum alpinum, Bryum algens, Andreaea* sp., *Psoroma cinnamomeum, Sphaerophorus globosus, Ceratidon* sp., and *Usnea* sp. may occur, being or not associated with lichens. Lichens such as *Leptogium puberulum*, *Ochrolechia frigida*, *Caloplaca* sp., *Haematomma erythromma*, *Physcia caesia*, *Ramalia tenebrata* and *Usnea* sp. are frequently associated with rocks, occasionally occurring with mosses. The algae *Prasiola crispa* is observed to occur in areas influenced by birds nesting. *Deschampsia antarctica* is frequently located at protected slopes of the peninsula (Bustamante et al., 1987; Bustamante et al., 1989; Torres-Mellado et al., 2011).

There is no meteorological station at Robert Island. The nearest station is located at Ecuadoran Station (Pedro Vicente Maldonado) in Greenwich Island. The average temperature during the austral summer at the latter station ranges between -2 and +2ºC, with about 600 mm of rainfall per year.

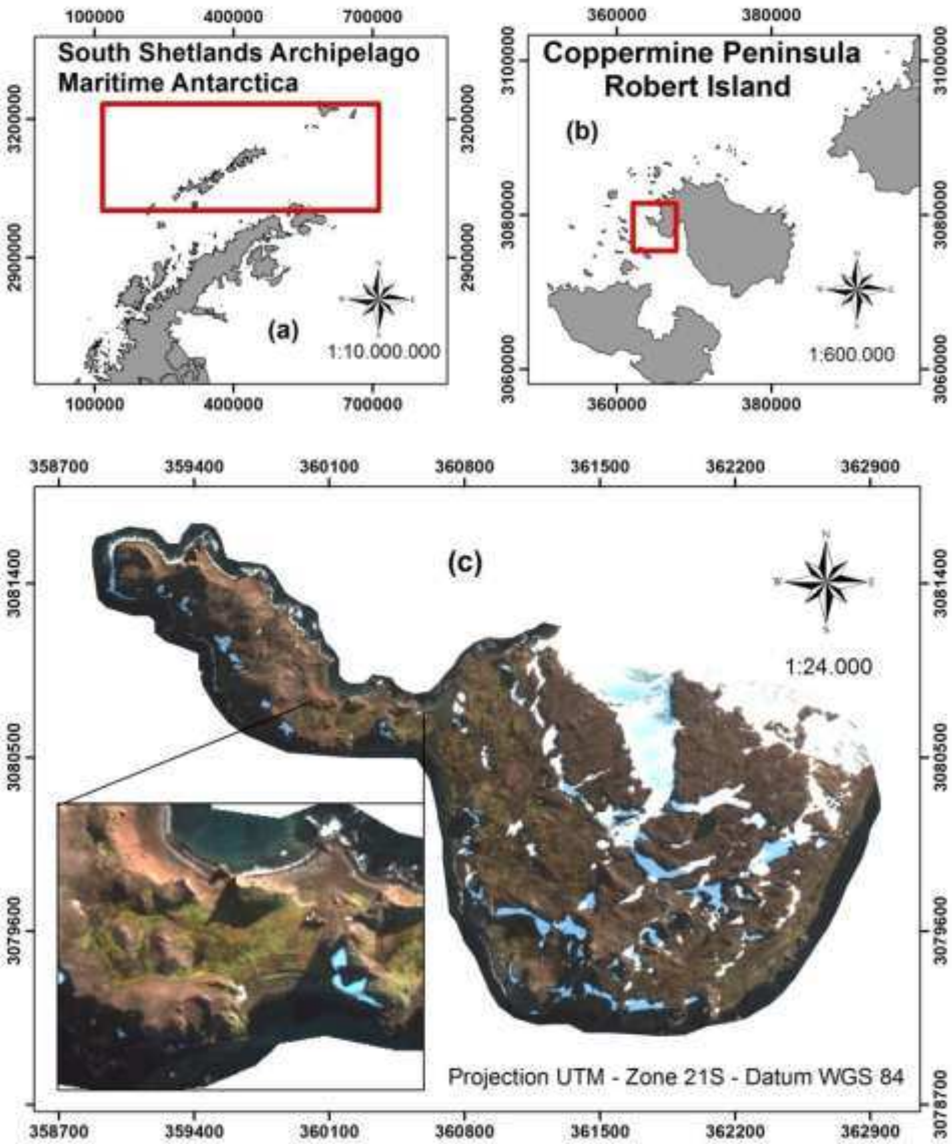

Fig 1. Illustrative map of South Shetlands archipelago (a), Coppermine Peninsula at Robert Island (b) and the selected area (c), where net ecosystem exchange and soil temperature were monitored.

2.2 Selected sites

Two typical vegetation communities were selected on February 2014 in a southeast part of a topossequence (Fig. 2). According to the World Reference Base for Soil Resources (WRB) classification system (IUSS Working Group WRB, 2006) soils in both sites are classified as Haplic Leptosol (Daher et al., 2015). This topossequence has low/or almost no influence of guano from birds. Based on Victoria et al. (2013) and Putzke et al. (2015), the selected area has a vegetation cover classified as “moss-carpet communities”. However, remarkable differences occur between the studied sites where NEE, soil temperature and moisture were evaluated, especially related to the floristic composition.

Site 1- It’s a marine terrace, highly influenced by ice/snow/permafrost melting on the bottom of the topossequence (20 m a.s.l). This site represents the most extensive moss carpet in Coppermine Peninsula, mainly constituted by *Sanionia uncinata* (Hedw.) Loeske, forming a dense carpet of 3-7 cm thickness, approximately. This extensive moss field is highly vigorous with intense green color.

Site 2 - An elevated area on basaltic ridge in the middle of the topossequence (29 m a.s.l.). This local has great influence of permafrost closer to the A horizon of the soil, being possible to find it at 30 cm depth. Vegetation species constitution is highly variable. This site is close to the “ecotone” between “moss-carpet communities” and “musciculous-lichens communities”, which in turn, has different floristic composition. However, there is a significant occurrence of *Polytrichastrum alpinum* G.L. Smith. Musiccolas lichens populations of *Psoroma cinnamomeum* Malme, *Ochrolechia frigida* (Sw.) Lynge and *Sphaerophorus globosus* (Huds.) Vain., as well as rare species of *Cladonia* spp. occur.

The selected areas represent the phenomena that may occur on the vegetation succession under climate change. First, the water will create wetter areas, such as site 1, with predominance of *Sanionia uncinata*. In other point of view, as lands uplifted or water from melting ceases, drier areas will progressively appear, being possible to have similar characteristics as found in site 2.

(a) **(b)**

Fig 2. Illustrative images showing the system used to collect data of NEE and soil temperature in the studied sites in Coppermine Peninsula without (a), and with snow (b) covering the surface.

2.3 Soil sampling

Soil was sampled in February 2014 to determine general soil properties, total soil organic carbon and total nitrogen at each investigated site. The soil sampling scheme was systematic using a sampling area divided into three experimental plots of 4 m² each. In each plot, three soil samples were taken at two layers (0-5 and 5-20 cm). The soil samples were air dried, grounded and sieved through a 2-mm sieve to remove larger pieces of root material and the stony fraction. All soil samples were analyzed in the soil laboratory at the Universidade Federal de Viçosa, Minas Gerais, Brazil.

2.4 General soil attributes

Particle size distribution (sand, silt, and clay) was performed by the pipette method (Embrapa, 1997). The pH was determined on a 1:2.5 soil: deionized water ratio; the potential acidity (H + Al) was extracted with $Ca(OAc)_2$ 0.5 mol L^{-1} buffered to pH 7.0, and quantified by titration with NaOH 0.0606 mol L^{-1}. Exchangeable Ca^{2+}, Mg^{2+} and Al^{3+} were extracted with 1 mol L^{-1} KCl and Na^+ and K^+ were extracted with Melich-1 (Embrapa, 1997). The element content in the extracts were determined by atomic absorption (Ca^{2+}, Mg^{2+} and Al^{3+}), flame emission (Na^+ and K^+) and photocolorimetry (P). The effective cation exchange capacity (CEC_E) was calculated by sum of cations (Ca^{2+}, Mg^{2+}, Na^+, K^+ and Al^{3+}). Total cation exchange capacity (CTC_T) was estimated by the sum of bases and potential acidity. Total soil organic carbon was determined by wet oxidation with $K_2Cr_2O_7$ 0.167 mol L^{-1} in the presence of sulfuric acid with external heating (Yeomans and Bremner, 1988). Total nitrogen was determined by sulfuric acid digestion followed by Kjeldahl distillation (Bremmer and Mulvaney, 1982.; Tedesco et al., 1995). Mean values of remaining phosphorus were obtained after shaking a $CaCl_2$ 10 mmol L^{-1} solution containing of 60 mg L^{-1} of phosphorus with 5 g of soil during one hour.

2.5 Soil temperature and water content

On February 2014, monitoring systems of soil temperature and moisture were set up in both sites. The monitoring systems consist of soil temperature probes (Campbell L107E thermocouple, accuracy of ± 0.2°C) and soil moisture probes (CS656 water content reflectometer, accuracy of ± 2.5%), placed in the active layer at 0-10 cm depths. Three probes were inserted at each site, spaced at 2 m from each other. Probes were inserted at the same local where PVC soil collar was placed to determine NEE. All probes were connected to a Campbell Scientific CR 1000 data logger, recording data at every 1 hour interval. This system recorded data of soil temperature and moisture from February 2014 to February 2016.

2.6 Net ecosystem exchange in situ

Long-term NEE measurements were carried out in January 2016, during the austral summer of Maritime Antarctica. To assess NEE data, we used closed automatic chamber system of CO_2 exchange (LI-COR Biosciences, Lincoln, NE, USA) containing an infra-red gas analyzer (model LI-8100A), a multiplexer system (model LI-8150) and one clear chamber (model LI-8100-104C). This system quantifies concentration of CO_2 through optical absorption spectroscopy. The system was calibrated at the factory using precision gases (CO_2 gas standards) at controlled temperatures. The clear chamber do not interrupt photosynthesis, allowing to determinate the difference between photosynthetic uptake of CO_2 by plants and the ecosystem respiration, which represent the net value of carbon exchange in a specific environment. Three PVC soil collars of 20 cm diameter were inserted into the soil prior measurements at each selected site (standard depth of 3 cm), spaced 2 m from each other, representing three replications in both sites. Measurement of NEE occurred *in situ* at the same local where probes of soil temperature and moisture were installed in February 2014. NEE data were recorded every 1-h interval, at the same time of the probes. NEE at each point were based on a single measurement over 1.5 min and the concentrations of CO_2 were made at 3 s intervals to determinate the current flux of CO_2. Mean values of NEE were obtained from 08th (00:00 h) to January 22th, 2016 (12:00 h). Positive values of NEE indicate that the ecosystem is acting as a source of CO_2. Contrarily, negative values indicate a sink effect of CO_2. When NEE is equal to 0, the ecosystem is equilibrated.

2.7 Data analysis

Data of general soil attributes (n=3) were interpreted in terms of general trends by mean values at each layer. Soil temperature and moisture temporal data were analyzed by hourly and monthly means. Also we calculated: (i) thawing days (TD): which are the days with all hourly measurements positive, being at least one warmer than +0.5 °C, (ii) freezing days (FD): which are the days with all hourly measurements negative, being at least one colder than -0.5 °C; (iii) number of isothermal days (ID): days in which all hourly measurements range only between ±0.5 °C, indicating the energy consumed to change the water phase both during thawing and freezing; (iv) number of freeze–thaw days (FTD): which are the days with both negative and positive temperatures, with at least one value greater than ±0.5 °C, indicating days in which freeze–thaw cycles may occur; (v) thawing degree days (TDD): obtained by the cumulative sum of the mean daily temperatures above 0 °C and (vi) freezing degree days (FDD): obtained by the cumulative sum of the mean daily temperatures below 0 °C. Thawed and frozen days indicate when the soil moisture is frozen or in a liquid state. All parameters were obtained according to Guglielmin et al. (2008) and Almeida et al. (2014). NEE values were interpreted by hourly and daily means (n=3). Correlations of NEE with soil temperature and moisture were tested using Pearson correlation analysis at 1% of significant level. Regression models between NEE and soil temperature were tested. Descriptive and statistical analyses were performed using the XLStat (XLStat, NY, USA, 2014) program. All graphs were performed with Sigmaplot v10 program (Systat Software Inc., Chicago, IL).

3 Results

3.1 General soil attributes

Table 1 shows the general soil attributes of the studied sites. In both sites, soil presented elevated soil exchangeable bases availability, reflecting in elevated bases sum and saturation of bases. In both sites and sampled depth, soil is eutrophic. There is an increment of fine particles and for the most determined soil attributes in depth. Total organic carbon contents tended to be higher in site 2 at 0-5 cm depth. However, incrementing of total organic carbon was observed to occur in site 1, tended to be higher at 5-20 cm in site 1 compared to site 2. No remarkable differences were observed to occur for N in the sampled depths.

Table 1. Soil chemical and physical attributes of the two selected sites in Coppermine Peninsula

	pH	P	K	Na	Ca	Mg	Al	H+Al	BS	CEC_E	CEC_T
		------mg kg^{-1}-----			---------------------------$cmol_c$ kg^{-1} ----------------------						
						0-5 cm					
Site 1	6.06	110.40	0.53	3.52	10.55	11.03	1.40	8.27	25.62	27.02	33.89
Site 2	5.74	273.20	0.67	4.07	8.65	10.37	4.68	14.43	23.76	28.44	38.19
						5-20 cm					
Site 1	6.12	156.43	0.60	3.49	12.50	10.39	1.50	8.43	26.98	28.47	35.41
Site 2	5.89	164.87	0.71	3.55	11.26	10.92	1.82	8.77	26.44	28.26	35.21

	S	m	ISNa	P-rem	C	N	CS	FS	Silt	Clay
	-----------%----------			mg L^{-1}	--g kg^{-1}--		-------------------g kg^{-1}------------------			
						0-5 cm				
Site 1	75.60	5.20	10.41	23.43	22.89	0.84	493.33	246.67	146.67	113.33
Site 2	62.53	5.23	10.73	20.90	27.84	0.82	550.00	170.00	146.67	133.33
						5-20 cm				
Site 1	76.23	16.37	9.90	23.03	17.94	0.72	523.33	226.67	133.33	116.67
Site 2	75.03	6.37	10.07	31.23	12.99	0.72	533.33	216.67	126.67	123.33

pH: active acidity (H_2O); P: phosphorus; K: potassium; Na: sodium; Ca: calcium; Mg: magnesium; Al: aluminium; H+Al: potential acidity; BS: bases sum; CEC_E: effective cation exchange capacity; CEC_T: total cation exchange capacity; S: saturation of bases; m: saturation of aluminium; ISNa: saturation of sodium; C: total organic carbon; N: total nitrogen; CS: Coarse sand (0.2-<2 mm); FS: Fine sand (0.05-<0.2 mm); Silt (0.002-<0.05 mm); Clay (<0.002 mm).

3.2 Long-term soil temperature and moisture measurement

Large differences in soil temperature and moisture were observed for the studied sites over the monitored period (Fig 3a,b). Variations on soil temperature and moisture are greater in the summer period (from December to March). The lowest soil temperature (hourly records) found was -5.35ºC on August 31th and -18.25ºC on June 15th in Site 1 and 2, respectively. On the other hand, the highest soil temperature registered was 4.30 and 5.12 ºC on February 18th for Site 1 and 2, respectively. In 2014, annual mean soil temperature was -1.51ºC (±0.02) in Site 1 and -5.84ºC (±0.05) in Site 2. During 2015, the highest and lowest soil temperature recorded was 6.79 and -5.52ºC (January 24th and June 17th) in Site 1, while a range of 6.25 to -25.88ºC

(February 19th and June 6th) was recorded in Site 2. Annual mean soil temperature in 2015 was -1.39ºC (±0.02) in Site 1 and -6.25ºC (±0.07) in Site 2.

In 2016, until February 22th, the maximum hourly record was 3.23 and 2.98ºC on January 18th, while the minimum was -2.79 and -6.99ºC on January 12th in Site 1 and 2, respectively. Soil moisture presented less variation compared to values of soil temperature along the monitored period (Fig 3c). During the summer, hourly records indicated that soil moisture can reach to 0.52 m^3 m^{-3} in Site 1 from 2014 to 2016. Also, in the same period, hourly measurements reached to 0.37 m^3 m^{-3} in Site 2, being approximately 30% lower. From May to November; soil moisture is low, varying between 0.03 and 0.17 m^3 m^{-3} (see monthly means in Table 2). Even in spring, fall and winter, soil moisture tended to be higher in Site 1 compared to Site 2. The minimum soil moisture found were 0.09 and 0.03 m^3 m^{-3} in Site 1 and 2, respectively.

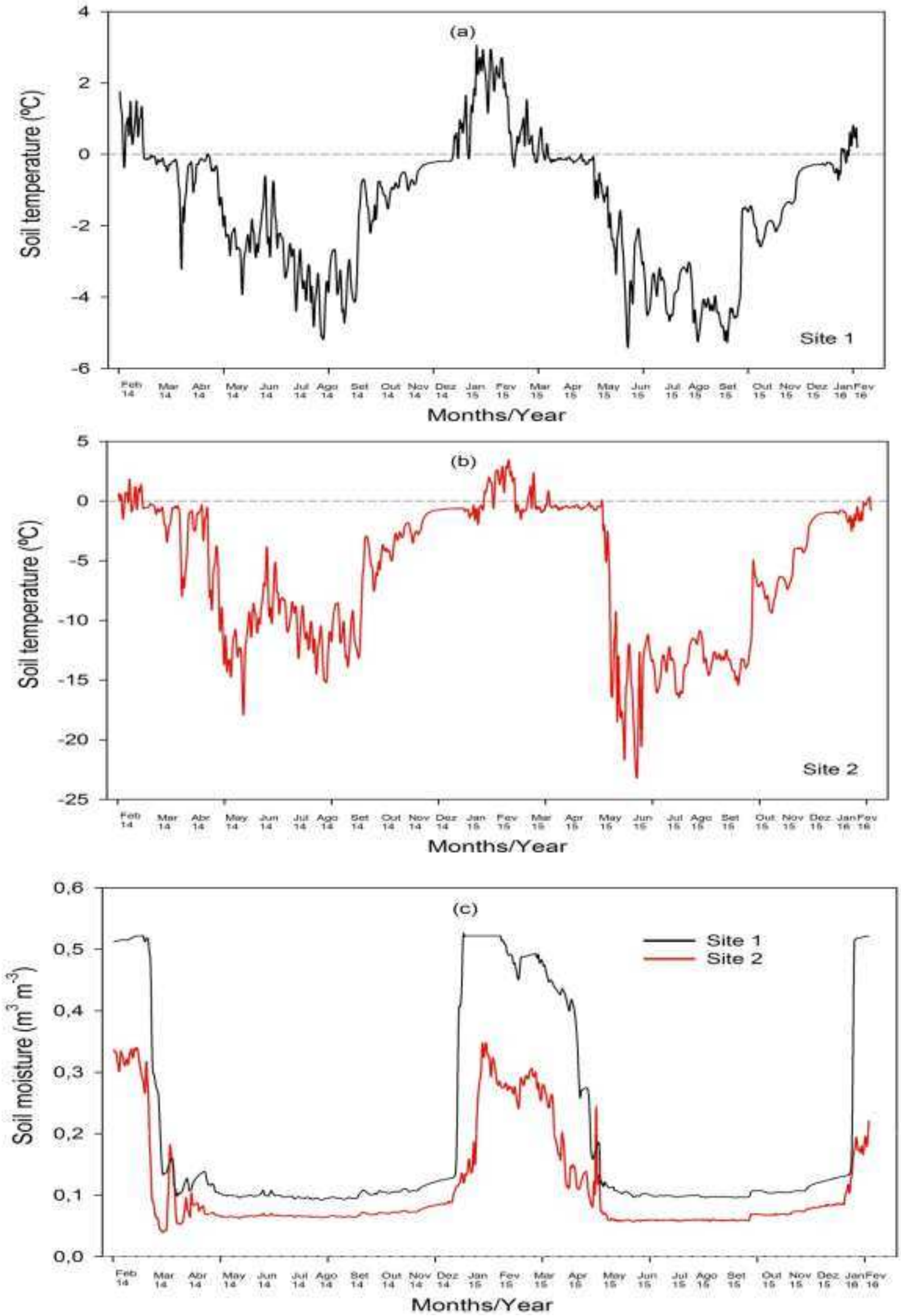

Fig 3. Daily mean soil temperature and moisture measurements at the studied sites in Coppermine Peninsula, from February 2014 to February 2016.

Monthly mean soil temperature tended to be negative after March in Site 1 for both years (2014 and 2015) and being positive in January (Table 2). On the other hand, monthly mean soil temperature tended to be negative before in Site 2, starting on March in 2014. In addition, only February showed negative monthly means in 2015. There were only 1 thawing day in Site 2 on 2016, being freezing days predominantly when compared to the Site 1. Results show that thawing days occurred more in 2015 in both sites, consequently reducing the number of freezing days. However, this result must be carefully interpreted, since data in January 2014 was not collected, where soil temperature tend to be higher. During the entire monitored period, thawing days were 32 times higher in Site 1, whilst freezing days were 1.27 times higher in Site 2, when comparing both sites.

Isothermal days are concentrated during the summer and fall (from December to May) in Site 1 for both years (Table 3). In Site 2, only one isothermal day was registered on May 2015. Isothermal days were up to 114 times higher in Site 1 than in Site 2. Freeze-thaw days also frequently occur during summer and fall. During the monitored period, freeze-thaw days were 1.31 times higher in Site 2 when compared to the Site 1. A predominance of freezing conditions was observed to occur in Site 2, by the cumulative freezing degree days, whilst thawed days and conditions are remarkable features of Site 1. In the entire monitored period, there were -587 and -650 freezing degree days, 116 and 53 thawing degree days in Site 1 and 2, respectively.

Table 2. Monthly mean soil temperature (MST), soil moisture (MSM), thawing days (TD) and freezing days (FD) during the monitored period at the two selected sites in the 0-10 cm depth.

			2014					
	--------------Site 1-----------------				---------------Site 2----------------			
	MST (ºC)	**MSM (m^3m^{-3})**	**TD**	**FD**	**MST (ºC)**	**MSM (m^3m^{-3})**	**TD**	**FD**
Feb	0.80	0.51	3.00	0.00	0.19	0.32	0.00	0.00
Mar	0.24	0.47	4.00	3.00	-0.24	0.25	0.00	9.00
Apr	-0.73	0.13	0.00	23.00	-2.50	0.08	0.00	26.00
May	-0.67	0.12	0.00	16.00	-5.88	0.07	0.00	31.00
Jun	-2.57	0.10	0.00	30.00	-11.84	0.07	0.00	30.00
Jul	-2.17	0.10	0.00	31.00	-8.26	0.07	0.00	31.00
Aug	-3.78	0.10	0.00	31.00	-11.68	0.07	0.00	31.00
Sep	-3.64	0.09	0.00	30.00	-11.20	0.07	0.00	30.00
Oct	-1.49	0.10	0.00	31.00	-5.41	0.07	0.00	31.00
Nov	-0.81	0.11	0.00	29.00	-2.67	0.07	0.00	30.00
Dec	-0.24	0.12	0.00	0.00	-0.78	0.08	0.00	31.00
Sum			7.00	224.00			0.00	280.00
			2015					
Jan	1.22	0.46	9.00	0.00	-0.42	0.19	0.00	11.00
Feb	1.80	0.51	19.00	0.00	1.45	0.29	0.00	0.00
Mar	0.35	0.48	4.00	0.00	-0.26	0.28	1.00	0.00
Apr	-0.13	0.40	0.00	3.00	-0.52	0.16	0.00	13.00
May	-0.63	0.17	0.00	18.00	-4.72	0.10	0.00	28.00
Jun	-2.97	0.10	0.00	30.00	-16.14	0.06	0.00	30.00
Jul	-3.89	0.10	0.00	31.00	-14.45	0.06	0.00	31.00
Aug	-3.91	0.10	0.00	31.00	-12.71	0.06	0.00	31.00
Sep	-4.53	0.10	0.00	30.00	-13.65	0.06	0.00	30.00
Oct	-2.13	0.10	0.00	31.00	-7.77	0.07	0.00	31.00
Nov	-1.42	0.11	0.00	29.00	-4.46	0.07	0.00	30.00
Dec	-0.31	0.12	0.00	4.00	-1.02	0.08	0.00	31.00
Sum			32.00	207.00			1.00	266.00
			2016					
Jan			0.00	3.00			0.00	3.00

Table 3. Isothermal days (ID), freeze-thaw days (FTD), thawing degree days (TDD) and freezing degree days (FDD) during the monitored period at the two selected sites in the 0-10 cm depth.

	2014							
	Site 1				Site 2			
	ID	**FTD**	**TDD**	**FDD**	**ID**	**FTD**	**TDD**	**FDD**
Feb	0.00	7.00	9.00	-1.00	0.00	10.00	7.00	-3.00
Mar	7.00	17.00	12.00	-19.00	0.00	22.00	8.00	-23.00
Apr	4.00	3.00	0.00	-30.00	0.00	4.00	0.00	-30.00
May	15.00	0.00	1.00	-30.00	0.00	0.00	0.00	-31.00
Jun	0.00	0.00	0.00	-30.00	0.00	0.00	0.00	-30.00
Jul	0.00	0.00	0.00	-31.00	0.00	0.00	0.00	-31.00
Aug	0.00	0.00	0.00	-31.00	0.00	0.00	0.00	-31.00
Sep	0.00	0.00	0.00	-30.00	0.00	0.00	0.00	-30.00
Oct	0.00	0.00	0.00	-31.00	0.00	0.00	0.00	-31.00
Nov	1.00	0.00	0.00	-30.00	0.00	0.00	0.00	-30.00
Dec	31.00	0.00	0.00	-31.00	0.00	0.00	0.00	-31.00
Sum	58.00	27.00	22.00	-294.00	0.00	36.00	15.00	-301.00
	2015							
Jan	2.00	20.00	28.00	-3.00	0.00	20.00	6.00	-25.00
Feb	0.00	9.00	26.00	-2.00	0.00	28.00	21.00	-7.00
Mar	1.00	26.00	24.00	-7.00	0.00	30.00	8.00	-23.00
Apr	12.00	15.00	2.00	-28.00	0.00	17.00	0.00	-30.00
May	13.00	0.00	1.00	-30.00	1.00	2.00	0.00	-31.00
Jun	0.00	0.00	0.00	-30.00	0.00	0.00	0.00	-30.00
Jul	0.00	0.00	0.00	-31.00	0.00	0.00	0.00	-31.00
Aug	0.00	0.00	0.00	-31.00	0.00	0.00	0.00	-31.00
Sep	0.00	0.00	0.00	-30.00	0.00	0.00	0.00	-30.00
Oct	0.00	0.00	0.00	-31.00	0.00	0.00	0.00	-31.00
Nov	1.00	0.00	0.00	-30.00	0.00	0.00	0.00	-30.00
Dec	27.00	0.00	0.00	-31.00	0.00	0.00	0.00	-31.00
Sum	56.00	70.00	81.00	-284.00	1.00	97.00	35.00	-330.00
	2016							
Jan	0.00	18.00	13.00	-9.00	0.00	18.00	3.00	-19.00

3.3 Net ecosystem exchange in situ

Hourly records of NEE and soil temperature during the monitored period on January 2016 are presented in Fig 4a,b. Despite presenting similar temporal variation over the course of a day, differences on NEE and soil temperature were observed to occur in both sites, where the variation is more pronounced in

Site 1. The lowest NEE (hourly records) found was -3.21 and -1.62 μmol CO_2 m^{-2} s^{-1} on January 13th (15:00) and 10th (12:00) in Site 1 and 2, respectively. On the other hand, the maximum NEE registered was 1.34 and 0.74 μmol CO_2 m^{-2} s^{-1} on January 8th (00:00) and 10th (04:00) for Site 1 and 2, respectively. From January 08th to 22th, mean values of NEE were -0.54 (±0.05) μmol CO_2 m^{-2} s^{-1} in Site 1 and -0.07 (±0.02) μmol CO_2 m^{-2} s^{-1} in Site 2.

The maximum hourly record of soil temperature during this period was 3.23 and 2.98ºC on January 18th (04:00 and 21:00), while the minimum was -2.79 and -6.99ºC on January 12th (10:00) in Site 1 and 2, respectively. From January 10th at 00:00 to 11th 07:00 there was a snow event that covered the soil surface. In this period, NEE tended to follow the same pattern in both sites with similar trend and amplitude. On 15th, daily cumulative NEE indicated a total of -22.98 μmol CO_2 m^{-2} s^{-1} or the equivalent of 87.36 g CO_2 m^{-2} dia^{-1} sequestered by the vegetation in Site 1 (Fig 4c). From 18th to 20th, daily cumulative NEE indicate a source effect (positive cumulative values of NEE) in Site 2, coupled with rising temperatures (Fig 4d). A total net uptake of 185.29 and 25.25 μmol CO_2 m^{-2} during the monitored period were recorded in Site 1 and 2. These values are equivalent of 704.39 and 95.99 g CO_2 m^{-2}. As shown in Fig 4 e, the sink strength of CO_2 is higher during the day in Site 1 when compared to Site 2. On the average, NEE tended to be positive (acting as a source of CO_2) after 21:00h in both sites (Fig. 4 e). After 22:00h, NEE values in Site 1 exceed the mean values in Site 2.

Based on hourly mean records from the entire monitored period, Site 1 act as a source of CO_2 from 22:00 to 06:00h. The source strength is higher during this period when compared to Site 2. Soil temperature tended to be almost always higher in Site 1 (Fig. 4f), for all hourly mean values. Hourly mean soil temperature indicates that both sites tended to have negative temperatures after 05:00h. However, positive temperatures occurred after 15:00h in Site 1 and 18:00h in Site 2. The maximum soil temperature occurred at 21:00 and 23:00h for Site 1 and Site 2, respectively. On the other hand, minimum was registered at the same time for both sites (12:00h). The maximum and minimum soil temperature had a strong relationship with the maximum and minimum of NEE. The relationship between NEE and soil temperature was best described by a third-order polynomial regression model (Fig 5) with a significant and positive correlation among them (Table 4). The best adjust and higher coefficient of correlation was obtained in Site 2.

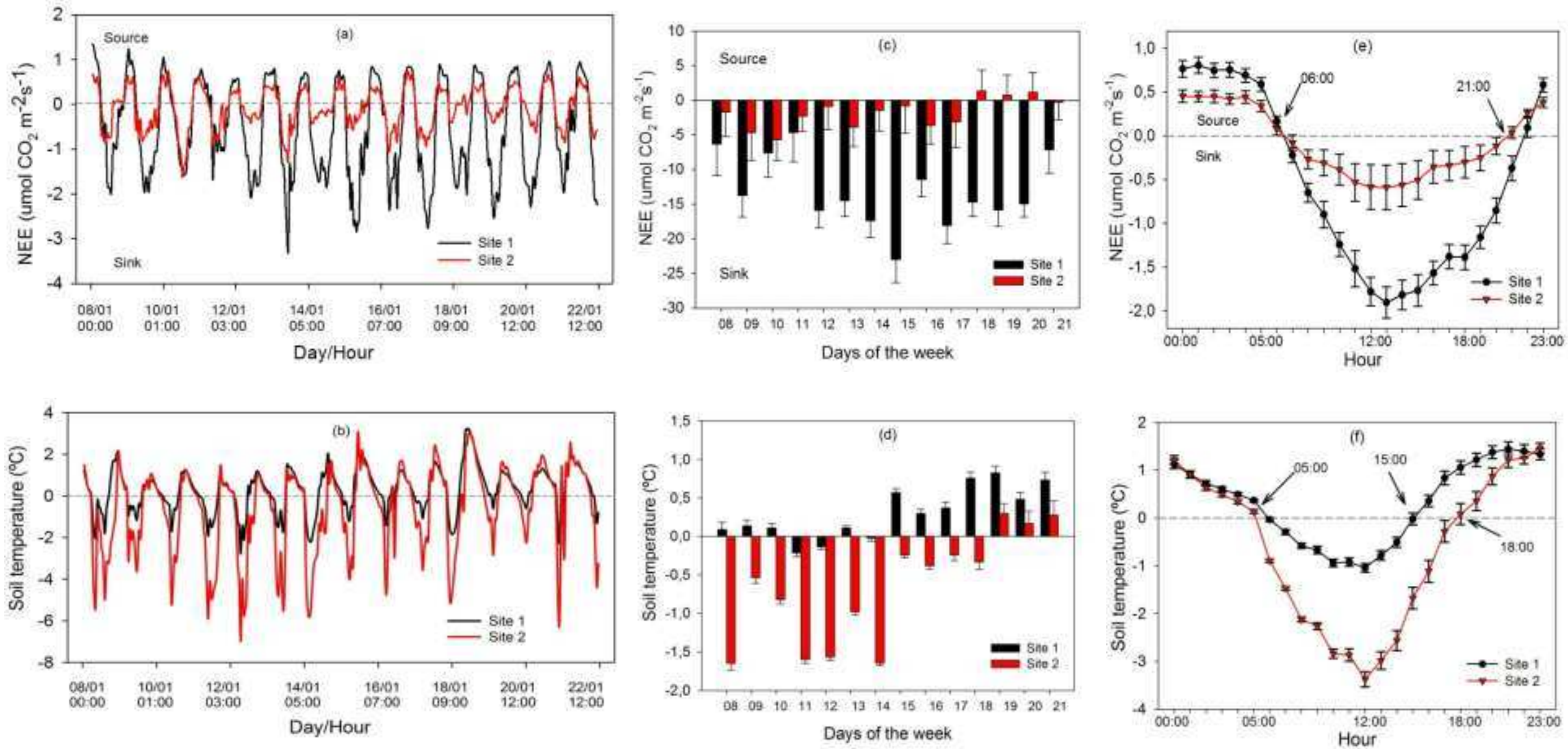

Fig 4. Hourly (a, b), cumulative and daily mean (c, d) net ecosystem exchange and soil temperature, respectively, during the monitored period at the two studied sites. Hourly mean net ecosystem exchange and soil temperature considering all of *in situ* measurements are shown in charts e and f, respectively. Vertical bars represent the standard error of mean.

Table 4. Pearson's pairwise correlation and the coefficient of determination between soil temperature and net ecosystem exchange in the studied sites

	r	***P***	**R^2**
Site 1	0.4	<0.0001	0.23
Site 2	0.61	<0.0001	0.42

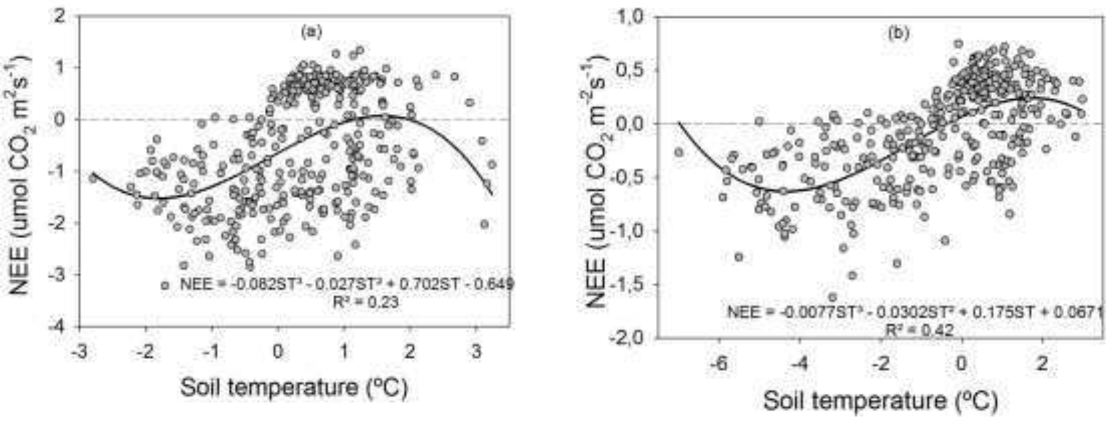

Fig 5. Bilinear relationship between values of NEE and soil temperature (ST) measured *in situ*, with the best adjusted model in the studied site 1 (a) and 2 (b). Each point represents mean values of NEE and its corresponding soil temperature at the same time, across the measurement period.

4 Discussion

In Coppermine peninsula, the rich parent material (olivine-basalt) strongly affected the soil nutrients status. Overall, both sites showed large amounts of exchangeable bases, mostly due the parent material characteristics. Basaltic material reflected in higher magnesium content, compared to calcium at 0-5 cm depth. Low phosphorus mean values indicate no strong ornithogenic influence (Tatur et al., 1997). This peninsula is less affected by penguins, which are reported to deposit large amounts of guano, responsible to form ornitoghenic soils (Simas et al., 2008). Coppermine peninsula presents only a few nesting of Skuas and Giant Petrels, occurring sparsely. Soil organic carbon contents appear to be more uniformly distributed on the soil profile up to 20 cm in site 1, compared to site 2. Possible, a greater variation on the soil horizons constitution occur in site 2, since it has been affected by permafrost. However, further research is needed to investigate in deeper soil layers to confirm.

The incrementing of fine particles (especially clay), total organic carbon and for the most determined soil general attributes in depth, is mainly due cryoturbation, which is common in Maritime Antarctica. In this case, the mixing of the soil matrix within the pedon results in irregular or broken horizons (Bockheim and Tarnocai, 1998). Significant amounts of coarse particles on the soil surface could be also attributed to the wind ablation, carrying particles over long distances (Moura et al., 2012). Rockiness reported in this paper is well-known on the literature (Simas et al., 2008; Michel et al., 2006; Pereira et al., 2013; Souza et al., 2014), and in some cases, reflecting in a skeletic character (Simas et al., 2008). Despite vegetation being widely responsible for the carbon accumulation and exchange in Maritime Antarctica (Thomazini et al., 2015), the stoniness associated with the levels of cryoturbation, translocation of exchangeable bases, melting of permafrost under rising temperatures would further affect the net carbon exchange in Maritime Antarctica by mineralization process and diffusion of gases on the soil profile, as evidenced in this study.

The behavior of soil temperature and moisture over the monitored period is mainly attributed to the influence of water melting in Site 1 and presence of permafrost in Site 2. As Site 2 is located in the middle of the topossequence, drainage is facilitated. Contrarily, Site 1 is highly influenced by water due its position on the landscape, where thawing of active layer continuously supply water. The parameters calculated in this work indicate the phase of water on the soil solution and also provide useful data to interpret the amount of energy necessary to change water phase along the monitored period. Most of the process involving soil temperature and moisture are strongly influenced by the rising air temperatures in the late spring and summer, promoting melting of snow/ice and altering the soil chemical and physical process, especially soil carbon mineralization, which will further influence NEE dynamic.

Overall, soil temperature varied more in Site 2 than Site 1. The proximity of the permafrost in the monitored soil layer in Site 2, delayed the thawing (Almeida et al., 2014). On the other hand, a large number of isothermal days were registered in Site 1, indicating the buffering effect of water (Guglielmin et al., 2008), since this site is almost always wetter than Site 2. Permafrost and the elevated water content of soil promote the so-called thermal buffering effect, controlling soil temperature variations (Guglielmin et al., 2008; Almeida et al., 2014). Results suggest that in Site 1 there is a more pronounced buffering effect (higher number of isothermal days) due the hydromorphic environment. Despite permafrost exists in Site 2 that also contribute to the buffering effect, it's down the soil profile, probably creating a buffering effect on deeper active soil layers. In a similar environment under mosses colonization, Michel et al. (2012) and Almeida et al. (2014) also observed the buffering effect of water, increasing the number of isothermal days at the uppermost soil layer, compared to a drier lichen site, such as Site 2, in Maritime Antarctica.

Thermal conditions facilitated soil chemical and physical processes/weathering in Site 1. It is possible since the availability of water is more abundant during thawing and isothermal days, conjugated with higher soil temperatures (see Fig. 4f). Freeze-thaw days occurred frequently at the uppermost soil layer (Michel et al., 2012), due the interaction with the atmosphere, whereas, down the soil profile it is smoothed. For this reason, soil temperature on both sites was not predominantly close to 0, suggesting a greater variation on soil temperature over the monitored period, also confirmed by the low number of isothermal days. In this work, results indicate that freeze-thaw days are more common in Site 2, suggesting that freezing and thawing processes frequently occur at this site, compared to Site 1. It is also observed in the Fig 4b, where the amplitude of soil temperature is greater in Site 2, further confirming the pronounced buffering effect in Site 1. Results indicated predominance of freezing conditions in Site 2, by the greater number of freezing degree days, mainly attributed to the proximity of active layer to the permafrost zone.

Results indicate that both studied sites are currently acting as a sink of atmospheric CO_2 based on long-term measurements. However, the extensive mosses carpets in Coppermine Peninsula have more capacity of CO_2 uptake (up to 7 times) compared to the mixed vegetation community (lichens/mosses). Mosses carpets (especially of *Sanionia uncinata*) were previously studied by their capacity of CO_2 release and uptake based on low number of measurements and no temporal series in Maritime Antarctica (La Scala et al., 2010; Mendonça et al., 2010), making it difficult to interpret NEE dynamic over a diurnal cycle. Supported by consistent and detailed NEE measurements over a long period, this pattern is now confirmed, regarding the net balance. However, differences may occur on NEE dynamics among years and periods in function of environmental variables such as air temperature fluctuations, snow events and rainfall, which may strongly vary in Maritime Antarctica.

Soil temperature, moisture, nutrients assembly and vegetation coverage are reported to strongly drive carbon uptake and release in Maritime Antarctica (La Scala et al., 2010; Mendonça et al., 2010; Cannone et al., 2012; Zhu et al., 2014; Thomazini et al., 2015). The CO_2 sink strength reported in Site 1 is mainly attributed to the vegetation coverage and the hydromorphic environment. Soil carbon mineralization is reduced due to the limitation of oxygen, which reduce ecosystem respiration, enhancing CO_2 uptake more than the release. On the other hand, Cannone et al. (2012) showed that vegetation patches with predominance of *Sanionia uncinata* presented positive NEE values. Results reported by these authors are associated to elevated ecosystem rates in Dry Valleys, possibly related to a drier soil with relatively high nitrogen and organic matter contents.

Mixed communities with lichens and mosses, such as Site 2, are usually reported to have ecosystem respiration rates higher than their capacity of CO_2 uptake, in equilibrium or with no sink effect (Cannone et al., 2012; Zhu et al., 2014; Thomazini et al., 2015). However, the proximity of permafrost reduced soil temperature in the uppermost soil layer and contributed to decrease the source effect, as reported in this work. In some cases, with rising temperatures, there will be days in which lichens/mosses sites will act as a source of CO_2 based on cumulative daily means. However, as temperature is decrease, this site will mainly act as a sink of CO_2. But, soils in Maritime Antarctica might have relatively high amounts of organic carbon and nitrogen, which can contribute to elevated ecosystem respiration in some cases (Zhu et al., 2014). In this scenario, similar terrestrial ecosystems may act as a source of carbon in the most part of the austral summer, especially in warmer periods.

In the most part of the summer in Maritime Antarctica, the number of sun light hours is high, having no night time in some days. During the monitored period, only from 23:00 to 02:00h there was low or no sun light, which directly affected NEE and soil temperature. For this reason, the maximum and minimum peaks of NEE and soil temperature occurred around the middle of the night and the day, respectively. It was also associated with the delay of the maximum and minimum peaks of soil temperature in polar zones and the buffering effect imposed by water and proximity of permafrost (Michel et al., 2012; Almeida et al., 2014). With this, in the late summer and the beginning of fall, the sink effect tends to be reduced due the decrease in sun light hours, where the source effect is progressively increasing. However, further research is needed to quantify these differences. In this study, snow did not limited NEE when both sites were completely covered by snow. Under this condition, NEE was similar in both sites. Hence, an approach occurs in the dynamic of carbon under snow events, being the hourly records strongly similar in the studied vegetation communities.

Soil temperature and moisture are reported to be the most important controlling factor of carbon exchange in Maritime Antarctica (La Scala et al., 2010; Thomazini et al., 2015). During the studied period, Site 1 is more subject to thawing days and higher soil temperatures, coupled with elevated water content of soil, suggesting that these variables have remarkable influence on the carbon exchange in Maritime Antarctica. Thus, in other similar sites, the increase in soil temperature under climate warming, and the consequently thaw of snow, ice and permafrost will create hydromorphic zones, depending on the position in the landscape. Hence, further potentiate the sink effect in periglacial landscapes. Additionally, the currently and expected increase in mean air temperatures will also positively affect permafrost thawing, and reducing the sink strength in similar zones as Site 2. Despite these trends, it’s important to note that spatial heterogeneity in periglacial landscapes is strongly high, especially regarding soil development and vegetation patches (Thomazini et al., 2014), which may also modify the NEE dynamics. Further research is needed to measure NEE in vegetation patches with different characteristics and soil nutrient status (especially in Phanerogamic Antarctic communities) to elucidate and model the potential of periglacial areas to act as a sink or source of atmospheric CO_2.

5 Conclusions

In a region where fieldwork is highly constrained by logistic practicalities, our work presented consistent data of net ecosystem exchange of CO_2 and its controlling factors based on *in situ* long-term measurements. Data presented in this work demonstrate that vegetation coverage, soil temperature and moisture directly affect net ecosystem exchange of CO_2 in terrestrial ecosystems of Maritime Antarctica. At moss sites a net gain of CO_2 occurs, mainly due the saturated status of soil. In this local, thaw processes are more pronounced, coupled with higher soil temperature than a permafrost-influenced area. Also, variations on soil temperature are lower due the buffering effect imposed by water. In the moss/lichen site a sink effect was also provided to be happening. The proximity of permafrost is leading to lower soil temperatures and enhancing ecosystem respiration, resulting in a sink effect. However, under current climate warming, soil temperature will further increase in the uppermost soil layer and the local will progressively act as a source of CO_2 to the atmosphere. Further research is needed to elucidate and model the current CO_2 dynamics in other different vegetation communities, to enhance the knowledge of the possible alterations under climate warming as well as the contribution to increase or decrease atmospheric CO_2.

6 References

Almeida, I.C.C., Schaefer, C.E.G.R., Fernandes, R.B.A., Pereira, T.T.C., Nieuwendam, A.T., Pereira, A.B., 2014. Active layer thermal regime at different vegetation covers at Lions Rump, King George Island, Maritime Antarctica. Geomorphol. 225, 36–46.

Bockheim, J.G., Tarnocai, C., 1998. Recognition of cryoturbation for classifying permafrost-affected soils. Geoderma 81, 281–293.

Bustamante, R., I. Serey Y. G. Guzmán. 1987. Importancia de península Coppermine (isla Robert) para el desarrollo de un programa de investigación en ecología terrestre. Bol. Antárt. Chileno 7 (2), 5-8.

Bustamante, R., I. Serey y G. Guzmán. 1989. Mortalidad de musgos y distribución de Usnea aurantiaco-atra: ¿Efectos alelopáticos?. Ser. Cient. INACH 39, 69-73.

Bremmer, J.M., Mulvaney, C.S., 1982. Total nitrogen. In: Page, A.L. (Ed.), Methods of Soil Analyses. American Society of Agronomy, Madison, pp. 595–624.

Cannone, N., Binelli, G., Worland, M.R., Convey, P., Guglielmin, M., 2012. CO_2 fluxes among different vegetation types during the growing season in Marguerite Bay (Antarctic Peninsula). Geoderma 189–190, 595–605.

Clarke L. J., Robinson S. A., Hua Q., Ayre D. J., Fink D. 2012. Radiocarbon bomb spike reveals biological effects of Antarctic climate change. Global Change Biology, 18, 301 -310.

Daher, M. Gênese e classificação de solos na península Coppermine (Ilha Robert) e ilha Barrientos, Antártica Marítima. 129p. Dissertação (Mestrado em Solos e Nutrição de Plantas) – Universidade Federal de Viçosa, 2015.

Embrapa. Centro Nacional de Pesquisa de Solos. Manual de Métodos de Análise de Solo. 2. ed. ver. atualiz. Rio de Janeiro, 1997. 212p. il. (EMBRAPA/CNPS-RJ. Documentos, 1).

Guglielmin, M., Ellis Evans, C.J., Cannone, N., 2008. Active layer thermal regime under different vegetation conditions in permafrost areas. A case study at Signy Island (Maritime Antarctica). Geoderma 144, 73–85

IUSS Working Group WRB, 2006. World Reference Base for Soil Resources 2006. World Soil Resources Report No.103. FAO. Rome.

La Scala, N., Mendonça, E.S., Souza, J.V., Panosso, A.R., Simas, F.N.B., Schaefer, C.E.R.G., 2010. Spatial and temporal variability in soil CO_2 emissions and relation to soil temperature at King George Island, Maritime Antarctica. Polar Sci. 4, 479-487.

Luo, Y., Zhou, X., 2006. Soil Respiration and the Environment. Academic Press, USA. 328p.

Machado, A., Lima, E. F., Chemale, F., Morata, D., Oteiza, O., Almeida, D. P. M., Urrutia, J. L. 2005. Geochemistry constraints of Mesozoic–Cenozoic calc-alkaline magmatism in the South Shetland arc, Antarctica. Journal of South American Earth Sciences, 18(3-4), 407–425.

Mendonça, E.S., La Scala, N., Panosso, A.R., Simas, F.N.B., Schaefer, C.E.G.R., 2010. Spatial variability models of CO_2 emissions from soils colonized by grass (*Deschampsia antarctica*) and moss (*Sanionia uncinata*) in Admiralty Bay, King George Island. Antarc. Sci. 23, 27-33.

Michel, R.F.M., Schaefer, C.E.G.R., Dias, L., Simas, F.N.B., Benites, V., Mendonca, E.S., 2006. Ornithogenic gelisols (cryosols) from Maritime Antarctica: pedogenesis, vegetation and carbon studies. Soil Sci. Soc. Am. J. 70, 1370–1376.

Michel, R.F.M., Schaefer, C.E.G.R., Poelking, E.L., Simas, F.N.B., Fernandes Filho, E.I., Bockheim, J.G., 2012. Active layer temperature in two Cryosols from King George Island, Maritime Antarctica. Geomorphology 155–156, 12–19.

Moura, P.A., Francelino, M.R., Schaefer, C.E.G.R., Simas, F.N.B., Mendonça, B.A.F., 2012. Distribution and characterization of soils and landform relationships in Byers Peninsula, Livingston Island, Maritime Antarctica. Geomorphology, 155-156, 45–54.

Newsham KK, Hopkins DW, Carvalhais LC, Fretwell1 PT, Rushton SP, O'Donnell AG, Dennis PG. 2015. Relationship between soil fungal diversity and temperature in the maritime Antarctic, Nature Climate Change, 6, 182-186.

Pereira, A.B. and Putzke, J. 2013. The Brazilian research contribution to knowledge of the plant communities from Antarctic ice free areas, Anais da Academia Brasileira de Ciências 85(3), 923-935.

Pereira, T.T.C., Schaefer, C.E.G.R., Ker, J. C., Almeida, C.C., Almeida, I.C.C., Pereira, A. B., 2013. Genesis, mineralogy and ecological significance of ornithogenic soils from a semi-desert polar landscape at Hope Bay, Antarctic Peninsula. Geoderma, 209-210, 98–109.

Putzke, J; Athanásio, C G ; De Albuquerque, M P ; Victoria, F C ; Pereira, A B . 2015. Comparative study of moss diversity in South Shetland Islands and in the Antarctic Peninsula. Revista Chilena de Historia Natural, 88, 6-6.

Simas FNB, Schaefer CEGR, Albuquerque Filho MR, Francelino MR, Fernandes Filho EI, Costa LM. 2007. Genesis, properties and classification of Cryosols from Admiralty Bay, maritime Antarctica. Geoderma,144, 116-122.

Simas F.N.B., Schaefer C.E.G.R., Albuquerque Filho M.R., Francelino M.R., Fernandes Filho E.I. da Costa L.M. 2008. Genesis, properties and classification of cryosols from Admiralty Bay, maritime Antarctica. Geoderma 144,116:122.

Souza, K.K.D., Schaefer, C.E.G.R., Simas, F.N.B., Spinola, D.N., De Paula, M.D., 2014. Soil formation in Seymour Island, Weddell Sea, Antarctica. Geomorphology, 225, 87-99.

Tatur A, Myrcha A, Niegodzisz J. Formation of abandoned penguin rookery ecosystems in the maritime Antarctic. 1997. Polar Biol, 17, 405–417.

Tedesco, M.J., Gianello, C., Bissani, C.A., Bohnen, H., Volkweiss, S.J., 1995. Análise de solo, plantas e outros materiais. 2nd ed. Universidade Federal do Rio Grande do Sul, Porto Alegre, p. 174.

Torres-Mellado, G.A., R. Jaña Y M.A. Casanova-Katny. 2011. Antarctic hairgrass expansion in the South Shetland archipelago and Antarctic Peninsula revisited. Polar Biol. 34 (11), 1679-1688.

Turner J, Barrand NE, Bracegirdle TJ, Convey P, Hodgson DA, Jarvis M, Jenkins A, Marshall G, Meredith MP, Roscoe H, Shanklin J, French J, Goosse H, Guglielmin M, Gutt J, Jacobs S, Kennicutt MC, Masson-Delmotte V, Mayewski P, Navarro F, Robinson S, Scambos T, Sparrow M, Summerhayes C, Speer K, Klepikov A. 2014. Antarctic climate change and the environment: an update. Polar Rec., 50, 237-259.

Thomazini, A., Mendonça, E.S., Teixeira, D.B., Almeida, I.C.C., La Scala, N., Canellas, L. P., Spokas, K.A., Milori, D.M.B.P. Turbay, C.V.G., Fernandes, R.B.A., Schaefer, C.E.G.R. 2015. CO_2 and N_2O emissions in a soil chronosequence at a glacier retreat zone in Maritime Antarctica. Sci. Total Environ. 521-522, 336–345.

Thomazini, A., Teixeira, D.B., Turbay, C.V.G., La Scala Jr, N., Schaefer, C.E.G. R., Mendonça, E.S., 2014. Spatial variability of CO_2 emissions from newly exposed paraglacial soils at a glacier retreat zone on King George Island, Maritime Antarctica. Permafr. Periglac. Process. 25, 233–242

Victoria, F.C., Alburqueque, M.P., Pereira, A.B., Simas, F.N.B., Spielmann, A.A., Schaefer, C.E.G.R., 2013. Characterization and mapping of plant communities at Hennequin Point. King George Island, Antarctica. Polar Res. 32, 19261.

Zhu, R., Bao, T., Wang, Q., Xu, H., Liu, Y. 2014. Summertime CO_2 fluxes and ecosystem respiration from marine animal colony tundra in maritime Antarctica. Atmosp. Environ. 98, 190–201.

Yeomans, J.C., Bremner, J.M., 1988. A rapid and precise method for routine determination of organic carbon in soil. Commun. Soil Sci. Plant Anal. 19, 1467-1476.

Conclusões gerais

O presente trabalho mostra o potencial de emissões e sequestro de carbono via CO_2 nos principais ecossistemas terrestres livres de gelo na Antártica Marítima, baseado em dados espaciais e temporais, bem como suas relações com os atributos, temperatura e umidade do solo. A temperatura, umidade e o status de nutrientes do solo afetam diretamente a troca de CO_2, bem como sua variabilidade espacial. Além disso, a variabilidade espacial dos atributos do solo foi fortemente relacionada com o tipo e/ou transição de cobertura vegetal, deposição de guano, bem como a dinâmica térmica e hídrica dos solos na Antártica Marítima.

Os extensos campos de musgos atuam como a maior fonte de dreno de CO_2 na Antártica Marítima. O potencial de dreno é mais acentuado à medida que se aumenta o conteúdo de água no solo. Nesses ambientes, a água promove um efeito tampão, aumentando o número de dias em que a temperatura varia entre ±0.5 °C. Quando este sítio é comparado com zonas mistas de liquens/musgos influenciadas por permafrost, o número de dias de degelo também é maior. Por outro lado, as comunidades mistas de liquens/musgos afetadas por permafrost apresentam maior variação na temperatura do solo na camada próxima a superfície. Esses locais apresentam um maior número de dias de congelamento, o que por sua vez também contribui para um aumento do efeito dreno de CO_2 na Antártica Marítima. Entretanto, à medida que a temperatura aumenta, esses sítios tendem a atuar como fonte de CO_2 para a atmosfera.

A tundra fanerogâmica antártica apresenta altas taxas de mineralização da matéria orgânica e respiração total do ecossistema, principalmente aquelas onde a atividade do guano é marcante. Dessa forma, essas áreas atuam como fonte de CO_2 para atmosfera. Solos desprovidos de vegetação sem influência de guano atuam como fonte de CO_2 para atmosfera. Apesar de apresentar baixas taxas de respiração total do ecossistema, mais estudos precisam ser realizados para verificar o potencial de perda de CO_2 das extensas áreas, desprovidas de colonização vegetal, uma vez que são muito comuns e ocupam grandes áreas livres de gelo.

A temperatura e umidade afetam fortemente a troca de CO_2 nas áreas livres de gelo na Antártica Marítima. O balanço líquido da troca de CO_2 irá depender fortemente do balanço entre as diversas áreas existentes, em formação e/ou transição, bem como novas áreas (úmidas ou bem drenadas devido ao soerguimento) que possam surgir frente a um cenário de aquecimento. Estudos nessa linha devem ser encorajados, uma vez que o balanço global ainda é desconhecido em escala maior.